

**Numerical Model Study of Potential Salinity  
Impacts Due to Proposed Navigation  
Improvements to the Sabine-Neches Waterway, Texas**

Gary L. Brown, Maria Soraya Sarruff, Rao Vemulakonda,  
Gregory H. Nail, Janelle Stokes, and Baldev Mann

**March 2006  
Revised March 2007**

Coastal and Hydraulics Laboratory  
US Army Corps of Engineers  
Engineer Research and Development Center, Vicksburg

## ADDENDUM

This Report **“Numerical Model Study of Potential Salinity Impacts due to Proposed Navigation Improvements to the Sabine-Neches Waterway – March 2006”** by ERDC was revised as a result of ITR review comments (ITRs in June 2006 and March 2007) by the U. S. Army Corps of Engineers, Mobile District, Alabama (SAM).

The following paragraph is to be added in the Chapter relating to ‘Model Analysis of the Impacts of Proposed Channel Deepening and Widening’.

New ship simulation study in order to achieve entrance channel width-reduction for the SNWW was completed in December 2006. This study for two-way simulations for large tankers and one-way LNG simulations were conducted at the Seamen’s Church Institute (SCI) at Houston, TX and ERDC. Based on that, a 700 ft width (instead of 800 ft) for the Sabine Bank Channel was established for its entire length except for the upper 5,300 ft at its junction (Sta. 18+000) with Sabine Pass Outer Bar Channel. Also, a transition length of 2,500 ft (from 800 ft to 700 ft width) was provided south of the 5,300 ft length with 800 ft width. No new hydrodynamic analysis for this 100 ft width-reduction was performed as it seemed to have minimal impact on current and salinity levels in the Sabine Bank Channel.

Also, add Figure 1 (shown below) just before the Chapter – Modeling Approach: TABS-MDS AND DOWSMM. Figure 1 shows location of some of the ‘Mitigation Measures’ considered in this plan. Other ‘Areas’ are shown in the EIS Section of the Feasibility Report.

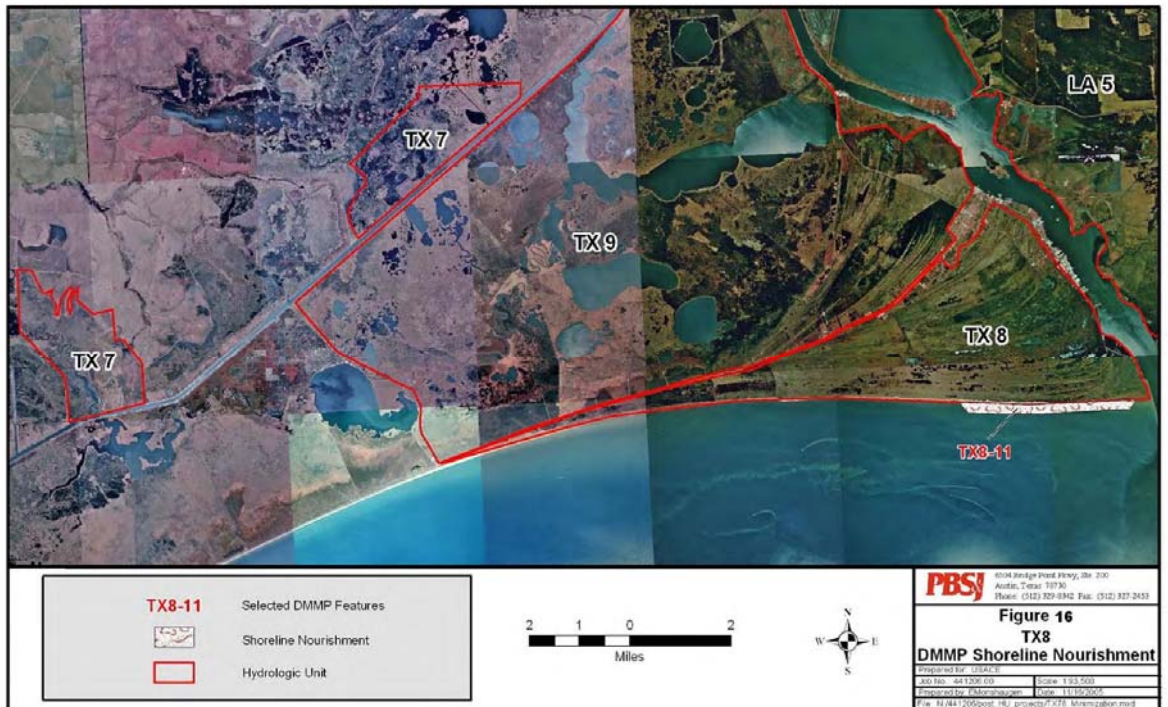
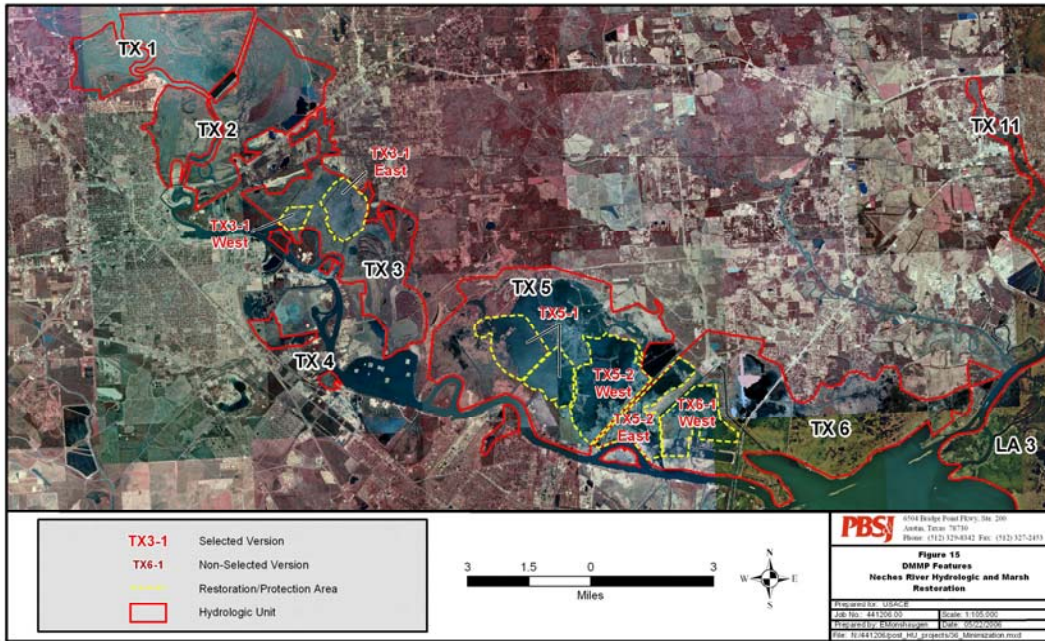


Figure 1: Showing Location of Mitigation Measures



**Numerical Model Study of Potential Salinity  
Impacts Due to Proposed Navigation  
Improvements to the Sabine-Neches  
Waterway, TX  
Volume 1: DRAFT Report**

Gary L. Brown, Maria Soraya Sarruff, Rao Vemulakonda, Gregory H.  
Nail, Janelle Stokes, and Baldev Mann

March 2006

# Preface

---

As part of the continuing studies of the Sabine-Neches Waterway, TX, The U.S. Army Engineer District, Galveston (SWG), requested the U.S. Army Engineer Research and Development Center, Waterways Experiment Station (ERDC-WES) to perform a numerical model study of circulation and salinity impacts resulting from modification of the Sabine-Neches Waterway (SNWW) in Texas. The study included development of a two- and three-dimensional (3D) model of the system, validating the model, and performing long-term simulations of impacts due to different deepening and widening plans.

The Galveston District provided funding for this study. Mr. Gary Brown served as principal investigator of the project. Additional work was performed by M. Soraya Sarruff, Rao Vemulakonda, and Greg Nail. Technical assistance and oversight was given by R. C. Berger and Joe Letter. The Hydraulic Analysis Group of CHL, led by Mr. Tim Fagerburg, undertook the field data collection efforts. Ms. Janelle Stokes, Mr. Baldev Mann provided pertinent data available at the Galveston District and the Modeling Workgroup of the SNWW Interagency Coordination Team (ICT) provided additional information on the study area.

The study was conducted under general supervision of Dr. Robert T. McAdory, Chief of the Estuarine Engineering Branch, and Mr. Thomas W. Richardson, Director, CHL.

At the time of this publication, Dr. James R. Houston was Director of ERDC, and COL James R. Rowan was Commander and Executive Director.

# Table of Contents

---

<b>INTRODUCTION .....</b>	<b>5</b>
<b>BACKGROUND AND PROBLEM STATEMENT .....</b>	<b>5</b>
<b>OBJECTIVE AND APPROACH.....</b>	<b>7</b>
<b>NUMERICAL MODEL DESCRIPTION .....</b>	<b>8</b>
<b>FIELD DATA COLLECTION AND ANALYSIS.....</b>	<b>8</b>
<b>HYDRODYNAMIC AND SALINITY MODELS.....</b>	<b>9</b>
<i>Computational Mesh .....</i>	<i>9</i>
<i>Mean Low Tide (MLT), ft.....</i>	<i>12</i>
<i>Mean Lower Low Water (MLLW), ft.....</i>	<i>12</i>
<i>NAVD 88, ft.....</i>	<i>12</i>
<i>Boundary Conditions.....</i>	<i>13</i>
<i>Vertical datum shift (ft).....</i>	<i>14</i>
<b>CALIBRATION AND VERIFICATION .....</b>	<b>21</b>
<b>MODEL CALIBRATION .....</b>	<b>21</b>
<b>MODEL VERIFICATION .....</b>	<b>22</b>
<i>Water Surface Elevation Data.....</i>	<i>22</i>
<i>ADCP Discharge Data.....</i>	<i>24</i>
<i>Velocity Data.....</i>	<i>26</i>
<i>Salinity Data.....</i>	<i>28</i>
<i>Salinity Sensitivity to the GIWW East Outflow.....</i>	<i>35</i>
<b>MODEL ANALYSIS OF THE IMPACTS OF PROPOSED CHANNEL DEEPENING.....</b>	<b>36</b>
<u><b>AND WIDENING</b></u>	
<b>DESCRIPTION OF PROPOSED CHANNEL DEEPENING AND WIDENING .....</b>	<b>36</b>
<i>REACH (EXISTING STATIONS) .....</i>	<i>36</i>
<i>BOTTOM WIDTH (FT).....</i>	<i>36</i>
<i>PROJECT DEPTH (MLT).....</i>	<i>36</i>
<i>ADVANCE MAINTENANCE ADDED (FT).....</i>	<i>36</i>
<i>ALLOWABLE OVERDEPTH (FT).....</i>	<i>36</i>
<i>TOTAL DEPTH (MLT).....</i>	<i>36</i>
<b>BOUNDARY CONDITIONS FOR ANALYSIS OF CHANNEL DEEPENING IMPACTS.....</b>	<b>38</b>
<i>Salinity.....</i>	<i>38</i>
<i>Storm Surge.....</i>	<i>42</i>
<b>RESULTS.....</b>	<b>42</b>
<i>Salinity.....</i>	<i>42</i>
<i>Storm Surge.....</i>	<i>59</i>
<b>MODEL ANALYSIS OF PROPOSED SALINITY MITIGATION ALTERNATIVES .....</b>	<b>60</b>
<b>DESCRIPTION OF PROPOSED SALINITY MITIGATION ALTERNATIVES.....</b>	<b>60</b>
<b>MODELING APPROACH: TABS-MDS AND DOWSMM.....</b>	<b>63</b>
<b>RESULTS.....</b>	<b>63</b>

*TABS-MDS results: General Observations* ..... 63  
*DOWSMM Desktop Modeling Results* ..... 69  
*Habitat Salinity Analysis* ..... 70  
**CONCLUSIONS**..... 73  
**REFERENCES** ..... 77

**APPENDIX A TABS-MDS**

---

**APPENDIX B DOWSMM**

**APPENDIX C MEAN AND HIGHEST 33% CONTINUOUS SALINITY VALUES FOR  
MITIGATION MEASURES 1-5**



# Introduction

---

## Background and Problem Statement

The Sabine-Neches Waterway is located on the border of Texas and Louisiana. The system consists of 6 major hydraulically significant features:

- 1) Sabine Pass, an artificially enlarged channel dredged between Sabine Lake and the Gulf of Mexico
- 2) The Sabine-Neches Canal and Port Arthur Canal, the artificial shipping channels dredged along the western shore of Sabine Lake, to link the Neches and Sabine Canals to Sabine Pass, and to provide shipping access for the ports of Port Arthur, Beaumont and Orange, Texas.
- 3) The Gulf Intracoastal Waterway (GIWW), which traverses the system and links it hydraulically with the Calcasieu Lake on the East, and Galveston Bay on the west.
- 4) The Sabine River, which empties into Sabine Pass via Sabine Lake and the Sabine – Neches Waterway
- 5) The Neches river, which empties into Sabine pass via Sabine Lake and the Sabine – Neches Waterway
- 6) Sabine Lake, a large, shallow (approximately 8 feet deep) estuary, receiving fresh water from the Sabine and Neches rivers, and salt water from Sabine Pass.

In addition, there are several sensitive and extensive wetland habitats within the system, including the Sabine National Wildlife Refuge, and McFaddin National Wildlife Refuge.

Figure 1 is a location map of the system..

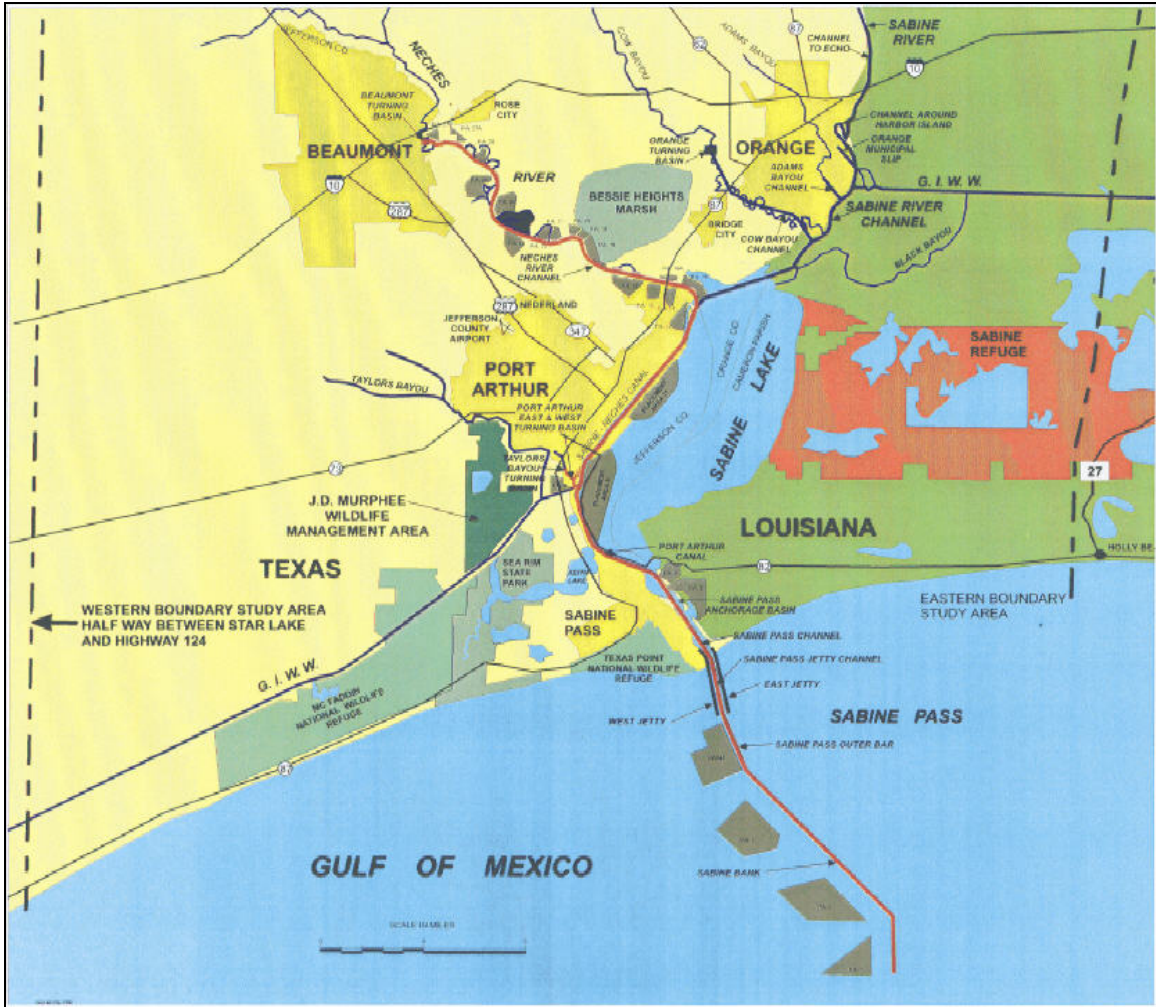


Figure 1: Location Map

## **Overview of Circulation and Salinity in the SNWW**

The SNWW system exhibits very complicated circulation and salinity patterns. Fresh water enters the system via several tributaries, including the Sabine River, the Neches River, and other smaller inflows. The Neches River flows directly into Sabine Lake and the Sabine –Neches Canal, whereas the Sabine River flows into Sabine Lake, the Sabine-Neches Wildlife Refuge, and into Calcasieu Lake via the GIWW.

The Sabine Neches canal acts as a flow pathway for both fresh water from the inflowing rivers, and saline water intruding via tidal propagation through Sabine Pass. This combination results in highly stratified conditions in the Sabine-Neches canal. This stratification contributes to salt water intrusion migrating up the Sabine-Neches canal and into the northwest corner of Sabine Lake and the lower reaches of the Neches River.

As a result of this intrusion, the observed salinity in Sabine Lake is highest at both the southern end (where the lake connects to Sabine Pass) and at the northern end (where the lake connects to the Sabine-Neches canal). The lowest salinities are observed in the central and eastern portions of the lake, which are furthest from the hydraulic connection to sources of saline water.

## **Objective and Approach**

This report details the development of a numerical model hydrodynamics and salinity in the Sabine-Neches waterway. The development and validation of the model are detailed, and the results of the model evaluation of salinity impacts due to proposed navigation improvements are presented.

The tasks performed and described by this report are:

- a. Development of a three-dimensional numerical model.
- b. Validation of the model for hydrodynamics and salinity using field data gathered for this undertaking,
- c. Evaluation of proposed plan conditions.
- d. Comparison and analysis of results.

# Numerical Model Description

---

The TABS-MDS code of ERDC-WES is used for computing hydrodynamics, plus salinity and sediment transport. The model was originally developed as RMA10 by Resource Management Associates (King, 1993) and extensively modified by ERDC-WES staff into its present configuration. In agreement with the original author, the ERDC version of the code was given the name TABS-MDS to distinguish it from RMA10. It is a finite element model, which gives it great flexibility in matching complex geometry. Through the solution of equations of conservation of mass and horizontal momentum, as well as the convective-diffusion equation for transport of salinity and heat, the code accounts for forcing due to tides, freshwater inflows, wind, Coriolis effects (where applicable), and density gradients due to salinity and temperature. It also considers evaporation and precipitation to complete an accurate description of the system under study. For further discussion of TABS-MDS, see Appendix A.

ERDC-WES personnel have used the code extensively over the last decade in a variety of field investigations with excellent results. Its proven effectiveness makes it well suited for this application.

## Field Data Collection and Analysis

A numerical hydrodynamic and transport model requires adequate field data to perform calibration and verification of the model. For this study, the Hydraulic Analysis Group of CHL performed an intensive data collection effort. These data include time-series observations of the following parameters:

- 16 tide observation locations
- 16 salinity observation locations
- 10 velocity observation locations
- 10 Acoustic Doppler Current Profiler (ADCP) 25-hour flow transects

The time-series data were collected between 16 May, 2001, and 10 January, 2002. The full data report is given in Fagerburg, et. al. (2001). The locations of the time-series data are given in Figure 2.

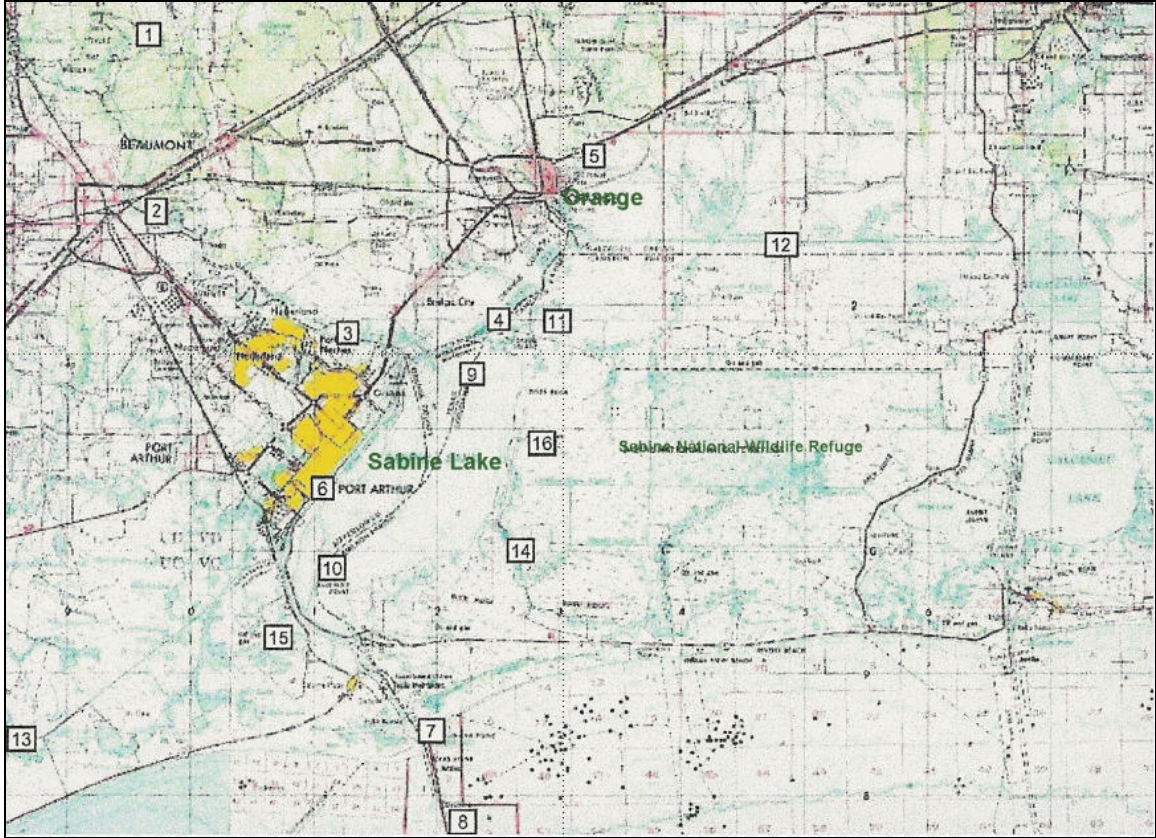


Figure 2: Instrument Location Map

## Hydrodynamic and Salinity Models

### Computational Mesh

The TABS-MDS code uses a computational mesh, as a mathematical representation of the physical environment under study. A mesh typically includes information on the shoreline geometry, the bathymetric features, and the bottom-type characteristics of the area involved. The extents of the model domain are given as follows:

- North to the Neches River at Evadale, TX, and the Sabine River at Ruliff, TX.
- East to a point approximately mid-way between the Sabine Lake and Calcasieu Lake, including approximately half of the Sabine-Neches Wildlife Refuge
- South approximately 55 miles into the Gulf of Mexico from the Gulf shoreline.
- West to a point approximately mid-way between Sabine Lake and Galveston Bay, including all of the McFaddin National Wildlife Refuge

The model mesh is given in Figure 3. It contains 33,321 surface nodes and 13,035 surface elements.

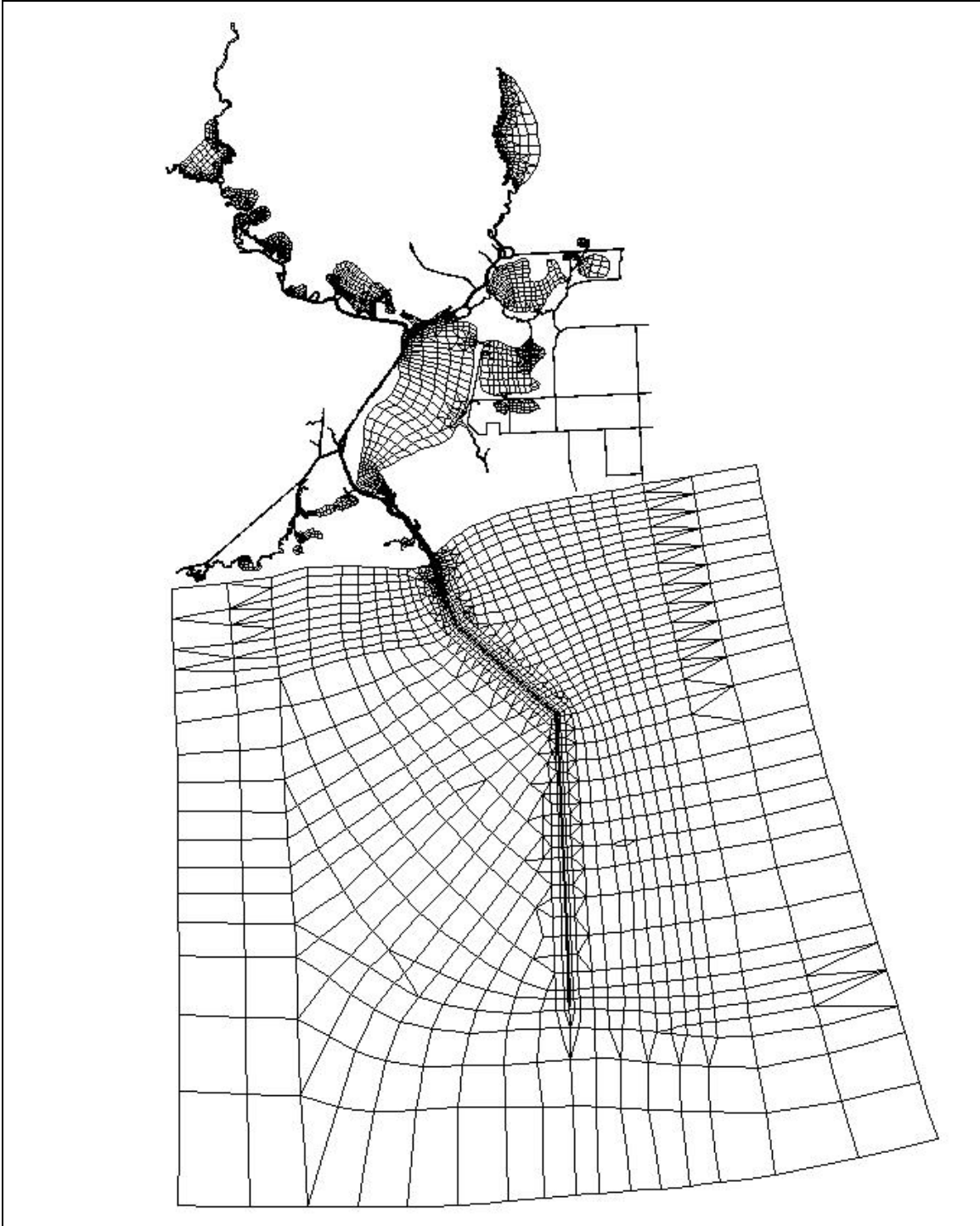


Figure 3: Model Mesh

The model mesh is assigned 3D resolution in all of the navigation channels and in Sabine Lake. This allows the model to simulate baroclinic forcing due to the density difference between salt water and fresh water. This resolution adds a significant computation burden to the model. The number of nodes and elements in the model with the 3D resolution included is 132,393 and

45,915, respectively.

The delineation of the shoreline in the model was accomplished with the use of National Oceanic and Atmospheric Administration (NOAA) charts, USGS Quad sheets, and of georeferenced satellite imagery provided by SWG. The bathymetry was taken from a variety of sources. Initially, the bathymetric data were taken from the NOAA charts of the region. The navigation channel bathymetry were taken from a comprehensive bathymetric survey provided by SWG. Additional bathymetric data was collected by SWG to confirm the accuracy of the bathymetric values taken from the NOAA charts for Sabine Lake.

The bathymetric data is given as Mean Low Tide (MLT). Table 1 gives the relationship between this datum and other commonly used datums, at Sabine Pass, TX.

**Table 1. Referencing Table for Different Datums for Sabine Pass, Texas\***

<b>Mean Low Tide (MLT), ft</b>		<b>Mean Lower Low Water (MLLW), ft</b>		<b>NAVD 88, ft</b>
0.0	=	-0.36	=	-0.78
0.36	=	0.0	=	-0.42
0.78	=	0.42	=	0.0
1.0	=	0.64	=	0.22
2.0	=	1.64	=	1.22
3.0	=	2.64	=	2.22
4.0	=	3.64	=	3.22

\* This table provides the best estimate of equal elevations at the three datums but the relationships between the datums have not been fully field-verified.

## Boundary Conditions

The applied boundary conditions and the data sources for each boundary condition are given in Figure 4.

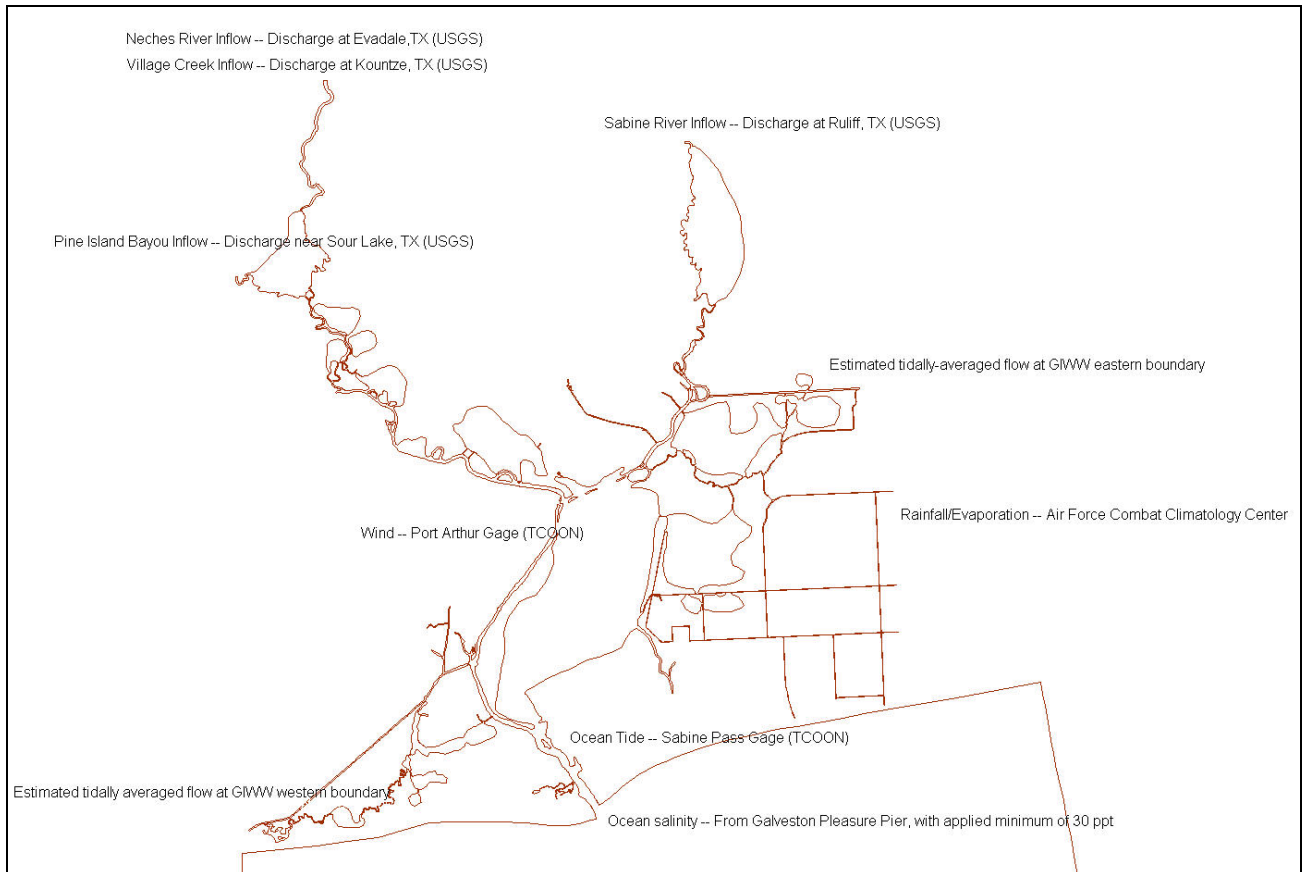


Figure 4: Applied Boundary Conditions

Ocean Tide – The tidal boundary condition applied at the ocean boundary was extrapolated from the observed tide at Sabine Pass. Since the tidal signal transforms dramatically between the offshore and Sabine Pass (due to nonlinear frictional effects) it was necessary to adjust the observed tidal signal such that the applied signal transformed into the observed signal at Sabine Pass as it propagated from the offshore inland. The signal was transformed by first decomposing it into several frequency bands (these bands were chosen to correspond roughly with the major tidal harmonic components), and then by adjusting the amplification factor and tidal plane adjustment of each frequency band consistent with observations of the model results. That is, model tides were extracted at both the offshore boundary and at Sabine Pass, the signals were decomposed, and the adjustment factors between each location were observed. These were applied to the model boundary, and the process was repeated until no further adjustment was required. The final adjustments are given in Table 2. A sample of the applied boundary tidal signal and the observed tidal signal as it propagates across the Sabine Pass gage are given in Figure 5.

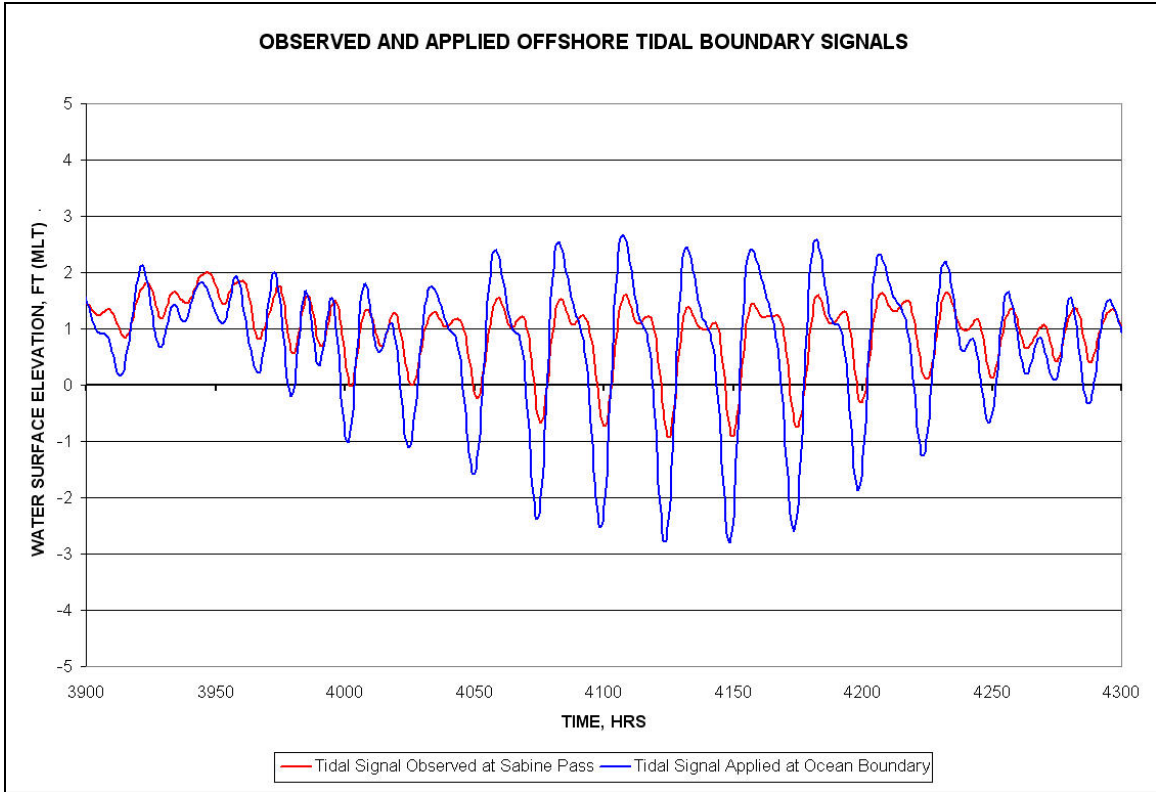


Figure 5: Observed and Applied Tidal Boundary

**Table 2. Tidal boundary condition adjustment factors**

Frequency Band (hrs)	Vertical datum shift (ft)	Phase shift (hrs)	Tidal amplitude multiplication factor
0-8	-.27	-1.0	.67
8-16	-.27	-1.0	1.67
16-30	-.27	-1.0	2.45
>30	-.27	-1.0	1.00

Ocean Salinity – The salinity at the ocean boundaries was taken from the 30-year, monthly averaged salinity, measured offshore at Galveston, TX (Cochrane and Kelly, 1986). These salinities reflect the seasonal variability in near shore salinity along the Texas coast, influenced in large part by the Mississippi River. The salinity was adjusted such that the minimum applied salinity was 30 ppt. This adjustment was made because the model boundary is sufficiently far offshore (approximately 60 miles) that consistent salinity below 30 ppt is unlikely to occur. The applied ocean salinity is given in Figure 6.

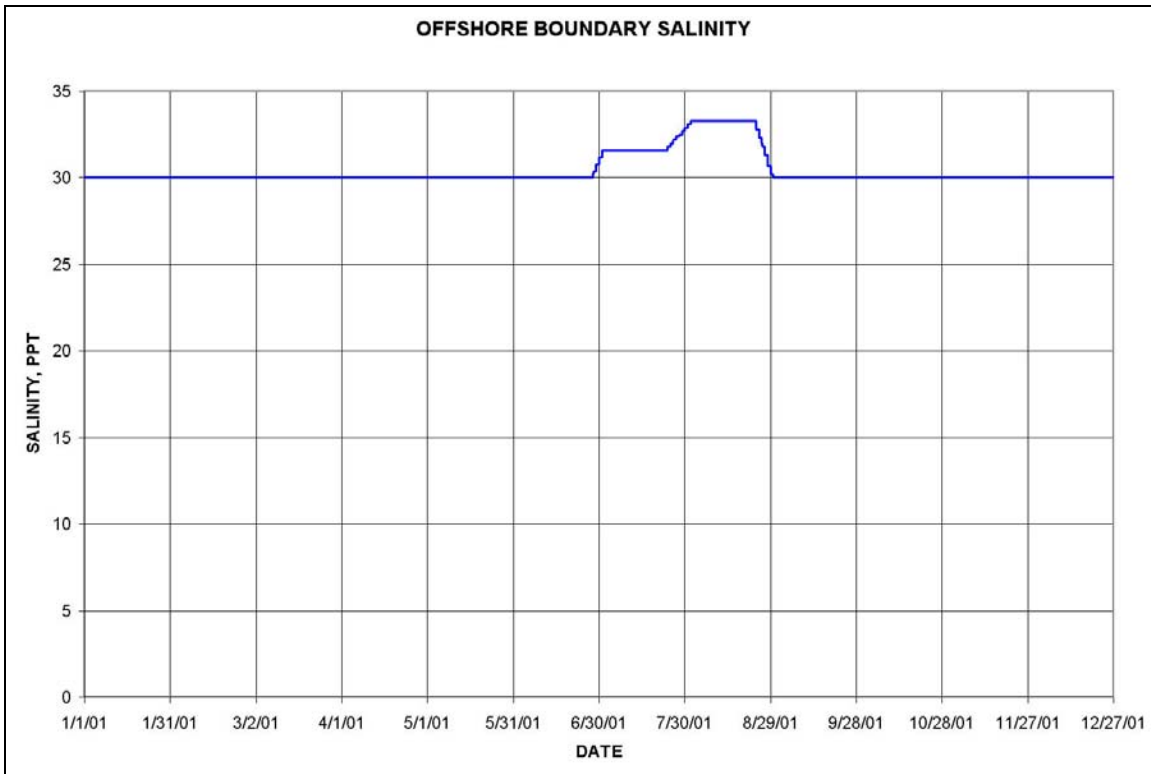


Figure 6: Applied Offshore Salt Boundary Condition

Wind – Hourly wind data were taken from the TCOON station at Port Arthur, TX. These were applied throughout the model domain. A plot of the applied wind magnitude and direction are given in Figure 7.

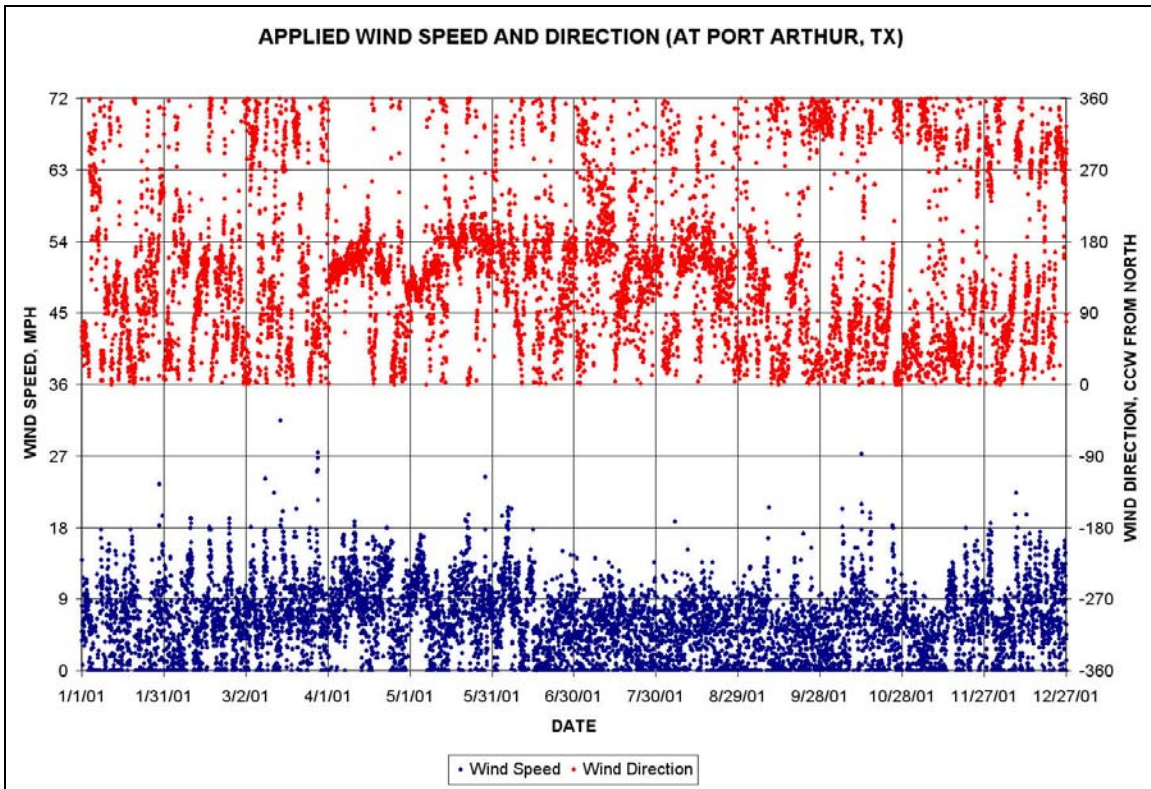


Figure 7: Applied Wind Speed and Direction

Rainfall and evaporation – Daily rainfall and evaporation values were taken from the Air Force Combat Climatology Center. These were applied throughout the model domain. The applied net precipitation (rainfall minus evaporation) is given in Figure 8.

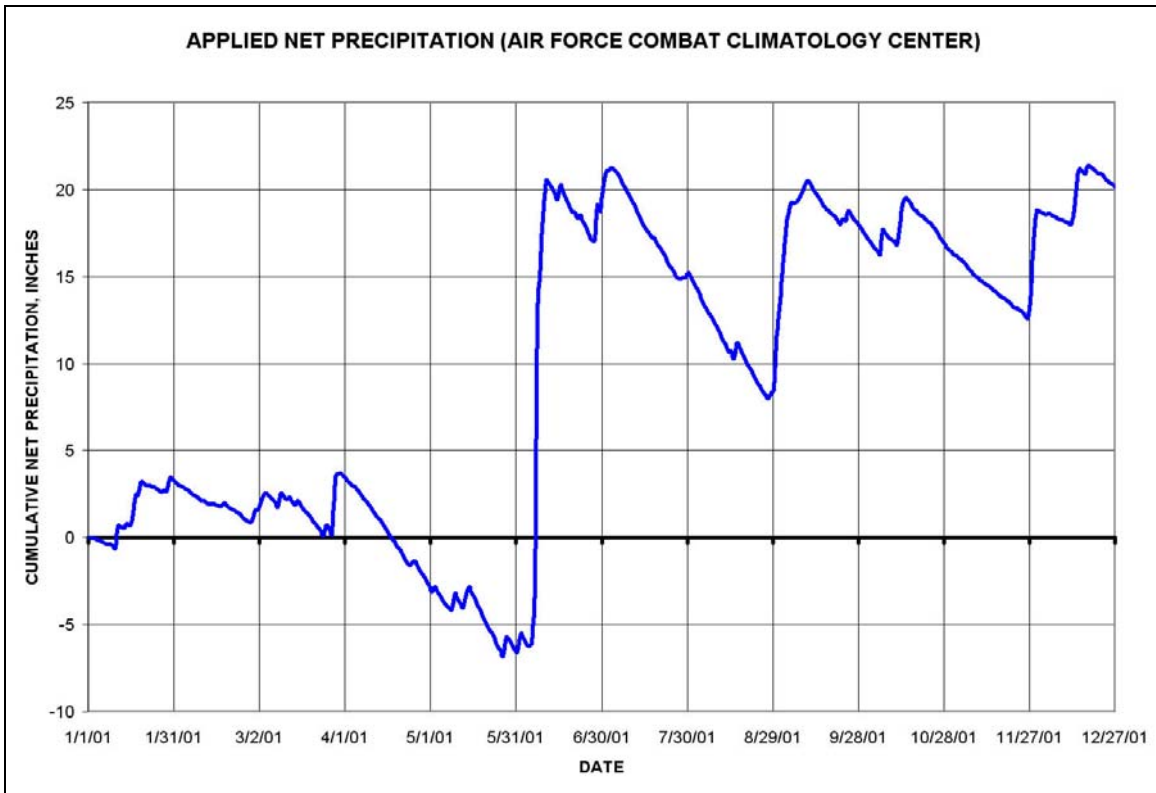


Figure 8: Applied Net Precipitation

River inflows – Daily river inflows for the 4 major freshwater sources to the system (The Sabine River, the Neches River, Village Creek, and Pine Island Bayou) were taken from USGS observations. The time series of these inflows for the model simulation period are given in Figure 9.

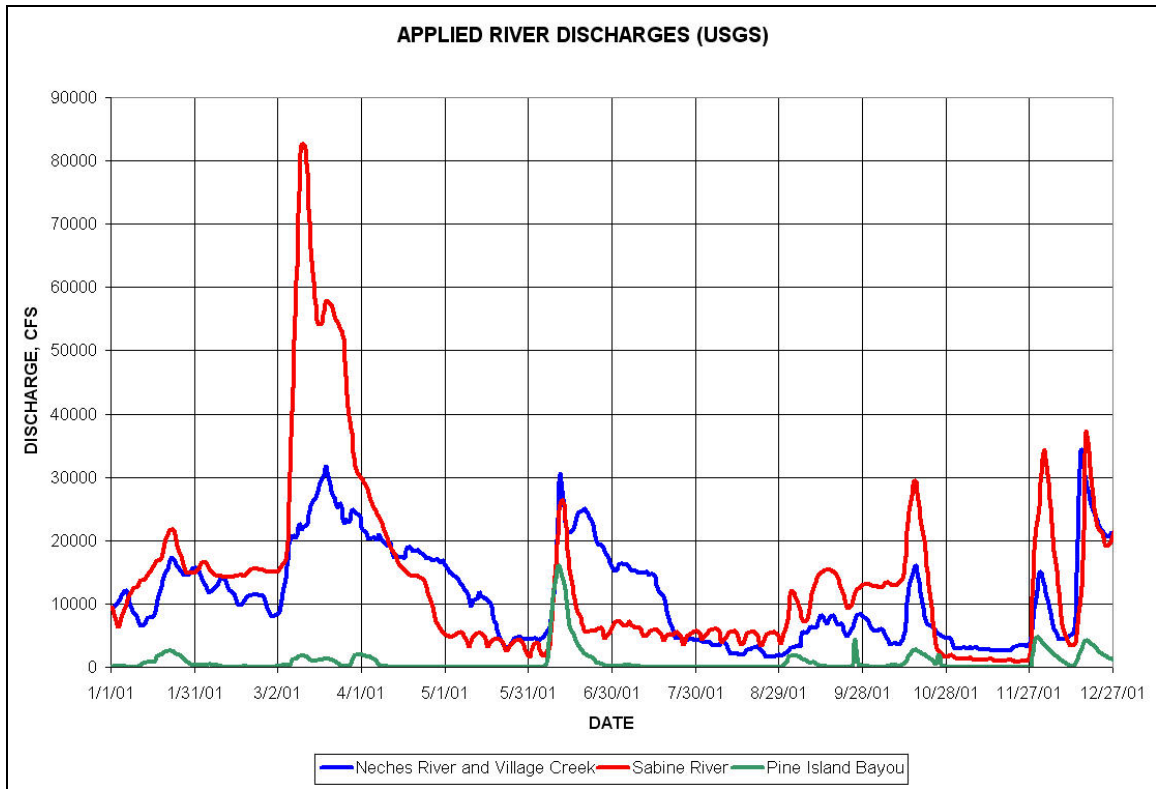


Figure 9: Applied River Discharges

GIWW eastern and western boundaries – Initially, both the GIWW eastern and western boundaries were modeled as no-flow boundaries. These boundaries were chosen such that their locations correspond to the typical locations of tidal nodes. Hence, the currents at these locations were presumed to be small. However, investigations by the Louisiana Department of Natural Resources (LDNR) indicate that there is net transport of Sabine River water to the east in the GIWW (LDNR, 2002). Hence, although the average tidal current may be near zero at this location, there is a net sub-tidal current that correlates with the discharge in the Sabine River.

The exact magnitude of this discharge is unknown. The field data collected for this study does include a 25-hour discharge transect observation at this location, but this observation is not of sufficient duration to generate a statistically significant correlation between the Sabine River discharge and the net GIWW flow.

Therefore, a functional relationship between river discharge and net GIWW flow was generated for both the eastern and western boundaries, using primarily engineering judgment. The resulting discharge was compared to the observed discharge at the GIWW east location, to ensure that they correspond. However, this only represents a correspondence for a specific 25-hour period, and therefore does not represent a verification of this correlation. The sensitivity of the model uncertainties in this relationship are discussed in the model verification section of this report.

There was no available data for comparison at the western GIWW boundary. However,

uncertainties at this boundary have little affect of the model results.

The functional relationships used to generate these flows are given in Equations 1 and 2. Plots of the discharges at these boundaries are given in Figures 10 and 11.

$$Q_{GIWW.E} = \frac{5}{11} Q_{SABINE} + 1000, \text{with a maximum allowable outflow} = 5000 \text{ cfs....} \quad (1)$$

$$Q_{GIWW.W} = \frac{1}{10} Q_{NVPIB}, \text{with a maximum allowable outflow} = 2000 \text{ cfs.....} \quad (2)$$

Where  $Q_{GIWW.E}$  is the outflow at the GIWW eastern boundary,  $Q_{SABINE}$  is the Sabine River inflow,  $Q_{GIWW.W}$  is the outflow at the GIWW western boundary, and  $Q_{NVPIB}$  is the combined inflow of the Neches River, Village Creek, and Pine Island Bayou.

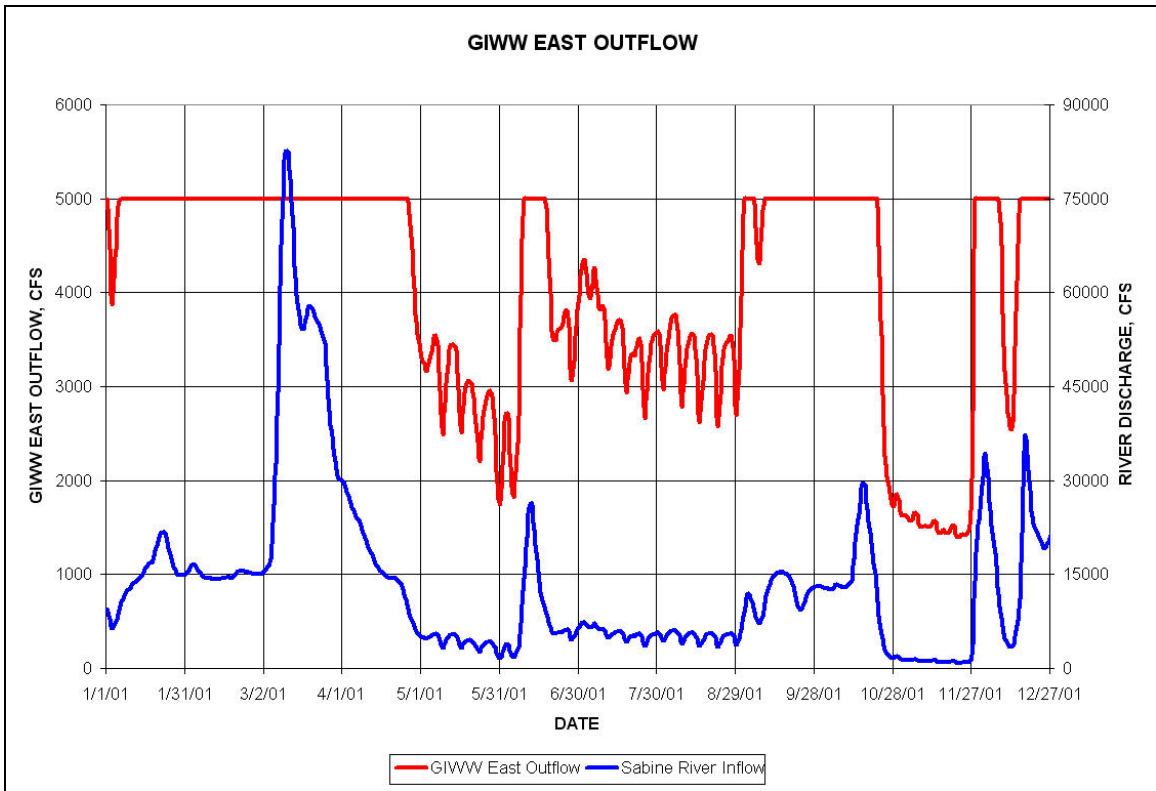


Figure 10: Applied GIWW East Outflow Boundary Condition

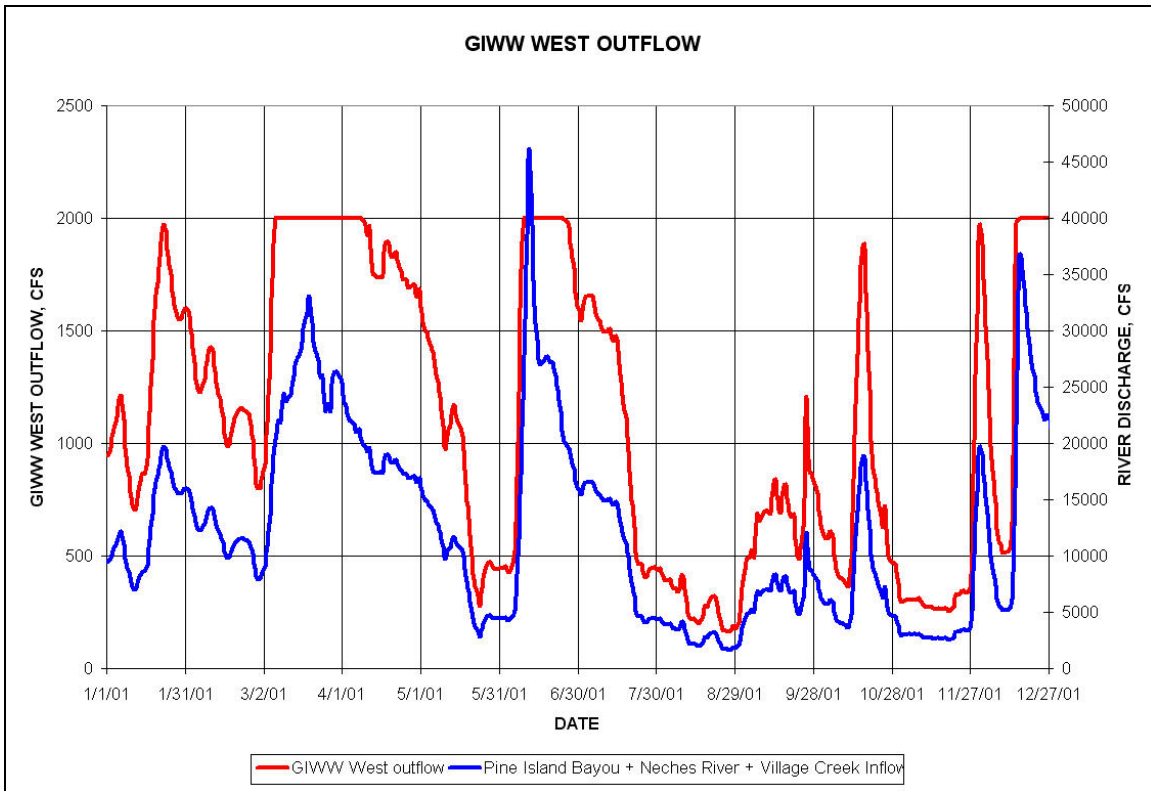


Figure 11: Applied GIWW West Outflow Boundary Condition

Power Plant Discharge at Bessie Heights– There is a constant intake of 5,000\_cfs from Old River Cove, used as a coolant for a power plant. This water is then discharged into a channel that flows into Bessie Heights. This is represented in the model by an intake of 5,000 cfs at Old River Cove, at the local ambient salinity. This intake is discharged at this same salinity in Bessie Heights.

# Calibration and Verification

---

The numerical model was calibrated and verified against the field data collected from June – December of 2001. The results of this effort are covered in this chapter. The specific data and procedures used for both calibration and verification are detailed, and the impact of uncertainties in the applied boundary conditions is analyzed with respect to their influence on the model verification.

## Model Calibration

The model was calibrated against the 12 water surface elevation stations. The calibration period was chosen from June through July, 2001. The model was calibrated by making adjustments to the friction coefficient (Manning's  $n$ ). Since the model relies on the Smagorinsky (1963) approximation for both horizontal turbulence closure and for horizontal salt diffusivity, these values were not adjusted as a calibration parameter. The Smagorinsky parameter was adjusted at specific locations within the domain, but this was done to provide numerical stability rather than to calibrate the model.

The discharge measurements and velocity measurements were not used for calibration per se. However, they were periodically inspected during the calibration process, in order to determine whether or not errors in the physical description of the system were present in the model. For example, early in the calibration process, it was noticed that some of the discharges measured in the model were much lower than those measured in the field. This discrepancy was not remedied by adjusting a calibration parameter. Rather, the model geometry was compared against satellite imagery of the system, and it was determined that the southern connection between the Sabine-Neches Canal and Sabine Lake was far too narrow in the mesh, due to an error in one of the charts used to define the original geometry. Since no calibration parameters were adjusted to force the model data to match the field data, this procedure is not classified as calibration, but rather as merely a correction of the system description, based on observations of the prototype.

The model was not specifically calibrated for salinity, since the only parameters that could be used to calibrate for salinity (horizontal and vertical turbulent mixing) are constrained by the physics of the system. That is, turbulent mixing is a function of the velocities and velocity gradients present in the flow field, and as such dramatic adjustment of these parameters could result in a model that no longer obeys the proper physics. The results may match observations well, but not for the right reasons. This would result in a model that is unsuitable for use in the analysis of plan conditions, since the impacts of these changes could not be ascertained by a non-physics based model.

Having stated that, the inability to achieve verification of the salinity in the model made some artificial adjustment of the horizontal mixing necessary, but only in specific locations that were

chosen to limit the liability associated with this modification. This is explained in detail in the salinity verification section of this report.

The Manning's  $n$  values used here are appropriate for a relatively smooth bay bottom with little or no vegetation (see Chow 1959). The values vary from 0.02 in the channel, to 0.03 in the shallows and wetlands (such as the Bessie Heights area). The system is generally homogeneous with respect to bottom roughness, except for the values assigned to the wetlands. Some of the eddy viscosity and turbulent diffusion values in regions of the domain adjacent to inflow and tidal boundaries were made artificially large, to ensure stability.

## **Model Verification**

The model hydrodynamics were verified against 3 separate types of data: water surface elevation data (from August – December, 2001), ADCP 25-hour discharge data (from August 17<sup>th</sup>-18<sup>th</sup>, 2001), and velocity data (from June- December, 2001). The model salinities were verified against salinity data (from June- December, 2001). The following section contains a summary and discussion of these results.

### **Water Surface Elevation Data**

A sample of the water surface elevation observations for both the model and the field for the verification period are given in Figure 12. The figure gives water surface elevations for a 28 day period (August 1<sup>st</sup> – August 28<sup>th</sup>). Since the field data are not referenced to a reliable vertical datum, the mean water surface elevation has been subtracted from the field data and the mean water surface elevation observed in the model has been added back in. This makes it easier to visually inspect the amplitude and phase comparisons between the model and the field.

Any of the field data that was obviously corrupted by bio-fouling of the sensor was omitted from this comparison and analysis. Also, the field data has been filtered to remove noise in the signal. Signals with a period of 6 hours or less were omitted from the data set.

The water surface elevation observations are given such that the gages in closest contact (hydraulically) with the ocean are shown at the top of the Figure. This is done so that the progression of the tide inland, and the consequent attenuation of the signal due to friction losses, can be readily observed for both the model and the field. The tide comparisons show that the model and field have good agreement with respect to the tidal signal, at all of the stations except for Station 5. This Station is far up the Sabine River, and shows that the model is overly dissipative in this reach. This increased attenuation could not be addressed by further reduction of friction coefficients, since the coefficients used are already representative of a relatively smooth bed.

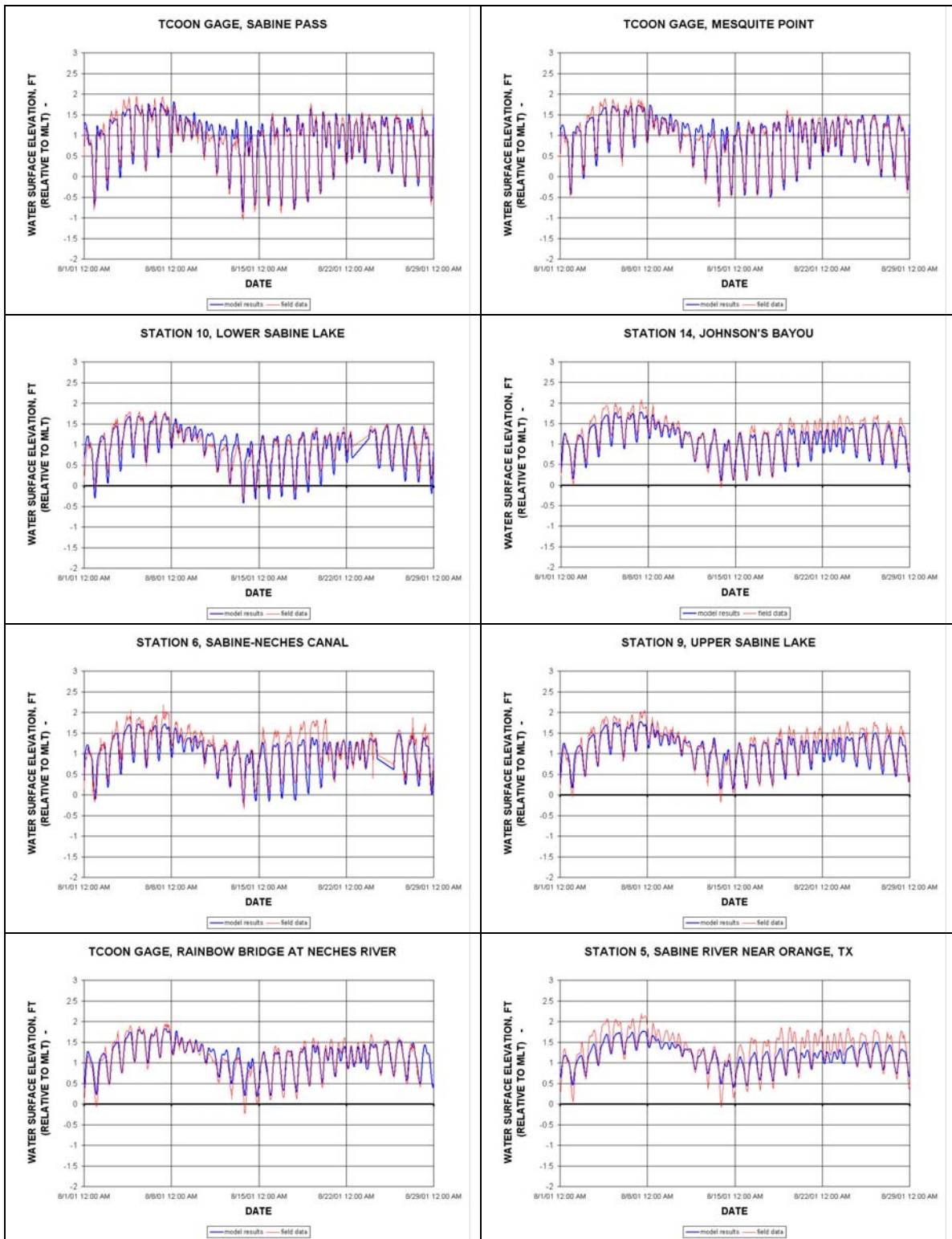


Figure 12: Tide Comparisons at Stations 5, 6, 9, 10, 14, and TCOON Gages at Sabine Pass, Mesquite Point, and Rainbow Bridge

## ADCP Discharge Data

The discharge observations at all 10 transects given in the field data are plotted against model results in Figures 13-16. The locations of each range are shown in the figures. Note that, although the total discharge in Ranges 3 and 5 appears low in the model, the total discharges observed in Ranges 6 and 8 appear appropriate. This indicates that the flow split between the Sabine-Neches Canal and Sabine Lake is somewhat different in the model than in the field, with a greater percentage of the total flow passing through the Lake in the model than in the field. Several attempts were made to ascertain the cause of this discrepancy, but none were found that could be justified physically.

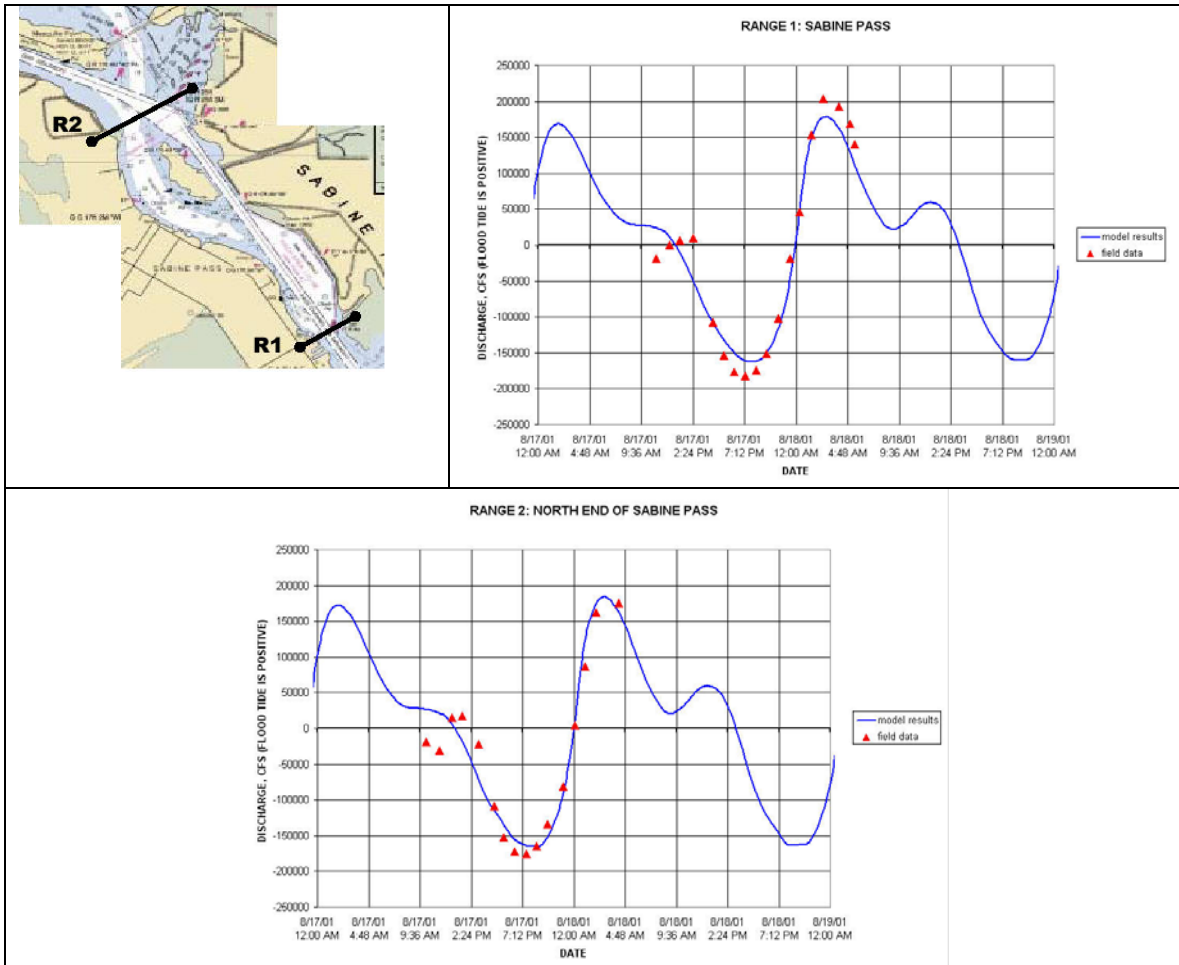


Figure 13: Discharge Comparisons at Ranges 1 and 2

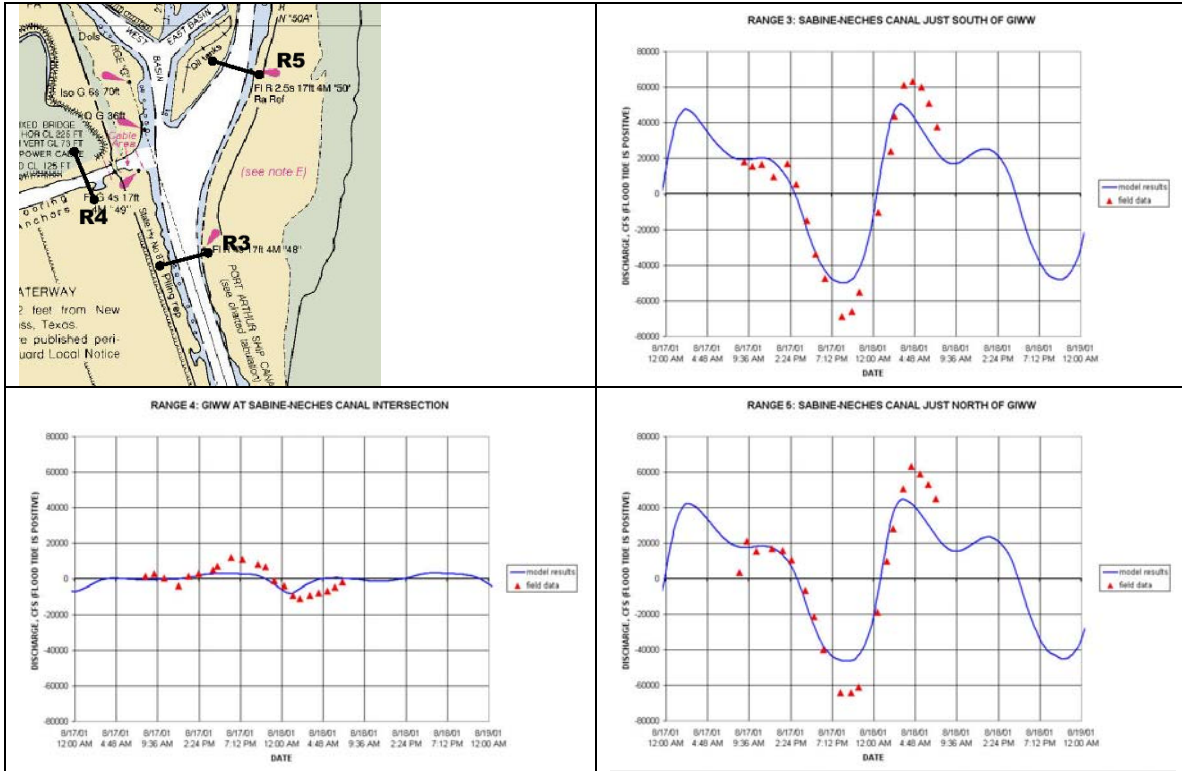


Figure 14: Discharge Comparisons at Ranges 3,4, and 5.

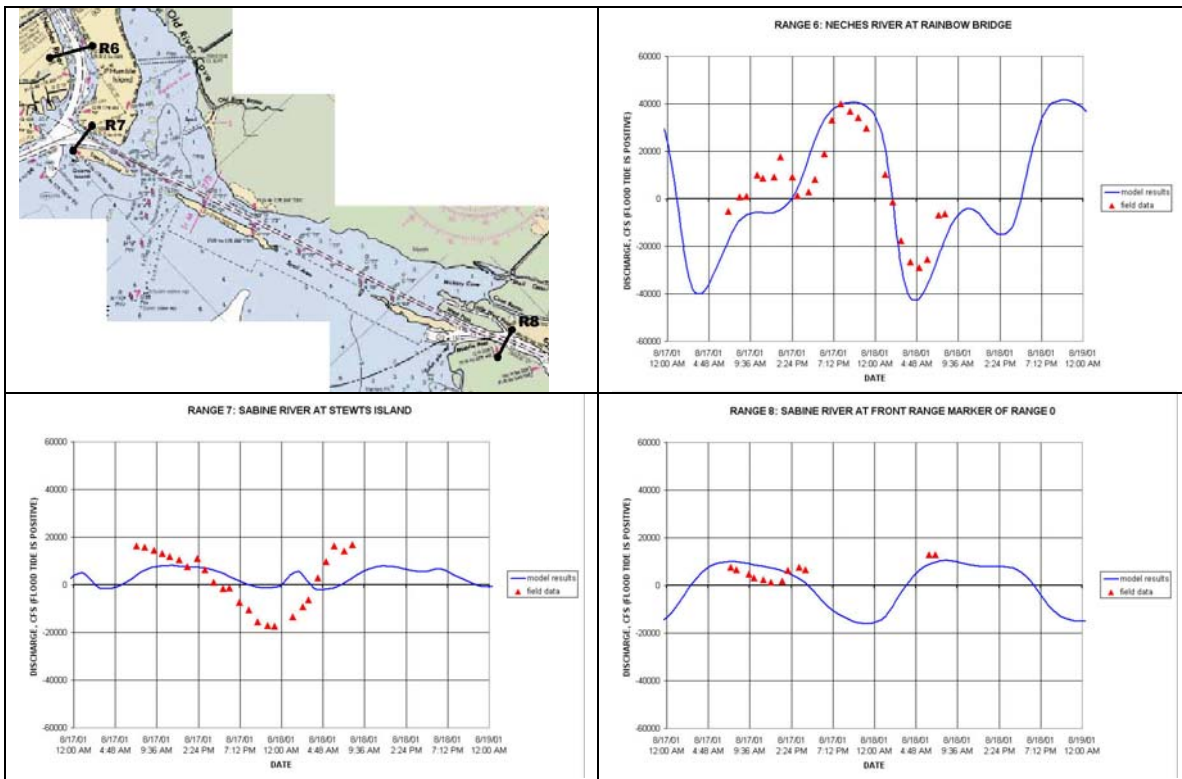


Figure 15: Discharge Comparisons at Ranges 6,7, and 8.

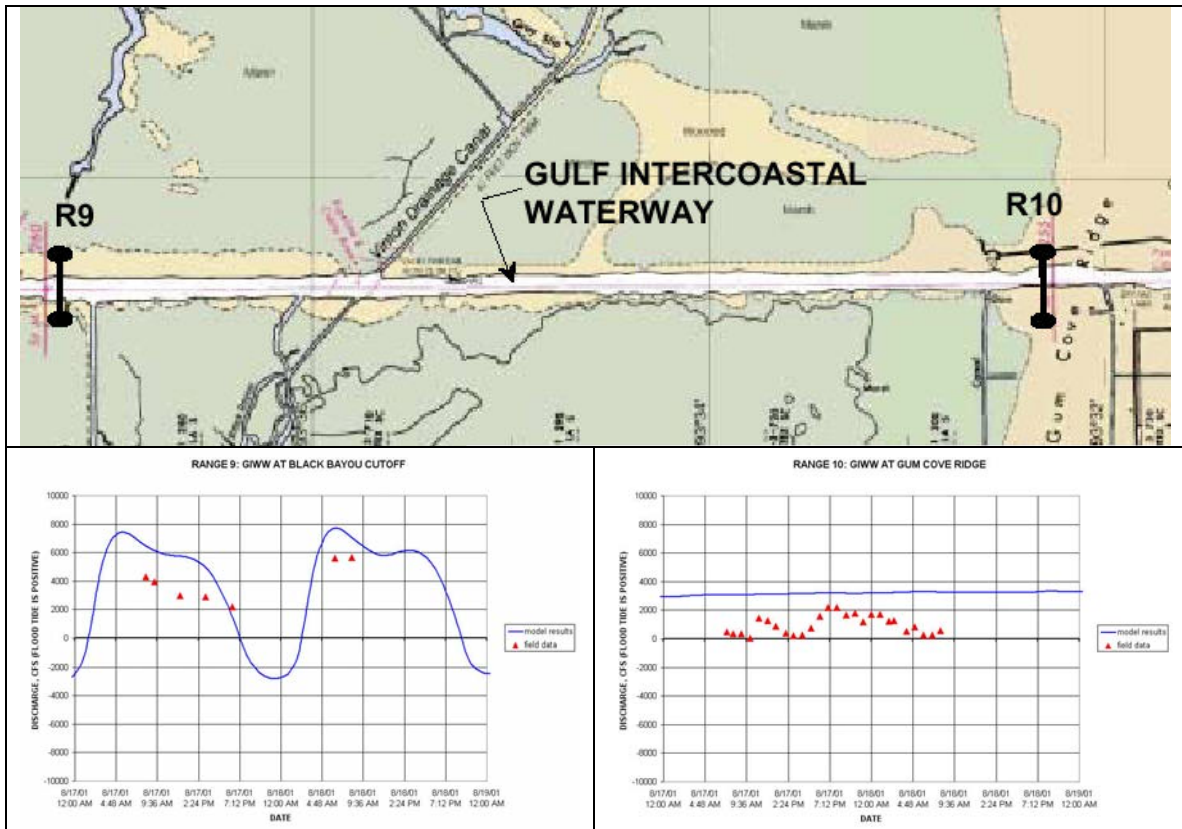


Figure 16: Discharge Comparisons at Ranges 9 and 10

### Velocity Data

The velocity observations are given in Figures 17 and 18. They show good agreement at most of the gage locations. However, at Station 6 (in the Sabine-Neches Canal) there is a noticeable difference in the strength of the ebb current in the model and the field. The ebb current in the model is much stronger than that observed in the field. This difference may account for some of the difficulties in promoting salt transport through the Sabine-Neches Canal in the model. However, repeated attempts to isolate and address the cause of this discrepancy were unsuccessful.

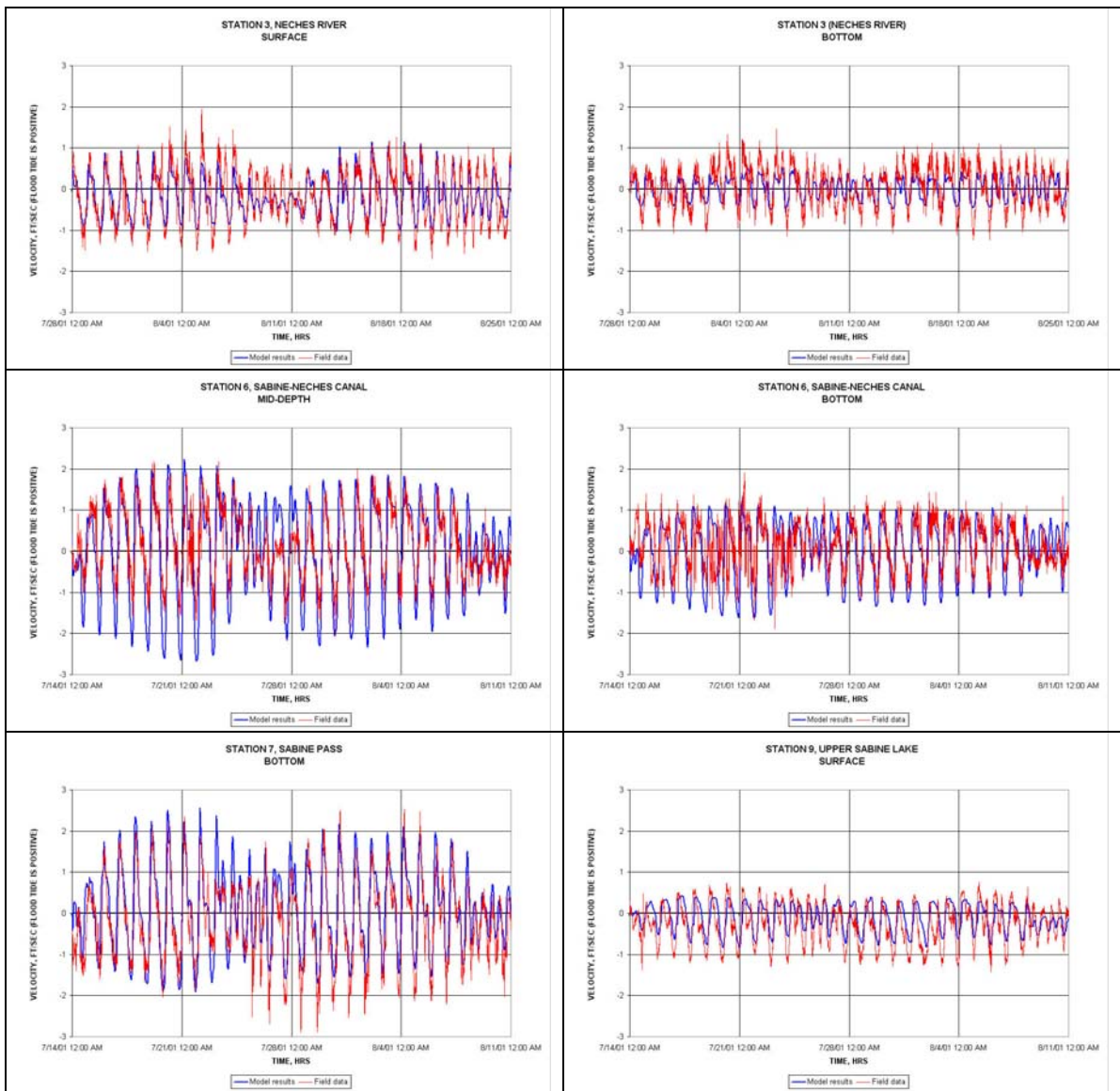


Figure 17 Velocities at Stations 3, 6, 7 and 9

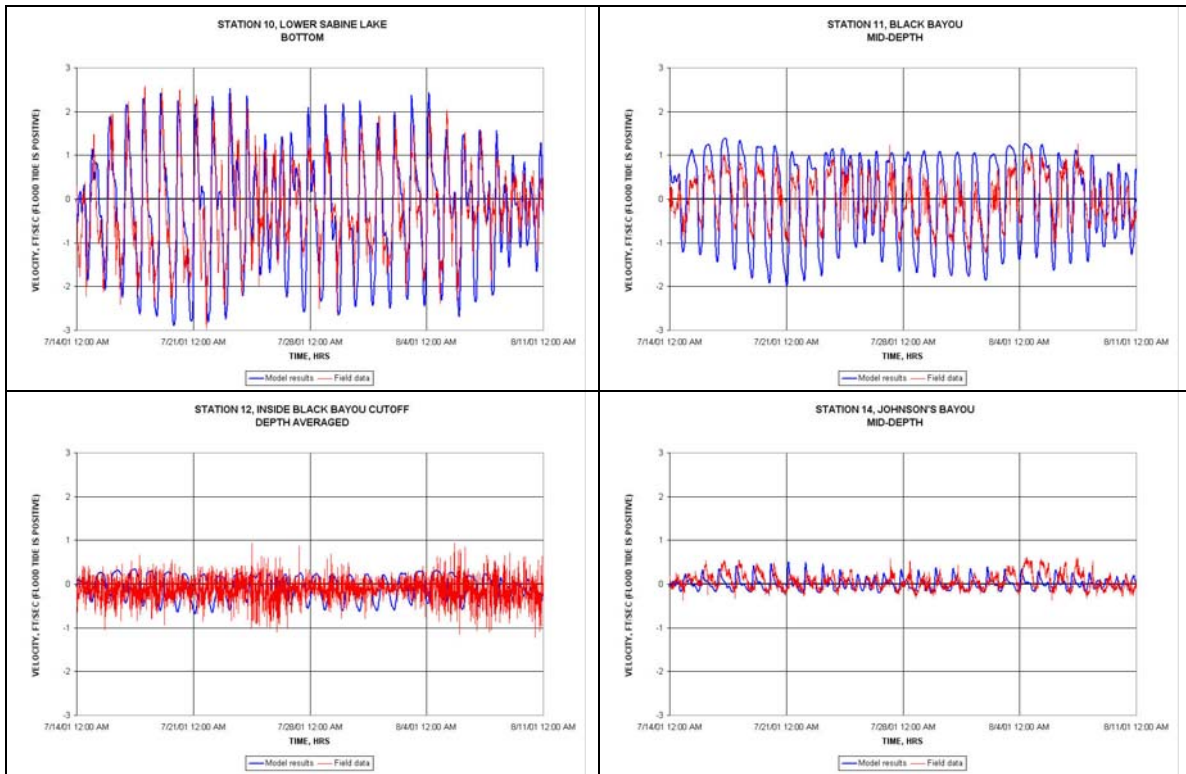


Figure 18: Velocities at Stations 10, 11, 12 and 14

### Salinity Data

The salinity observations for both the model and the field for the verification period are given in Figures 19-21. Any of the field data that was obviously corrupted by bio-fouling of the sensor was omitted from this comparison and analysis. Also, the field data has been filtered to remove noise in the signal. Signals with a period of 6 hours or less were omitted from the data set.

The figures contain field data, and 2 different sets of model results. The results given in blue represent the results obtained from the model with the horizontal mixing coefficients determined by the method of Smagorinsky (“low channel diffusion” in following tables). The results given in green are results that are determined by a model run where the horizontal mixing coefficient in a portion of the Sabine-Neches canal is elevated dramatically (“high channel diffusion” in following tables).

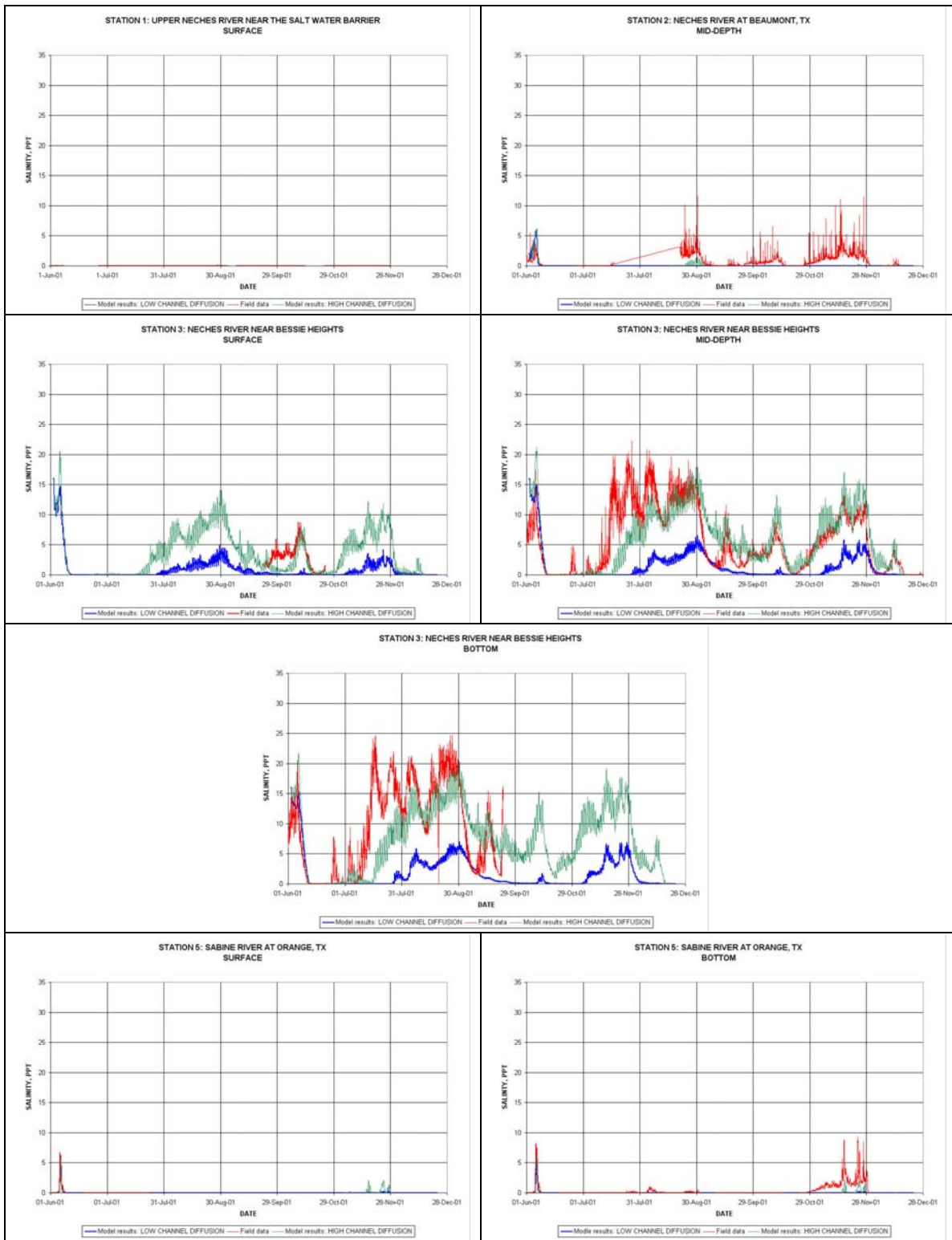


Figure 19: Salt Comparisons for Stations 1, 2, 3 and 5

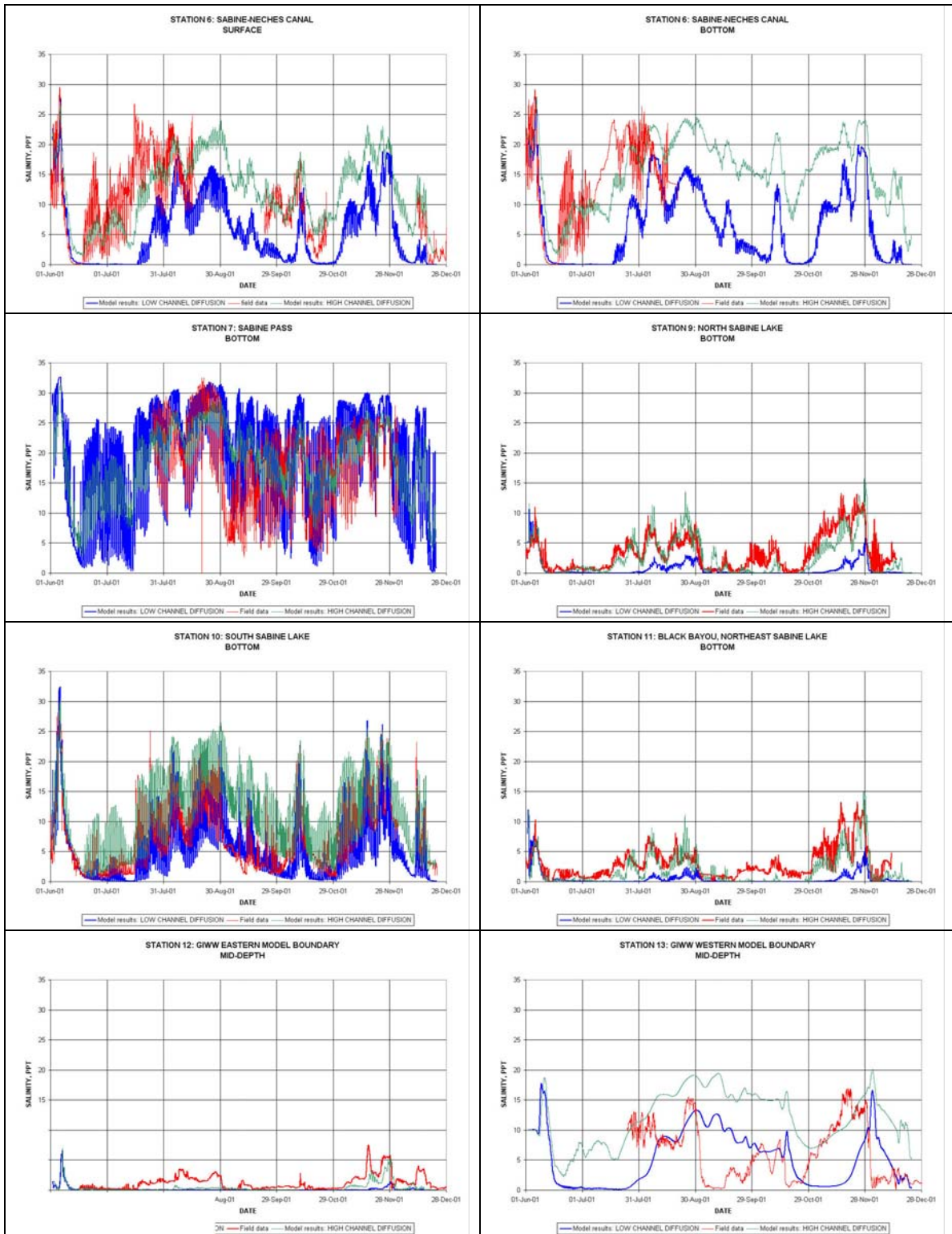


Figure 20: Salt Comparisons for Stations 6, 7, 9, 10, 11, 12, and 13

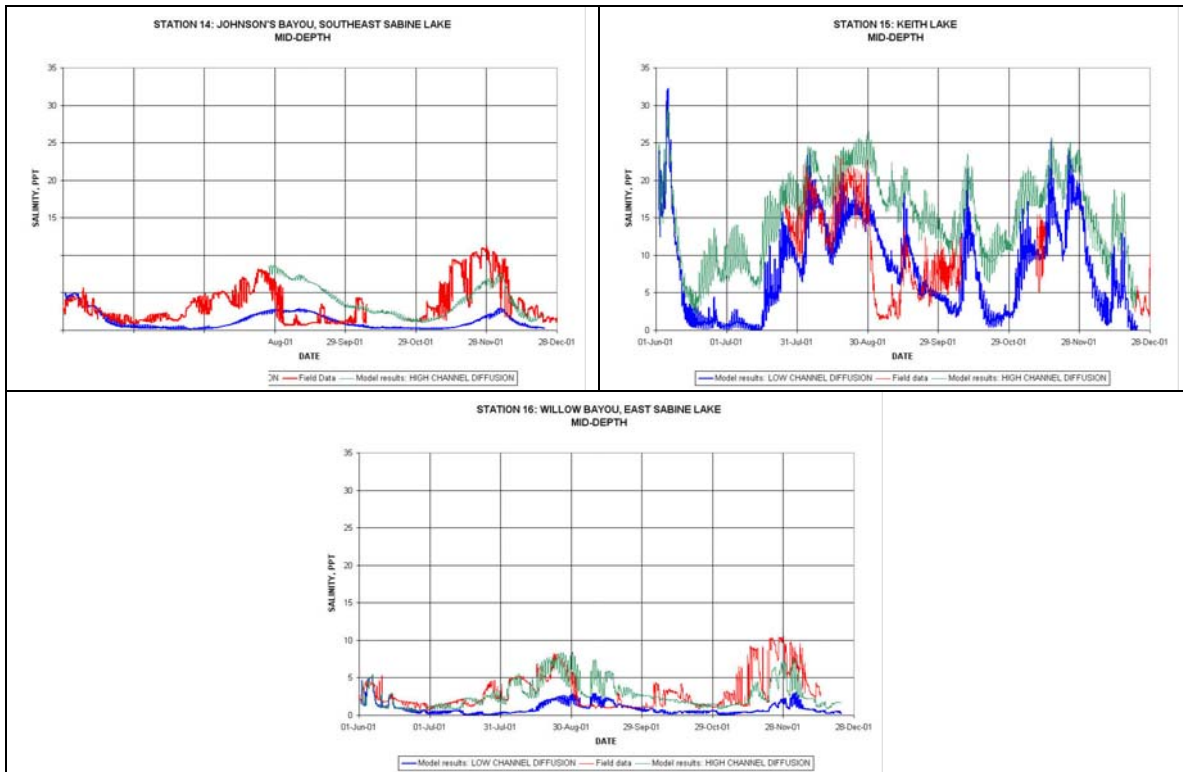


Figure 21: Salt Comparisons for Stations 14, 15, and 16

The region of the canal over which the elevated horizontal mixing coefficient was applied is depicted in Figure 22. This was done to promote the transport of salt through the Sabine-Neches Canal. As was discussed in the calibration section, this is a non-physical adjustment, and has to be made with caution. The adjustment was applied only to that section of the SNWW south of the intersection with the Neches River. This was done so that the fidelity of the physical description of the system in the Neches and Sabine Rivers is still valid, and hence, changes due to modifications of the plan condition could still be investigated.

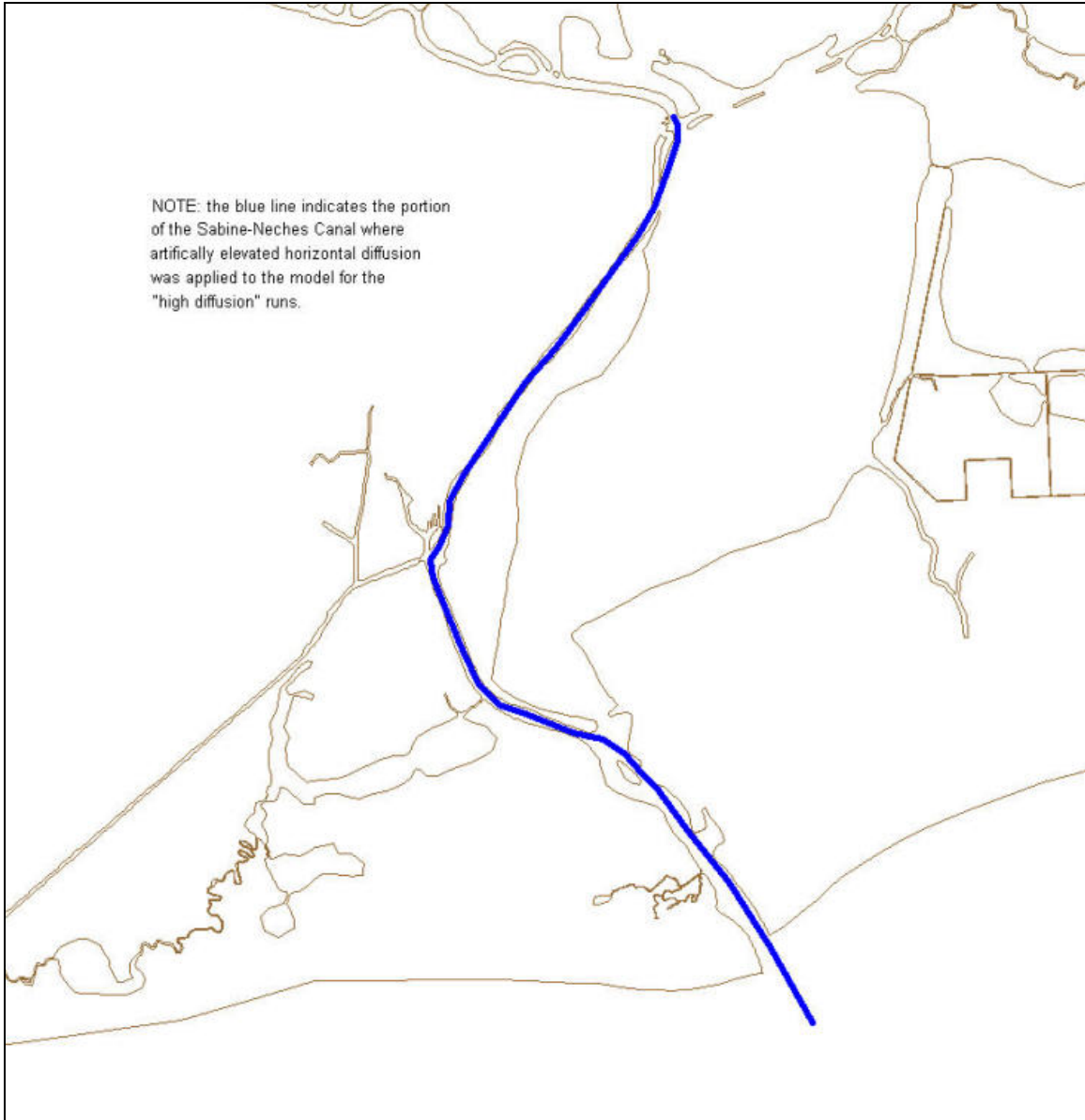


Figure 22: Portion of the Sabine-Neches Canal with Artificially Elevated Horizontal Diffusion

Since this diffusion adjustment represents a non-physics based contribution to the model, it introduces an additional uncertainty into the reliability of the model with respect to the evaluation of plan scenarios. Therefore, for all the plan scenarios, the model was run both with and without the high diffusion adjustment, and the run that yielded the largest change at a given location was generally used to define the salinity impact at that location. The high diffusion version yielded the largest change at nearly all locations and it was, therefore, used to define salinity impacts over the vast majority of the study area. However, the low diffusion version was used to predict salinity impacts for areas adjacent to the SNWW south of the GIWW where the low diffusion verification results were closer to field data than high diffusion results. This represents a conservative approach to impact assessment, and is intended to ensure that the additional uncertainty introduced by the artificially elevated horizontal diffusion does not result in assessments that underestimate the potential salinity impacts.

Overall, the model runs together yield predictions of salinity that faithfully replicate the response of the system to variations in freshwater inflow, wind, and tidal forcing. Of note are the Stations located in north and east Sabine Lake (Stations 9, 11, 14 and 16). The correlation between the model results and field data at these stations demonstrate the capability of the model to predict salinity variation at points far removed (hydraulically) from the source of salinity (i.e. from Sabine Pass). Hence, they implicitly demonstrate that the circulation patterns and the energy of the system are well represented in the model.

The reason for the inability of the model to accurately simulate the salt transport into the system (without artificial adjustment of the horizontal mixing) is not known with certainty. However, the two most likely factors are as follows:

- The model is overly diffusive with respect to the salinity stratification. The model does indeed simulate stratification, and the degree of stratification is on the order of that observed in the field (see Figure 23 for an example of the salinity stratification in the Neches River over one tidal cycle). However, the salt wedge interface is potentially much sharper in the field than in the model (i.e. the gradient occurs over a shorter vertical length). This, in turn, would result in a greater net upstream momentum of the salt wedge in the field than is observed in the model.
- The model does not drain as effectively as the actual system in the field. The hydraulic outlets available to flood waters in the field are far more numerous than those included in the model. Therefore, the fresh water inputs to the system would tend to have a greater impact on the salinity in the model than they do in the field. This is especially pertinent for the specific simulation period shown here. In early June of 2001, Tropical Storm Allison contributed over 2 feet of rain to the system, as well as significant flood flows in the rivers (see the rainfall and inflow boundary conditions). The consequent overland flooding that was observed in the field after this event is not represented in the model, since the land surface is not incorporated into the domain. In the model, all of this water must be contained in the defined flow pathways, and must exit the domain either through Sabine Pass, or through the GIWW East or West boundaries. Therefore, the potential exists for much higher residence times for this fresh water flood flows in the model than in the field, and this in turn serves to mitigate the salinity intrusion to a much greater degree in the model than in the field.

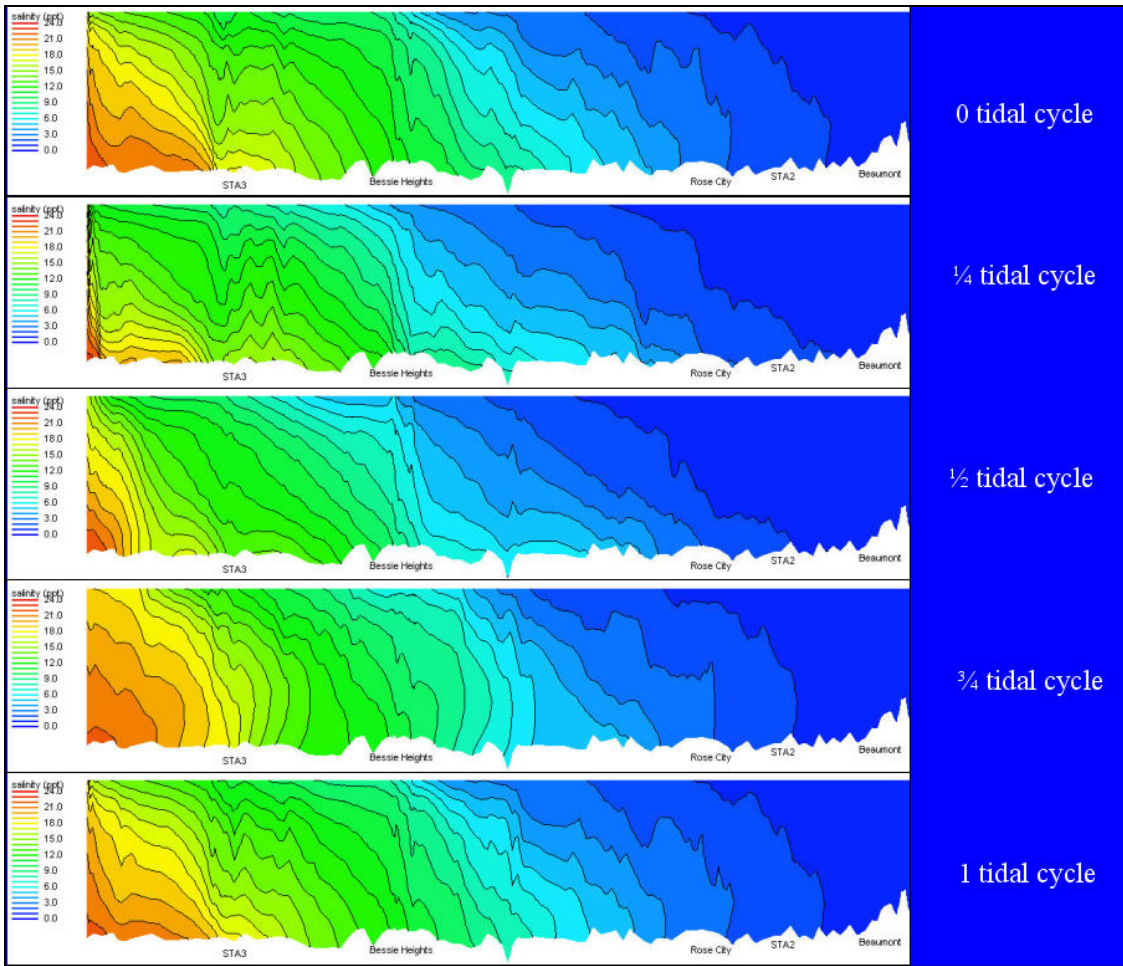


Figure 23: Plot of Salinity Stratification in the Neches River over 1 Tidal Cycle.

## Salinity Sensitivity to the GIWW East Outflow

The outflow defined for the GIWW is not based on observed data, but rather based (primarily) on engineering judgment. In order to determine the influence of this uncertainty on the model salinity, a sensitivity test was conducted. The model was run with the standard applied output of the GIWW East, and also with the applied outflow doubled at the GIWW East. The salinity impacts of the doubled GIWW East outflow at several stations are shown in Figure 24. Note that the impact is significant, even in the Neches River. This demonstrates the complexity and interconnectedness of the system.

It is tempting to maximize the outflow at the GIWW East, since this tends to drive the observed salinity in the model closer to the observed salinity in the field. However, all available observational evidence suggests the outflow defined for this study is likely about right, if not a little high (see the Discharge at Range 10, in Figure 16). Therefore, without supporting observational evidence, an increase in this applied discharge is unwarranted.

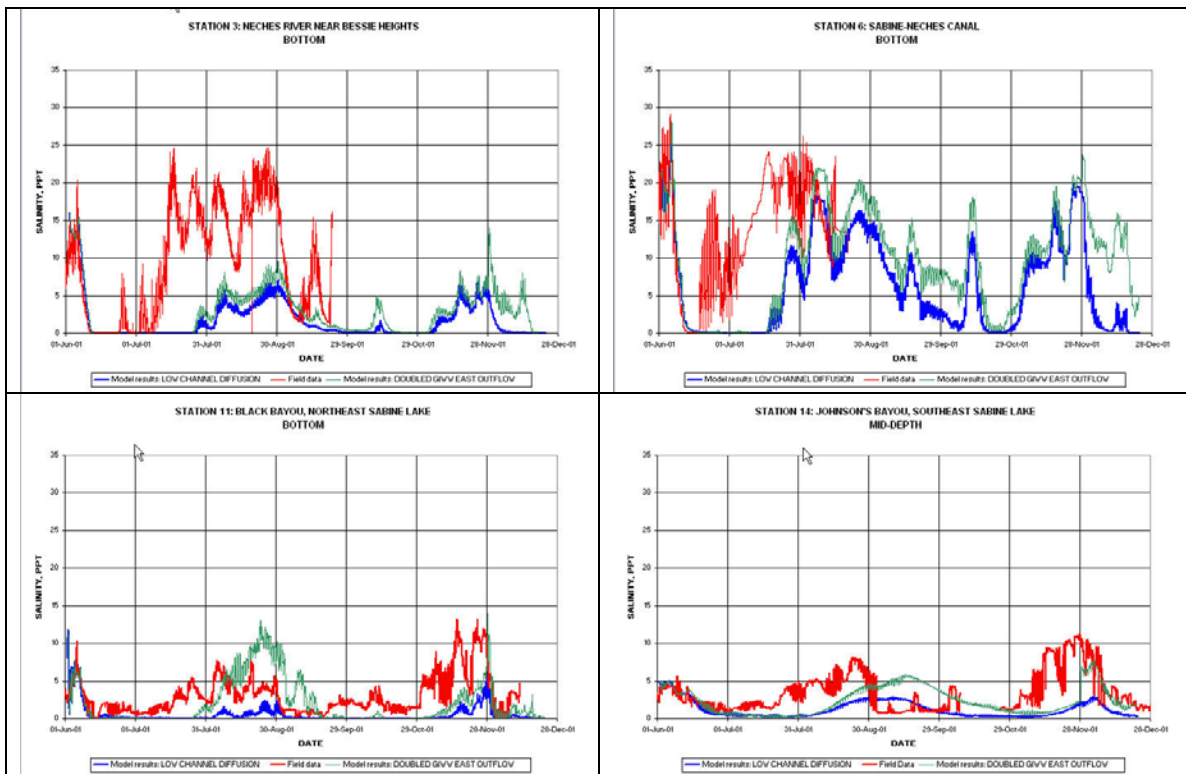


Figure 24: Salt Sensitivity (Due to Doubled GIWW East Outflow) at Stations 3, 6, 11 and 14

# Model Analysis of the Impacts of Proposed Channel Deepening and Widening

This chapter contains the results of model simulations design to assess impacts to both salinity and storm surge inundation that would result from implementing a 48-foot channel deepening project.

## Description of Proposed Channel Deepening and Widening

The recommended plan for the proposed SNWW 48-Foot project consists of deepening the existing navigation channel from 40 to 48 ft to the Port of Beaumont, extending the existing entrance channel into the Gulf of Mexico, widening the existing channel to provide for two-way navigation from Sabine Pass to the junction with the Taylors Bayou turning basin in the vicinity of Port Arthur, bend easings on the Sabine-Neches Canal and Neches River channel, deepening and widening of the Taylors Bayou navigation channel and turning basins, and the addition of new anchorages/turning basins on the Neches River channel. Table 3 gives the proposed changes to the project depth. Figure 25 shows the extents of the modified channel.

It should be noted that the project was originally modeled as a 50' channel because this depth would capture impacts for the three alternatives (45', 48', and 50') considered during final screening. The 48x700-foot alternative was modeled when it was identified as the NED Plan. When results from the modeling of the 48' and 50' channels are compared, the difference in impacts at each of the observation points does not exceed the standard deviation of the salinity differences observed at those points. Therefore, the impacts from the 48' channel are not significantly different from the impacts of the 50' channel.

**Table 3. Proposed Specifications for the 48-Foot Channel Deepening Option**

REACH (EXISTING STATIONS)	BOTTOM WIDTH (FT)	PROJECT DEPTH (MLT)	ADVANCE MAINTENANCE ADDED (FT)	ALLOWABLE OVERDEPTH (FT)	TOTAL DEPTH (MLT)
EXTENSION CHANNEL	700	50	2	2	54
SABINE BANK CHANNEL	700-800	50	2	2	54

SABINE PASS OUTER BAR	800	50	2	2	54
SABINE PASS JETTY CHANNEL	800-700	48	2	2	52
SABINE PASS CHANNEL	700	48	2	2	52
PORT ARTHUR CANAL	700	48	2	1	51
SABINE- NECHES CANAL	400	48	2	1	51
NECHES RIVER CHANNEL	400	48	2	2	52
NECHES RIVER CHANNEL	400	48	2	2	52
NECHES RIVER CHANNEL	400	48	2	2	52
NECHES RIVER CHANNEL	400	48	2	1	51
<b>TAYLORS BAYOU</b>					
ENTRANCE CHANNEL	275-678	48	2	1	51
EAST TURNING BASIN	370-547	48	2	1	51
WEST TURNING BASIN	350-550	48	2	1	51
CONNECTIN G CHANNEL	200-250	48	2	1	51
TAYLOR BAYOU TURNING BASIN	90-1233	48	2	1	51

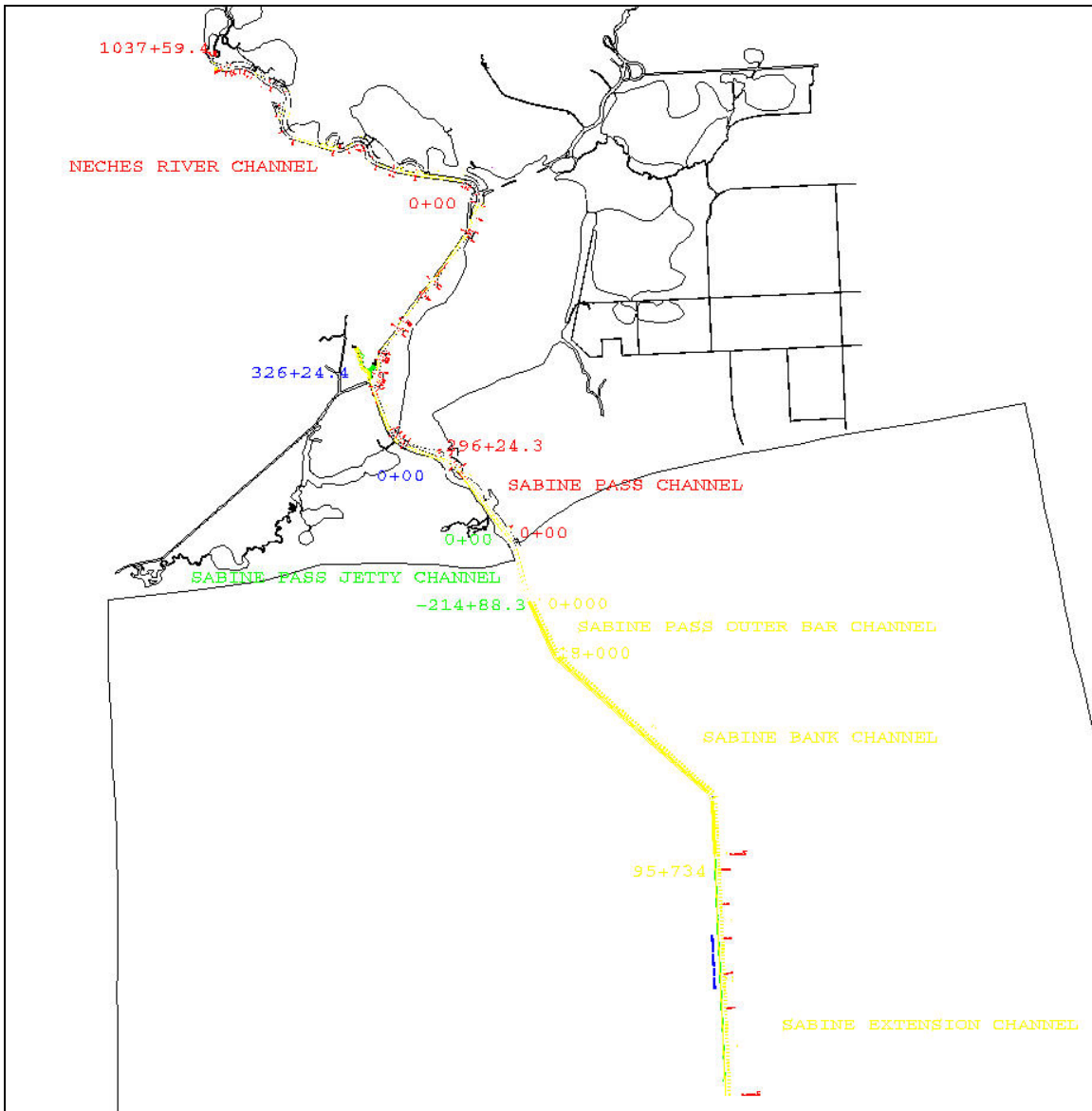


Figure 25: Proposed Extent of the Channel Deepening Project.

## Boundary Conditions for Analysis of Channel Deepening Impacts

### Salinity

The boundary conditions used to assess the salinity impacts were chosen to be representative of two separate freshwater inflow conditions: median inflow and low (10<sup>th</sup> percentile) inflow. These conditions were derived from a statistical analysis of inflow records conducted by the Texas Water Development Board. The data represent flow records spanning the period 1941-1997. This data was distributed to each of the 3 major freshwater sources to the system: The Sabine River, the Neches River, and Pine Island Bayou. The flow was distributed according to the statistical proportion of total inflow associated with each tributary. Figure 26 depicts the low

inflow hydrographs, and Figure 27 depicts the median inflow hydrographs.

The low inflow runs were run for 5 months, with the first 2 months used as spin-up. The spin-up period is used to allow sufficient time for the system to reach dynamic equilibrium with respect to salinity concentration. It is not included in the analysis. Therefore, the low inflow analysis is conducted only for the final 3 months of the simulation period. This represents roughly the period from August through October.

The median inflow runs were run for 7 months, with the first month used as spin-up (i.e. 6 months are used for analysis). This represents roughly the period from April through September. The median flow runs only require 1 month of spin-up because the higher inflows result in lower average residence times in the system, which in turn correlates directly to the required spin-up time.

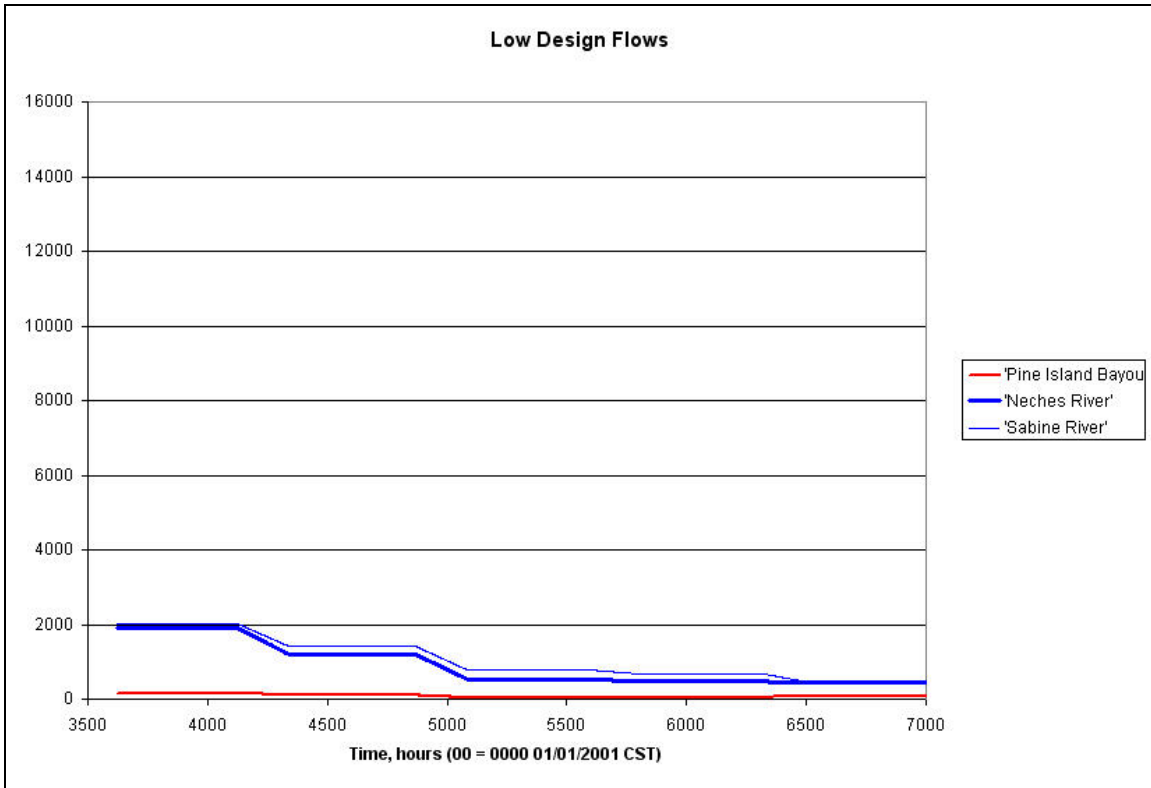


Figure 26: Low Inflow Hydrographs

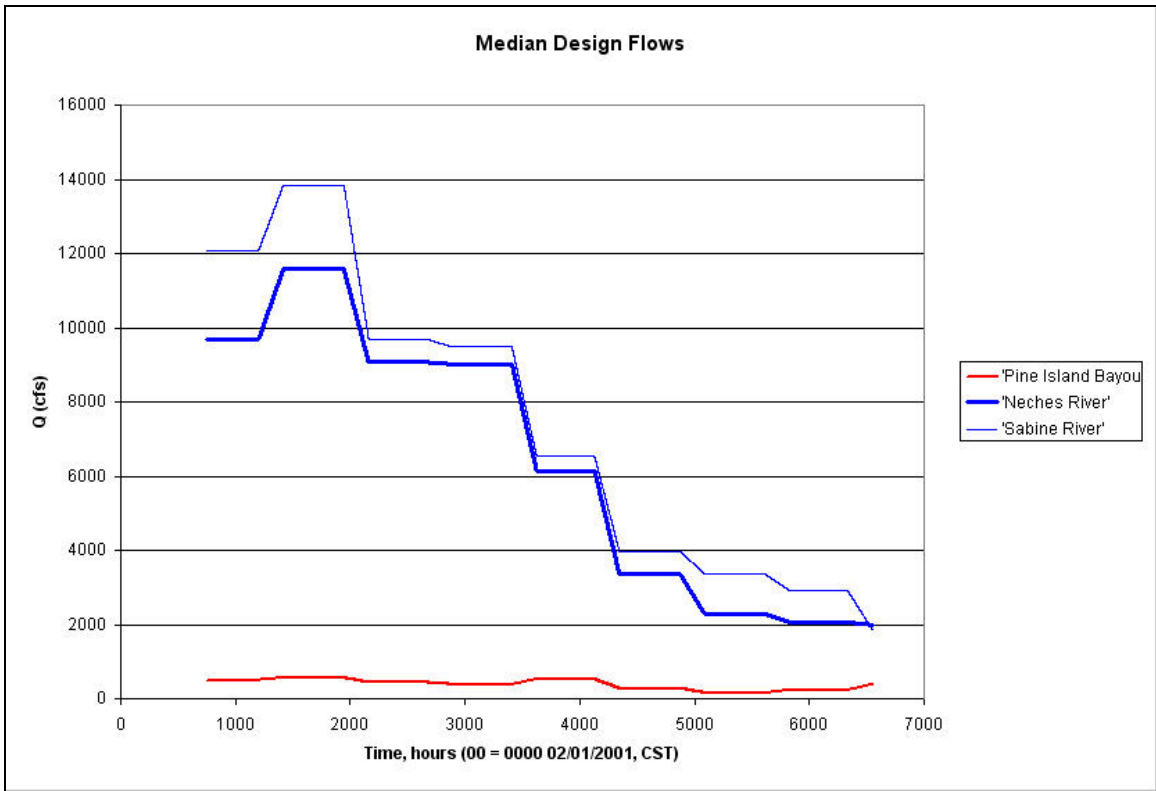


Figure 27: Median Inflow Hydrographs

Statistical correlations were also used to generate applied rainfall and evaporation hydrographs for the low and median flow runs. These are given in Figures 28 and 29.

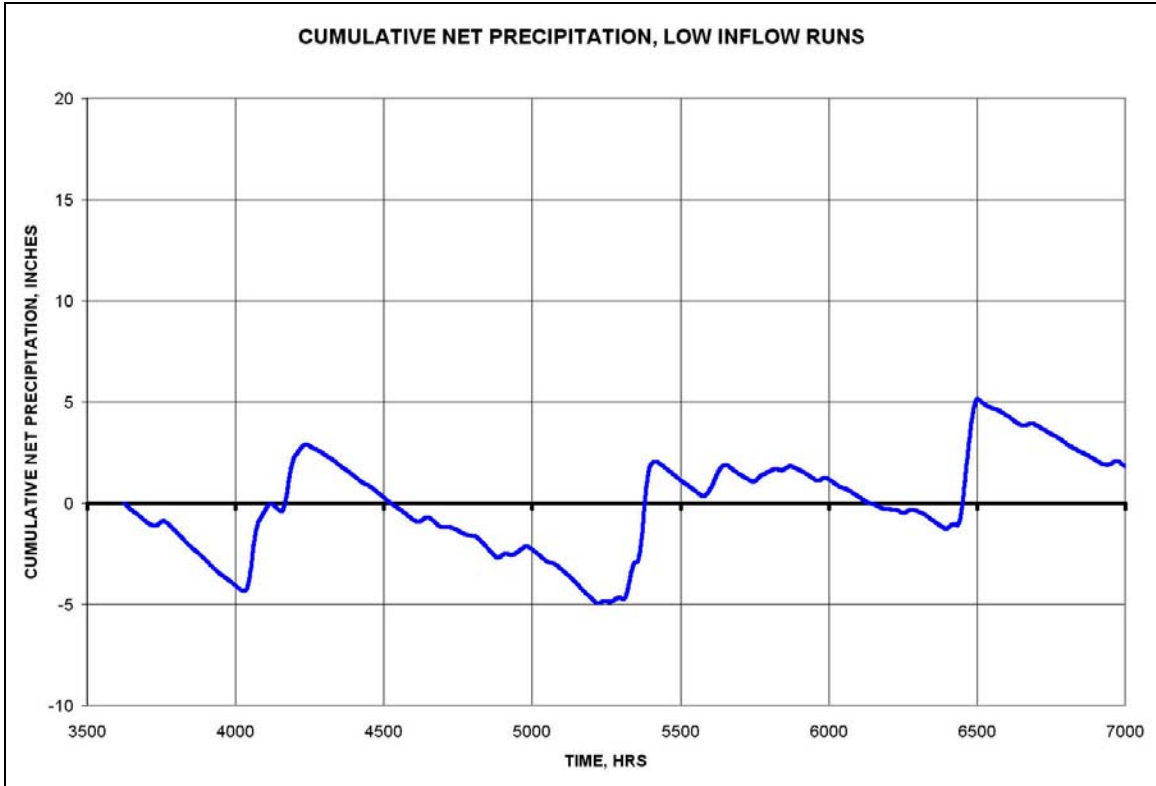


Figure 28: Low Inflow Cumulative Net Precipitation

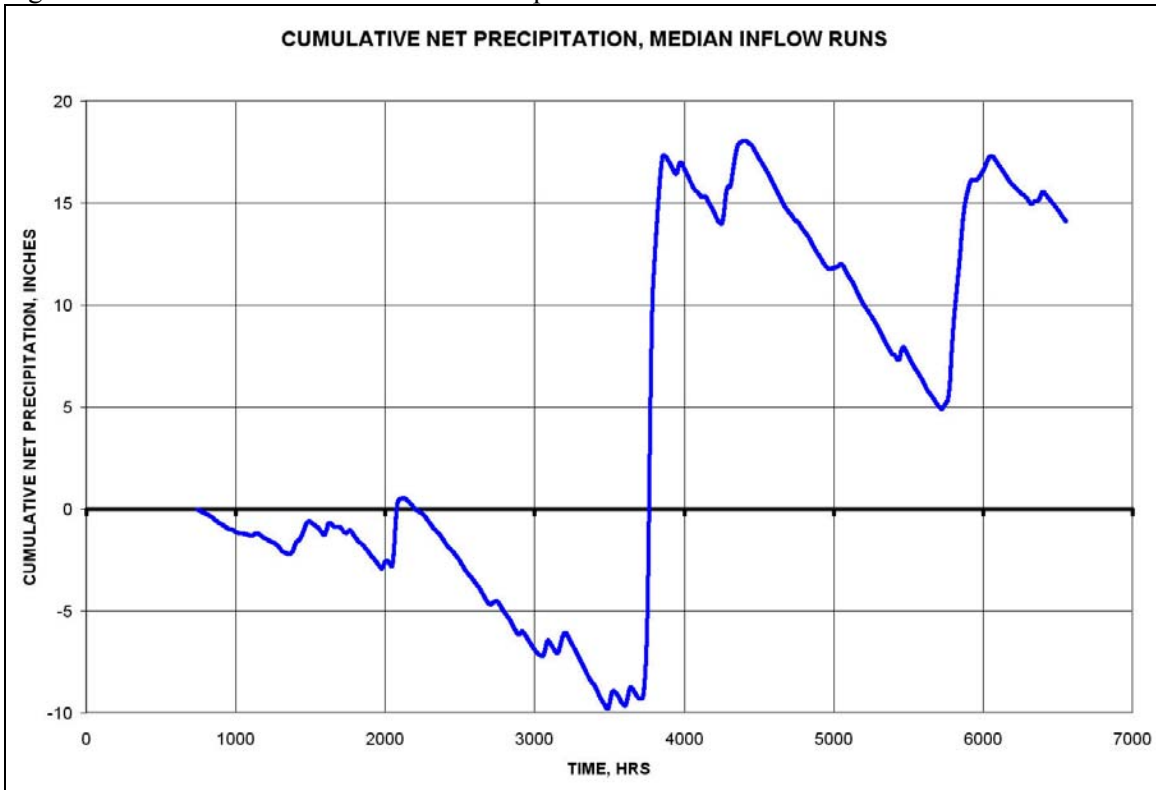


Figure 29: Median Inflow Cumulative Net Precipitation

The applied outflow at the GIWW East and West boundaries are governed by Equations 1 and 2.

using the low and median river inflows as input to the equations. The tide and wind conditions are the same as those used over the verification period.

## Storm Surge

In order to simulate the impact of the channel deepening project on storm-surge inundation, a boundary tidal signal was generated that was taken from the tidal signal recorded at Sabine Pass during Tropical Storm Frances, which hit the Texas Coast on September 11<sup>th</sup>, 1998. This signal is given in Figure 30. The rivers were assigned constant inflows, which represent moderate inflow conditions (4000 cfs on the Neches River, 5000 cfs on the Sabine River).

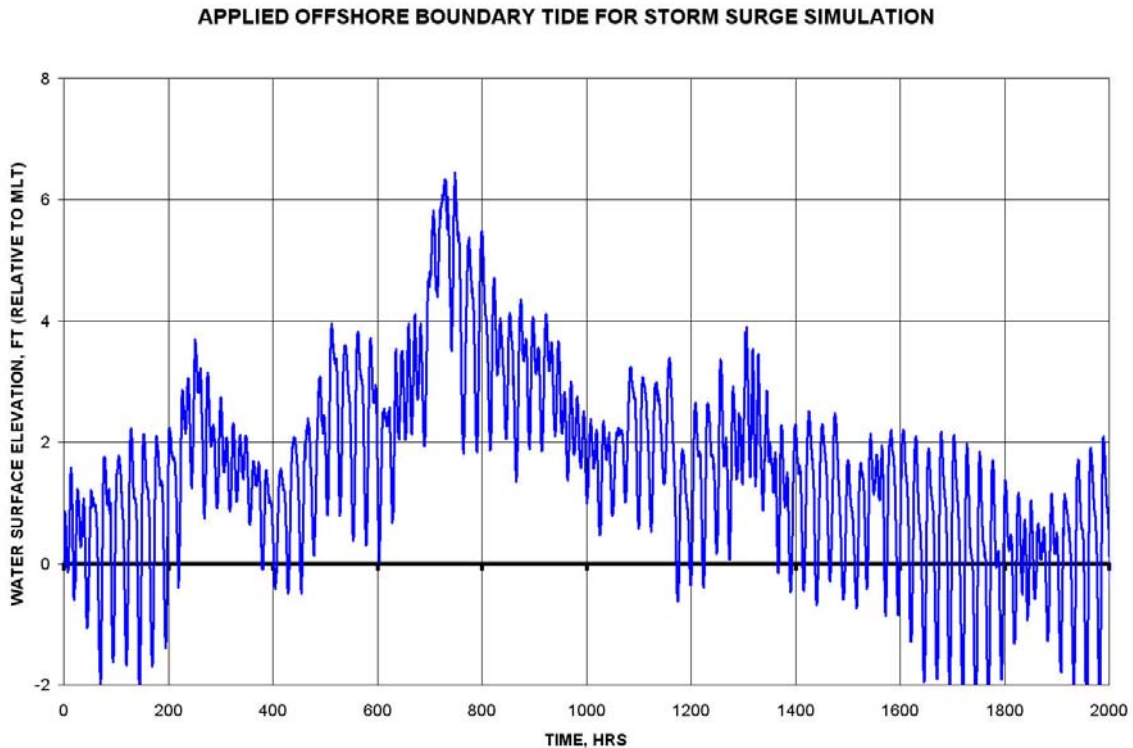


Figure 30: Applied Offshore Boundary tide for Storm Surge Simulation

## Results

### Velocity and Water Surface Elevation

The channel deepening and widening project results in some increased velocities in the study area. However, these increases are generally small (ranging from 0 to 20% increase in peak velocity). The largest changes are observed in the Sabine-Neches canal. However, it is not expected that increases in velocity in the canal will contribute significantly to erosion of the banks, since the principle cause of erosion at this location is vessel traffic.

The average water surface elevation is altered slightly by the widening and deepening. The water surface is lower by about -.05 feet at Sabine Pass. This due to an increased Venturi effect due to additional tidal flow in the Pass. The average water surface elevation is somewhat higher in the upper reaches of the model, with the highest elevation change observed in the upper reaches of the Neches river. This average elevation change is approximately +0.075 feet, or about 1 inch. This change likely results from the landward migration of the hydraulic backwater curve, resulting from an increase in the landward extent of the tidal propagation.

## **Salinity**

In order to perform the analysis of the impact of the channel deepening with respect to salinity, the model was run both with low channel diffusion and high channel diffusion (see the previous chapter). Generally, the largest impact (i.e. difference between base and plan simulations) was chosen as the predicted impact at that location. This yields a conservative estimate of impacts, relative to environmental concerns.

Figures 31-42 represent color contour plots of the average salinity values in both the base and plan runs. Also, a plot of the salinity difference (plan minus base) is given. Note that, for the median flow runs, the results are only averaged over 200 hours. This was done because the inflow is relatively high near the beginning of the simulation, so in order to show salinity values throughout the domain it was necessary to choose a period of time where the inflow was constant and somewhat low. The 200 hour period chosen is hour 5000-5200, which corresponds to a period in late July-Early August.

Figures 43 and 44 represent a statistical analysis of the salinity differences between base and plan at each of the salinity sampling stations used for the calibration and verification of the model. Included in this analysis is an additional station (Station 17) which is located in the GIWW west of the Sabine-Neches Canal, just west of the Taylor Bayou outfall.

Note that the salinity differences in all of the runs are most pronounced near the leading edge of the salinity intrusion. This is because the horizontal salinity gradients are high at this leading edge, and hence the additional intrusion facilitated by the channel deepening advances these high horizontal gradients further upstream.

For this system, this results in the highest salinity impacts in the following locations.

### Low Flow:

- Neches River, between Bessie Heights and Rose City (approximately 0.5-1.5 ppt)
- Sabine River (approximately 0-1 ppt)
- Eastern Shore of Sabine Lake (approximately 2-3 ppt)

### Median Flow:

- Keith Lake Fish Pass (approximately 2-4 ppt)
- Lower Sabine Lake (approximately 2-4 ppt).
- Sabine-Neches Canal (approximately 2-4 ppt).

Each of these locations corresponds to sensitive environments. This is especially true of the cypress-tupelo swamps on the Neches and Sabine Rivers; the eastern side of Sabine Lake, where Willow Bayou and Johnson's Bayou link the Lake to the Sabine National Wildlife Refuge (SNWR); and Keith Lake Fish Pass which links the navigation channel to the J.D. Murphree Wildlife Management Area.

Specific statistics were generated from the salinity analysis to support the Wetlands Value Assessment (WVA) ecological model (USFWS, 2002). The WVA requires input of “mean salinity” during the growing season for the assessment of impacts to brackish and saline habitats, and the "mean high salinity" statistic for impacts to fresh and intermediate habitats. The "mean high salinity" statistic is defined by the WVA as the average of the highest 33 percent consecutive salinity readings taken during a specified period of record. These statistics were provided to the Habitat Evaluation Workgroup of the SNWW ICT for use in predicting future-without project and future with-project conditions.

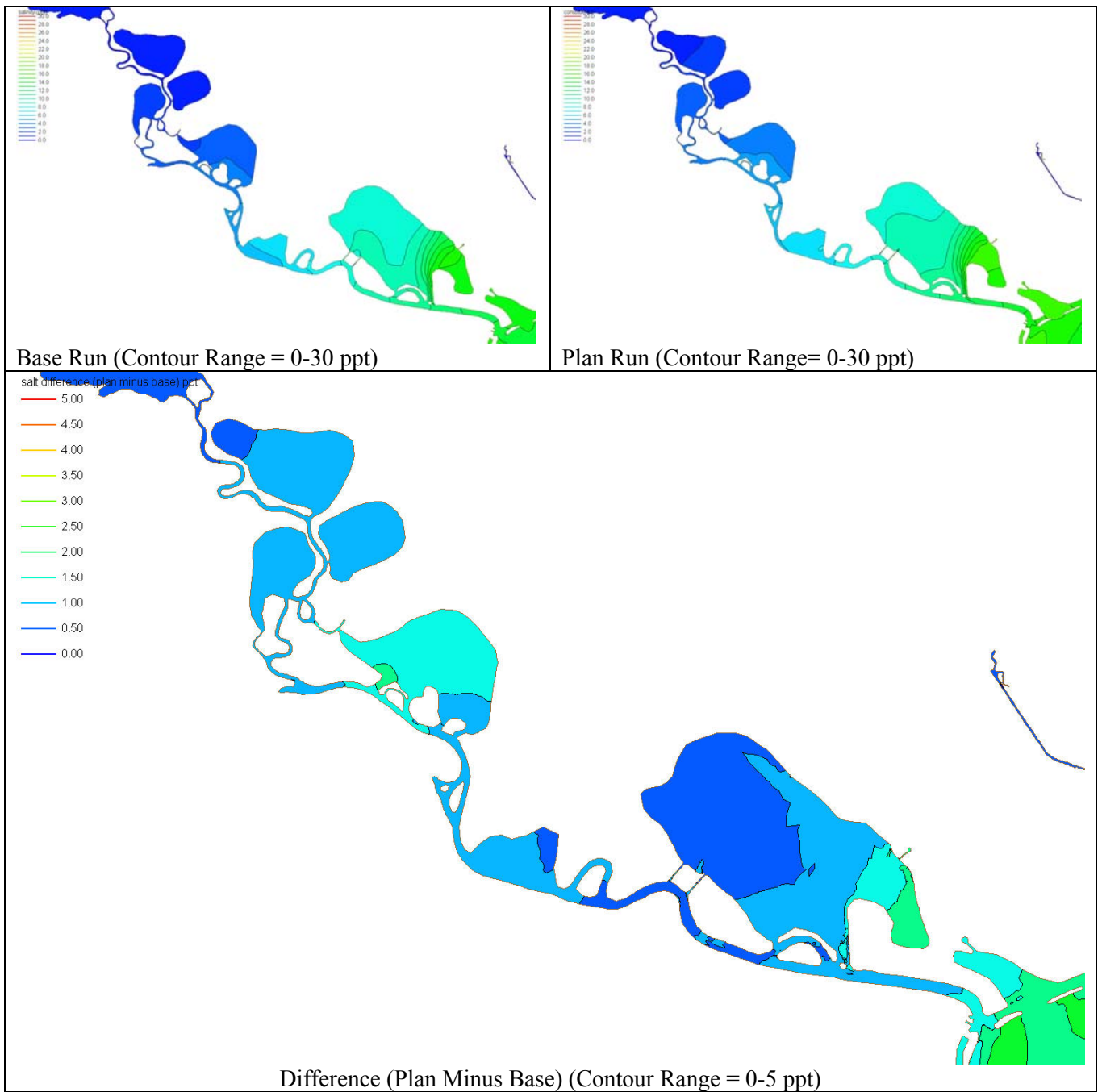


Figure 31: Average Base and Plan Salinity For the Low Inflow Condition, Low Channel Diffusion: Neches River

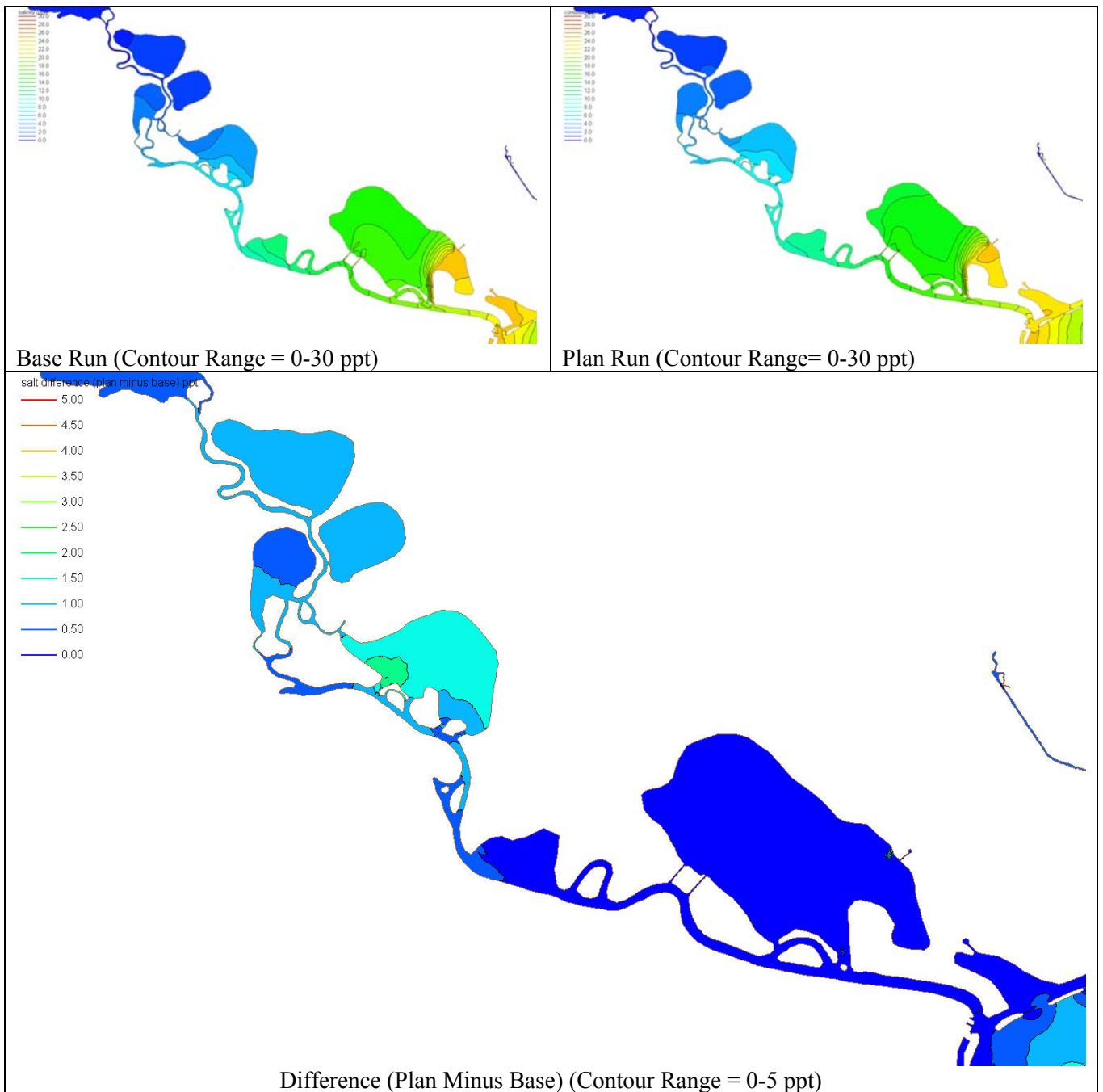


Figure 32: Average Base and Plan Salinity For the Low Inflow Condition, High Channel Diffusion: Neches River

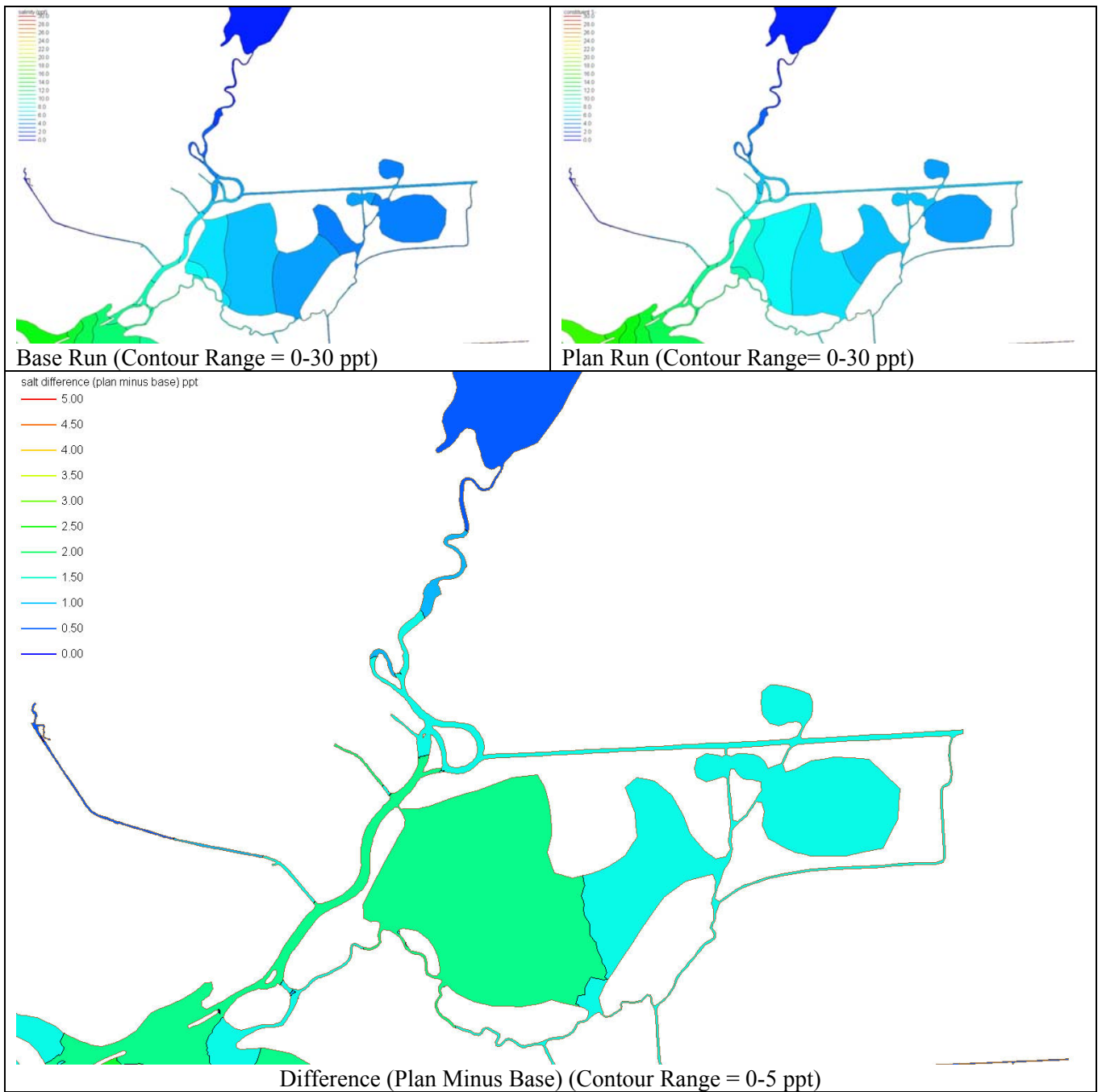


Figure 33: Average Base and Plan Salinity For the Low Inflow Condition, Low Channel Diffusion: Sabine River

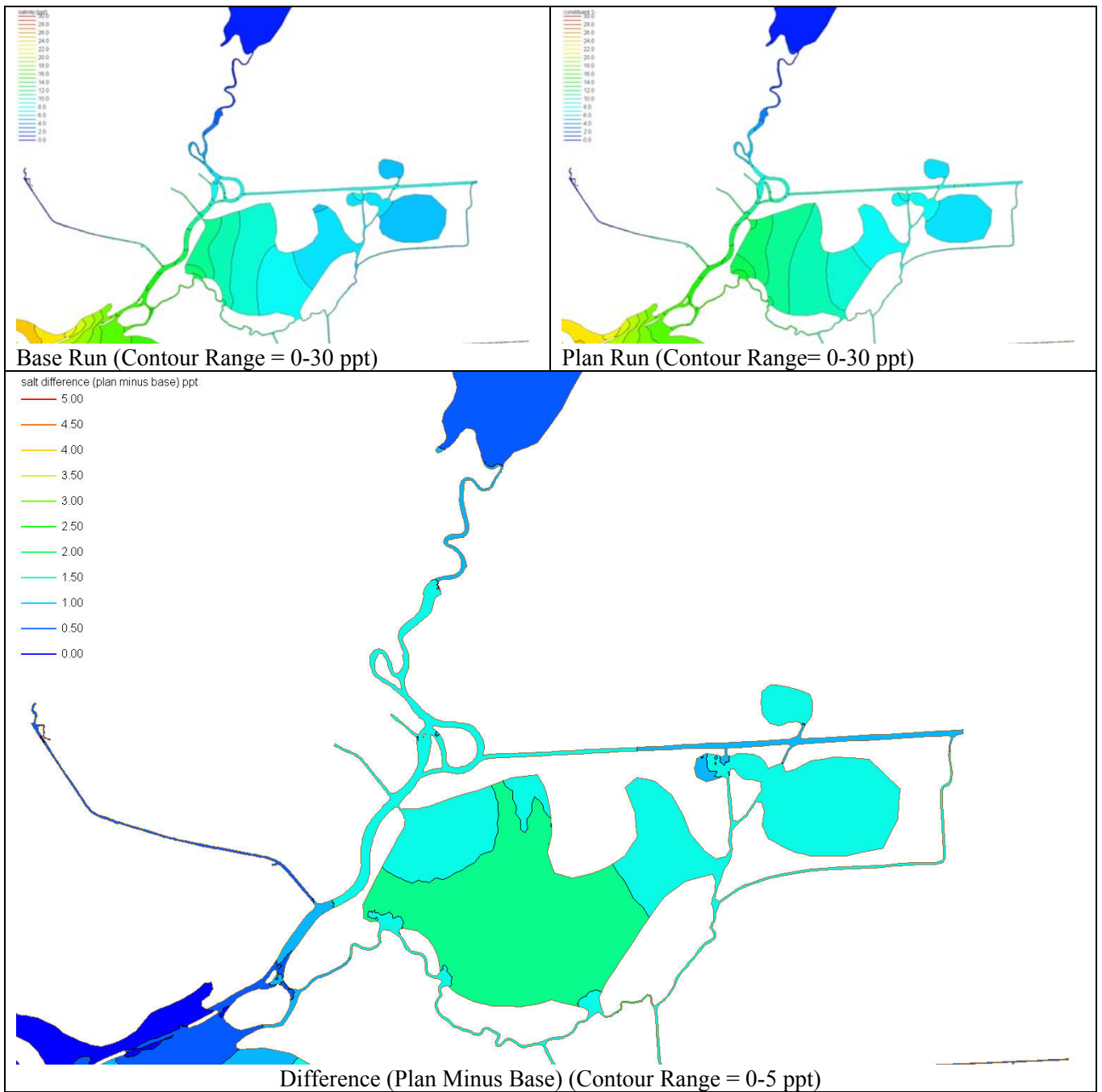


Figure 34: Average Base and Plan Salinity For the Low Inflow Condition, High Channel Diffusion: Sabine River

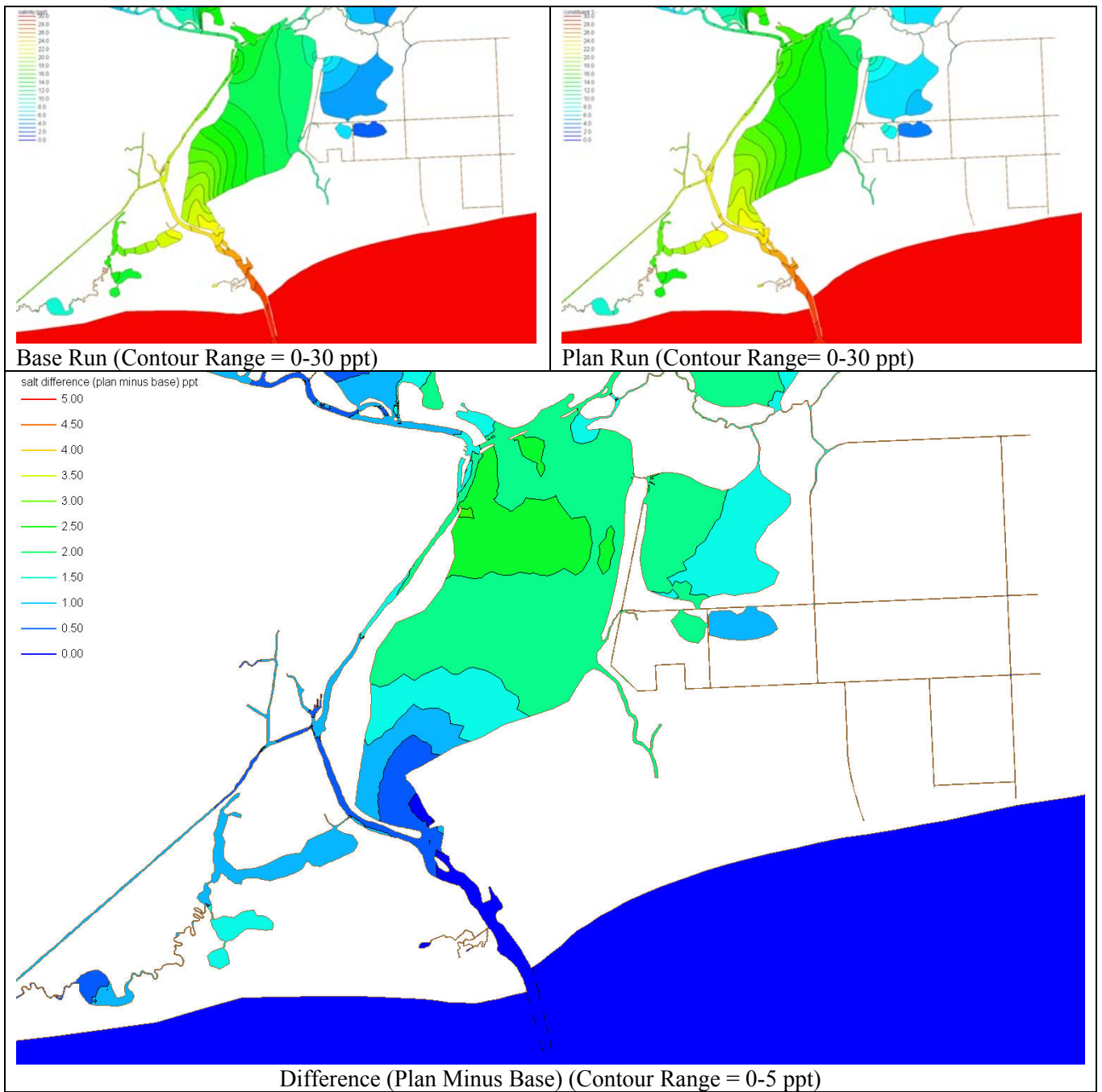


Figure 35: Average Base and Plan Salinity For the Low Inflow Condition, Low Channel Diffusion: Sabine Lake

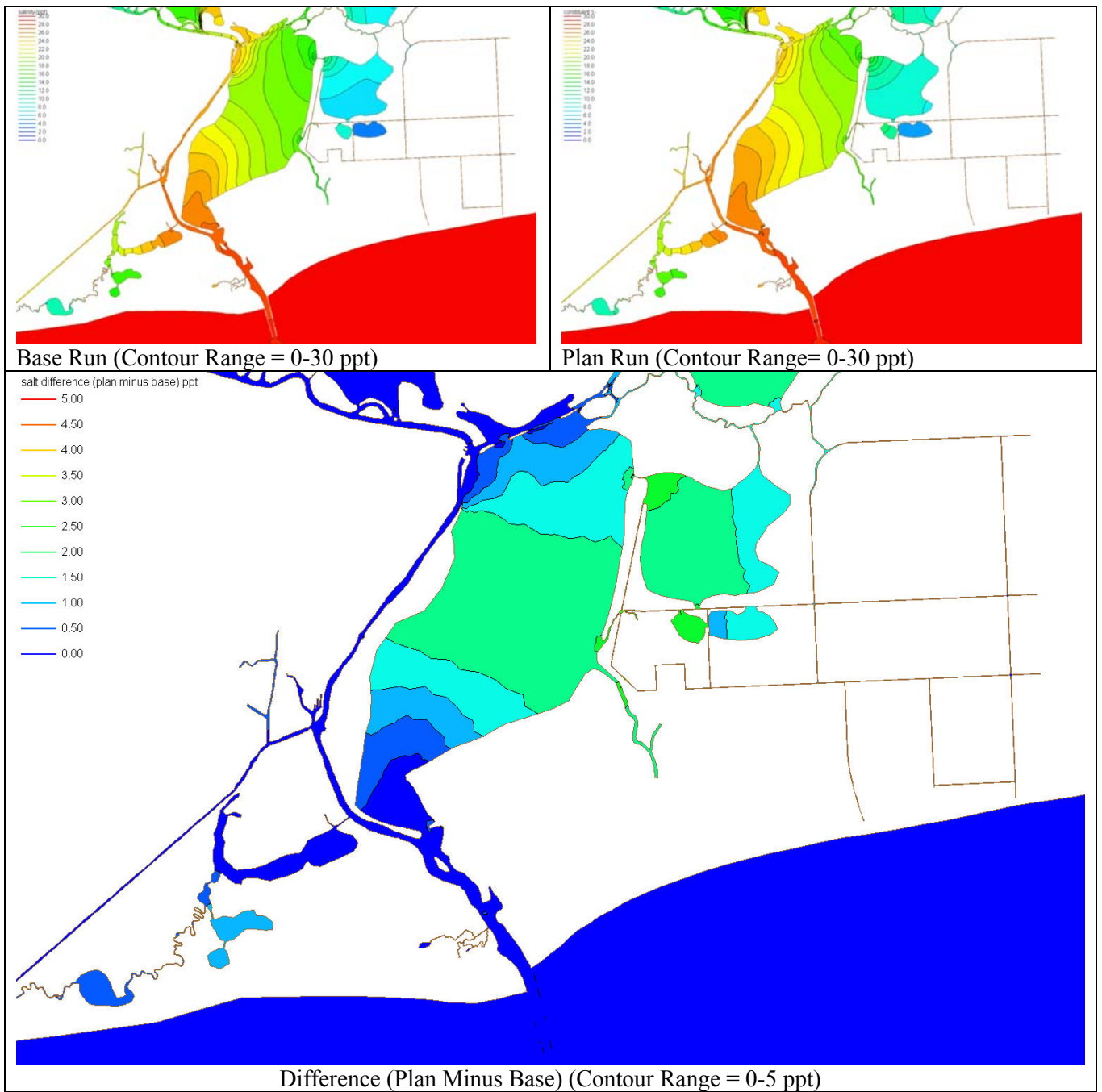


Figure 36: Average Base and Plan Salinity For the Low Inflow Condition, High Channel Diffusion: Sabine Lake

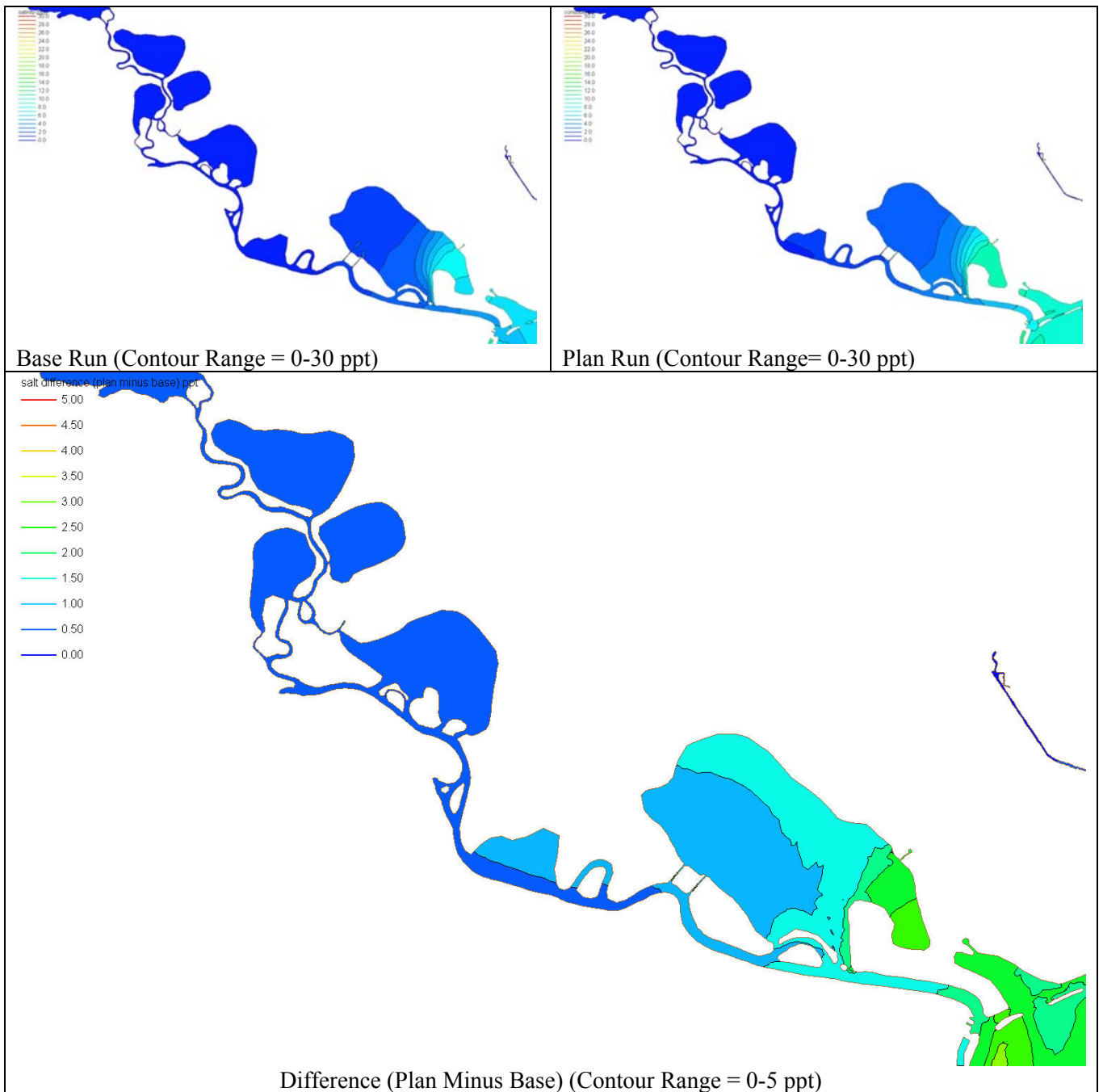


Figure 37: 200-Hour Average Base and Plan Salinity For the Median Inflow Condition, Low Channel Diffusion: Neches River

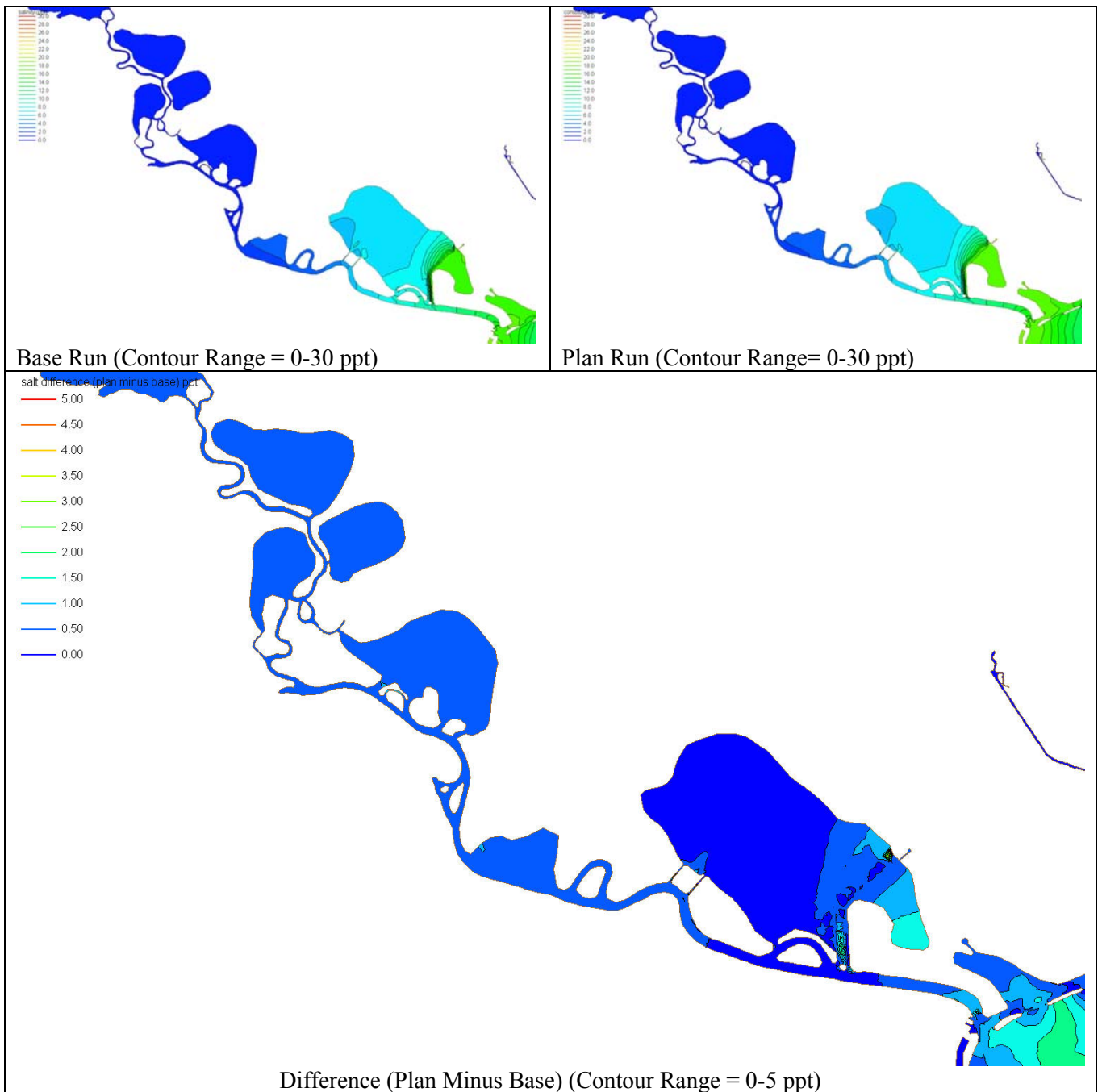


Figure 38: 200-Hour Average Base and Plan Salinity For the Median Inflow Condition, High Channel Diffusion: Neches River

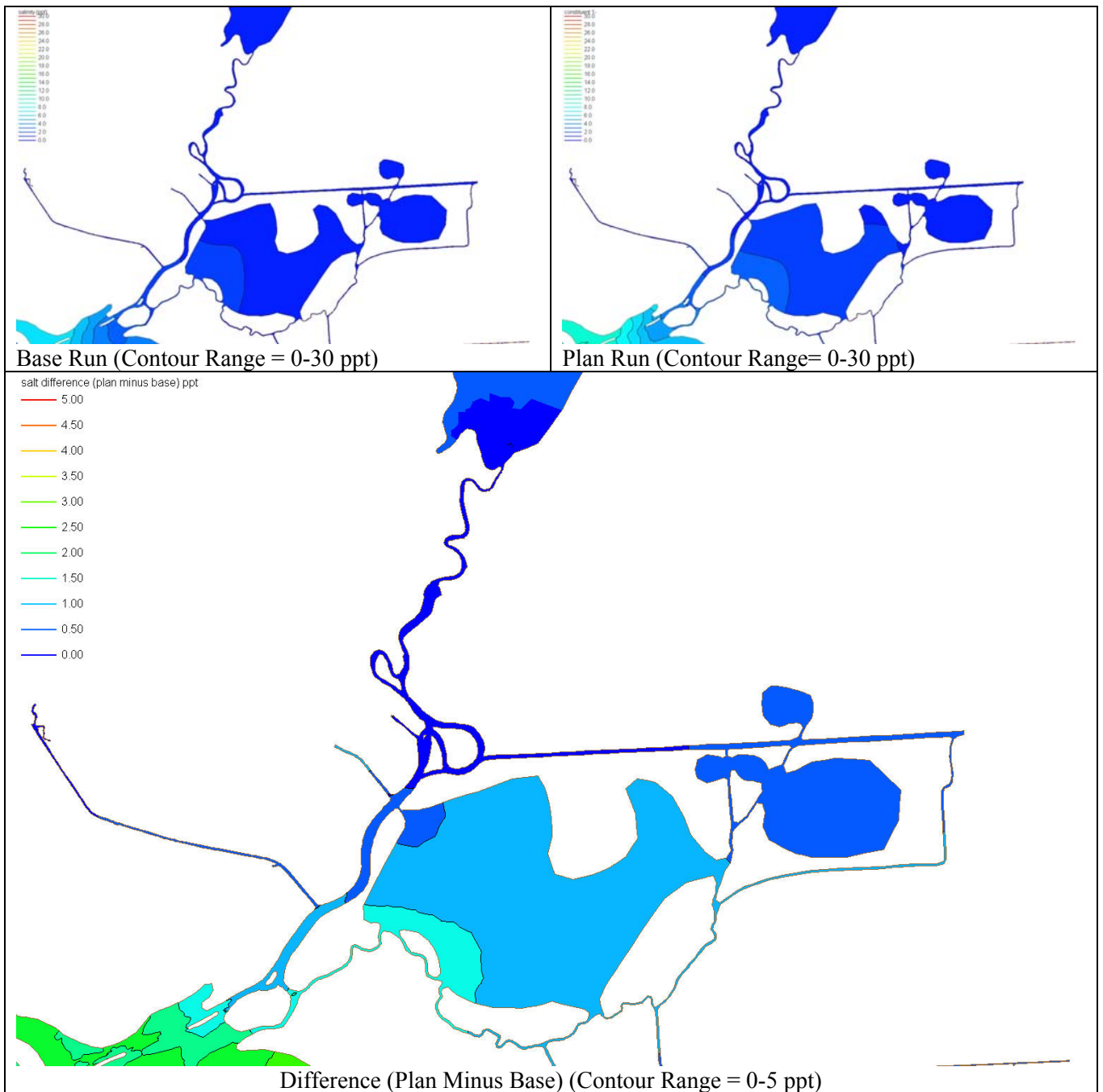


Figure 39: 200-Hour Average Base and Plan Salinity For the Median Inflow Condition, Low Channel Diffusion: Sabine River

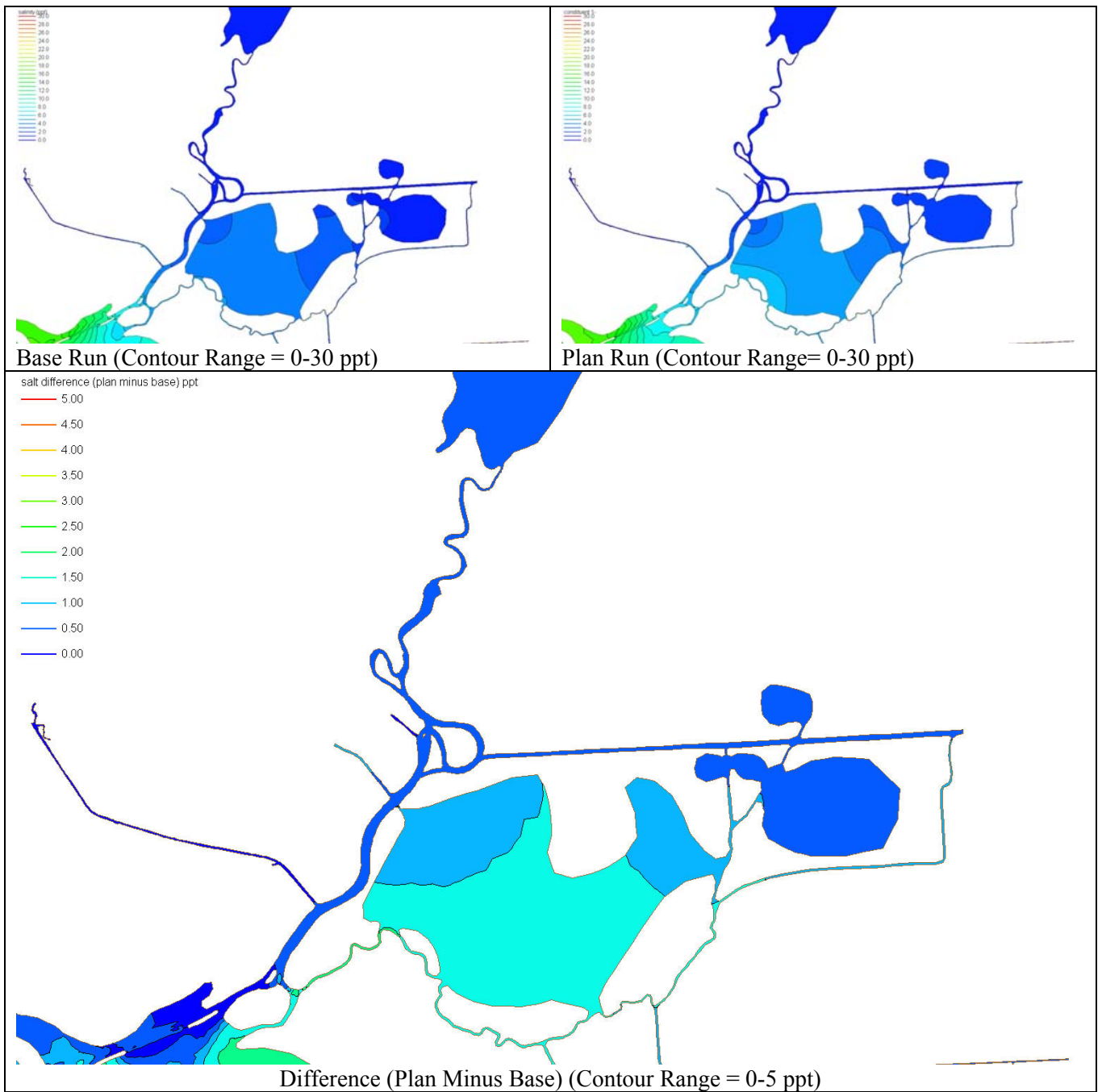


Figure 40: 200-Hour Average Base and Plan Salinity For the Median Inflow Condition, High Channel Diffusion: Sabine River

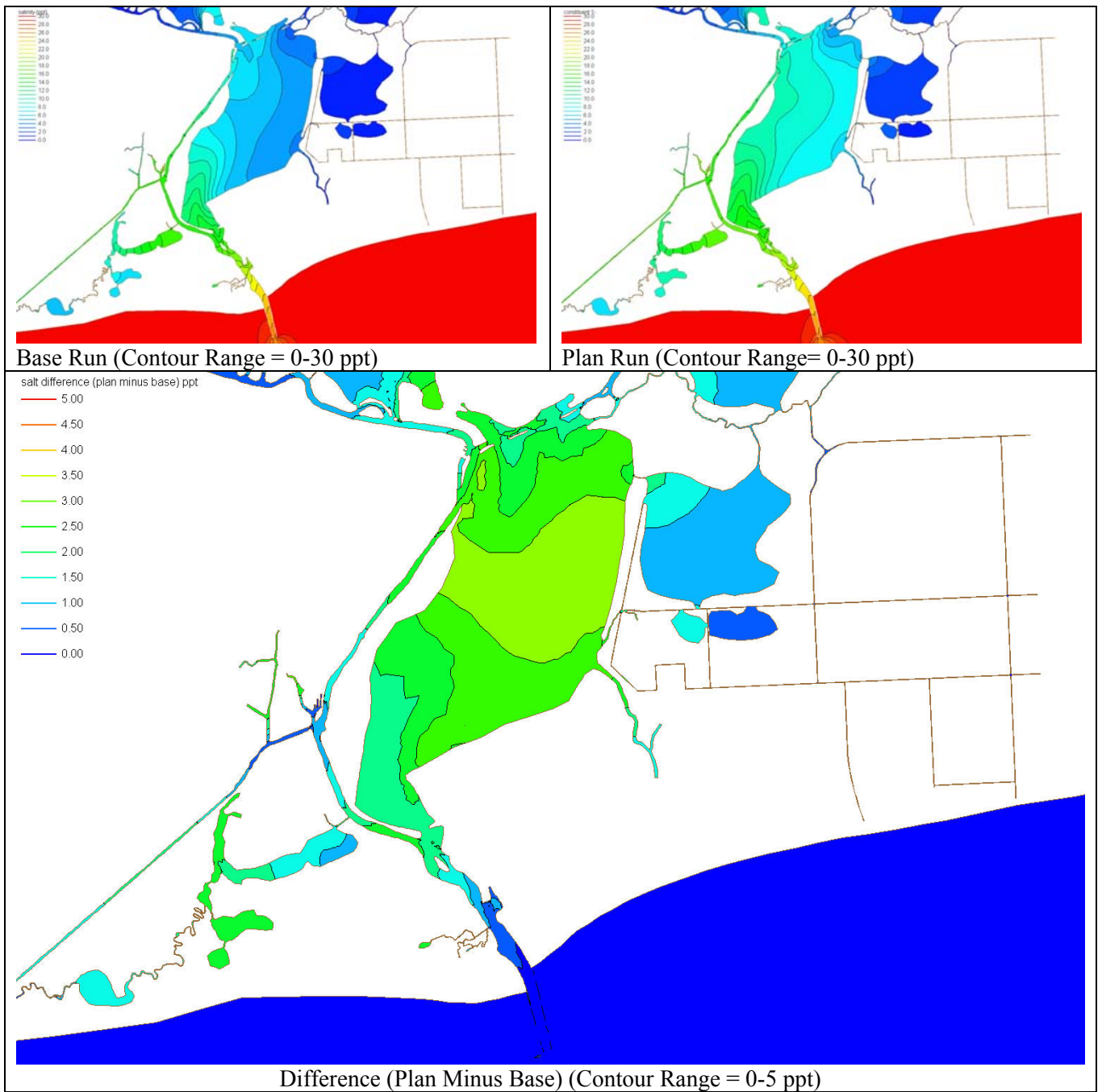


Figure 41: 200-Hour Average Base and Plan Salinity For the Median Inflow Condition, Low Channel Diffusion: Sabine Lake

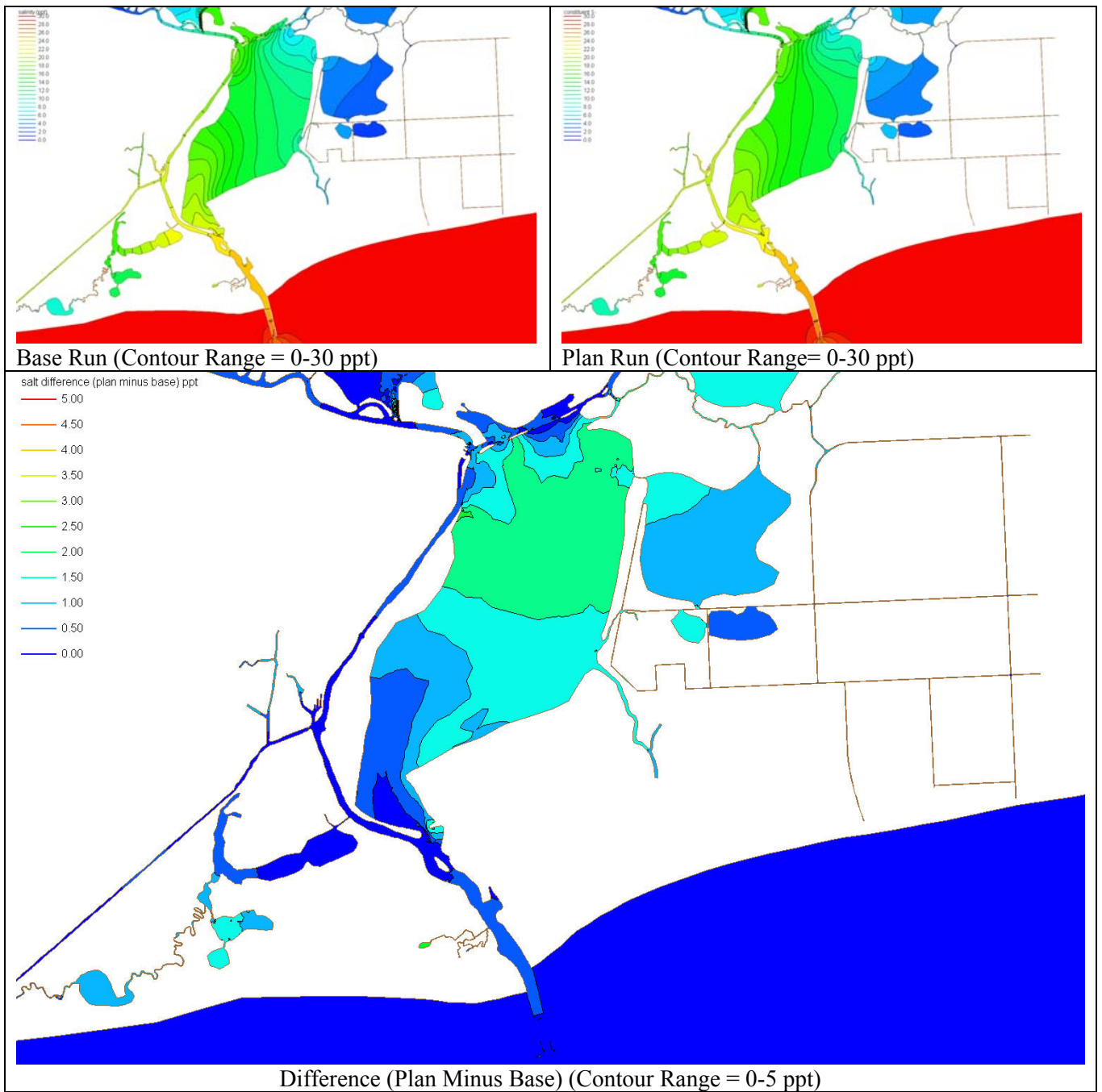


Figure 42: 200-Hour Average Base and Plan Salinity For the Median Inflow Condition, High Channel Diffusion: Sabine Lake

<b>LOW FLOW, LOW CHANNEL DIFFUSION, PLAN CHANNEL</b>													
AVERAGE DIFFERENCES													
STATION #	1	2	3	5	6	7	9	10	11	14	15	16	17
SURFACE SALINITY	0.45	1.10	0.67	0.70	0.96	-0.51	1.32	0.11	1.34	1.81	0.51	2.00	0.51
MIDDEPTH SALINITY	0.45	1.16	0.94	0.71	0.77	-0.10	1.32	0.13	1.33	1.80	0.55		0.48
BOTTOM SALINITY	0.46	0.79	0.98	0.71	0.71	0.07	1.32	0.13	1.33	1.80	0.55		0.47
STANDARD DEVIATION OF THE DIFFERENCES													
STATION #	1	2	3	5	6	7	9	10	11	14	15	16	17
SURFACE SALINITY	0.35	0.44	0.72	0.56	0.76	0.65	0.97	1.37	0.98	0.23	0.84	0.42	0.87
MIDDEPTH SALINITY	0.35	0.30	0.72	0.56	0.79	0.74	0.95	1.36	0.98	0.25	0.87		0.97
BOTTOM SALINITY	0.36	0.35	0.76	0.56	0.86	0.86	0.95	1.36	0.98	0.25	0.88		0.98
NOTE: statistics calculated after the spin-up period (hr 5088 - 7296)													

<b>LOW FLOW, HIGH CHANNEL DIFFUSION, PLAN CHANNEL</b>													
AVERAGE DIFFERENCES													
STATION #	1	2	3	5	6	7	9	10	11	14	15	16	17
SURFACE SALINITY	0.61	0.57	-1.13	0.93	-0.54	-0.03	0.44	-0.20	0.82	1.81	-0.52	2.55	-0.21
MIDDEPTH SALINITY	0.61	0.50	-0.88	0.93	-0.53	0.00	0.42	-0.19	0.82	1.78	-0.51		-0.23
BOTTOM SALINITY	0.62	-0.06	-0.84	0.93	-0.52	0.01	0.42	-0.19	0.82	1.78	-0.51		-0.23
STANDARD DEVIATION OF THE DIFFERENCES													
STATION #	1	2	3	5	6	7	9	10	11	14	15	16	17
SURFACE SALINITY	0.49	0.60	0.85	0.72	0.27	0.28	1.04	0.72	1.11	0.22	0.22	0.86	0.23
MIDDEPTH SALINITY	0.52	0.42	0.80	0.72	0.20	0.29	1.02	0.72	1.11	0.24	0.20		0.22
BOTTOM SALINITY	0.57	0.46	0.66	0.72	0.23	0.29	1.02	0.72	1.11	0.24	0.20		0.22
NOTE: statistics calculated after the spin-up period (hr 5088 - 7296)													

Figure 43: Statistical Analysis of Base/Plan Differences for the Low Inflow Runs

<b>MEDIUM FLOW, LOW CHANNEL DIFFUSION, PLAN CHANNEL</b>													
<b>AVERAGE DIFFERENCES</b>													
STATION #	1	2	3	5	6	7	9	10	11	14	15	16	17
SURFACE SALINITY	0.00	0.06	0.67	0.00	2.31	0.30	0.97	1.51	0.67	1.09	2.66	0.92	1.94
MIDDEPTH SALINITY	0.00	0.12	1.02	0.00	2.46	1.56	0.97	1.46	0.67	1.09	2.75		1.87
BOTTOM SALINITY	0.00	0.16	1.17	0.00	2.42	2.02	0.97	1.46	0.67	1.09	2.74		1.86
<b>STANDARD DEVIATION OF THE DIFFERENCES</b>													
STATION #	1	2	3	5	6	7	9	10	11	14	15	16	17
SURFACE SALINITY	0.00	0.12	0.73	0.00	1.26	1.63	1.19	1.25	0.93	1.00	1.25	0.90	1.40
MIDDEPTH SALINITY	0.00	0.22	1.03	0.00	1.53	2.03	1.19	1.32	0.93	1.00	1.37		1.52
BOTTOM SALINITY	0.00	0.27	1.15	0.00	1.59	2.37	1.19	1.32	0.93	1.00	1.37		1.54
<b>HIGHEST 10% OF DIFFERENCES</b>													
STATION #	1	2	3	5	6	7	9	10	11	14	15	16	17
SURFACE SALINITY	0.00	0.23	1.82	0.00	4.11	2.70	2.63	3.11	1.90	2.55	4.07	2.26	3.85
MIDDEPTH SALINITY	0.00	0.50	2.51	0.00	4.55	4.53	2.64	3.12	1.90	2.55	4.33		3.86
BOTTOM SALINITY	0.00	0.64	2.77	0.00	4.58	5.45	2.64	3.12	1.90	2.55	4.33		3.86
NOTE: statistics calculated after the spin-up period (hr 2136 - 6552)													

<b>MEDIUM FLOW, HIGH CHANNEL DIFFUSION, PLAN CHANNEL</b>													
<b>AVERAGE DIFFERENCES</b>													
STATION #	1	2	3	5	6	7	9	10	11	14	15	16	17
SURFACE SALINITY	0.00	0.12	0.43	0.00	0.66	0.74	0.79	0.90	0.81	0.67	0.20	0.62	-0.09
MIDDEPTH SALINITY	0.00	0.29	0.77	0.00	0.53	1.39	0.78	0.81	0.81	0.65	0.30		-0.17
BOTTOM SALINITY	0.00	0.27	0.89	0.00	0.30	1.55	0.78	0.81	0.81	0.65	0.31		-0.18
<b>STANDARD DEVIATION OF THE DIFFERENCES</b>													
STATION #	1	2	3	5	6	7	9	10	11	14	15	16	17
SURFACE SALINITY	0.00	0.21	0.74	0.02	0.77	0.60	0.91	0.94	0.98	0.47	0.64	0.57	0.81
MIDDEPTH SALINITY	0.00	0.41	0.92	0.02	0.78	1.07	0.90	0.97	0.98	0.46	0.63		0.94
BOTTOM SALINITY	0.00	0.38	0.87	0.02	0.85	1.21	0.90	0.97	0.98	0.46	0.63		0.96
<b>HIGHEST 10% OF DIFFERENCES</b>													
STATION #	1	2	3	5	6	7	9	10	11	14	15	16	17
SURFACE SALINITY	0.00	0.47	1.32	0.00	1.65	1.51	2.11	2.03	2.26	1.42	1.01	1.50	0.77
MIDDEPTH SALINITY	0.00	0.96	2.01	0.00	1.56	2.89	2.09	1.96	2.27	1.40	1.13		0.76
BOTTOM SALINITY	0.00	0.88	1.93	0.00	1.45	3.24	2.09	1.96	2.27	1.40	1.13		0.76
NOTE: statistics calculated after the spin-up period (hr 2136 - 6552)													

Figure 44: Statistical Analysis of Base/Plan Differences for the Median Inflow Runs

## Storm Surge

Figure 45 depicts the maximum storm surge differences observed in the model runs. These occur at or near the peak storm surge, and vary between 0 and 0.4 ft increase in water surface elevation.

Note, however, that the model does not allow for the significant overbank flooding that would occur in an actual storm, and hence this estimate of water surface elevation increase should be considered exceedingly conservative. Therefore, a 0.4 ft increase or less should be the maximum expected at any location in the study area during a storm surge event.

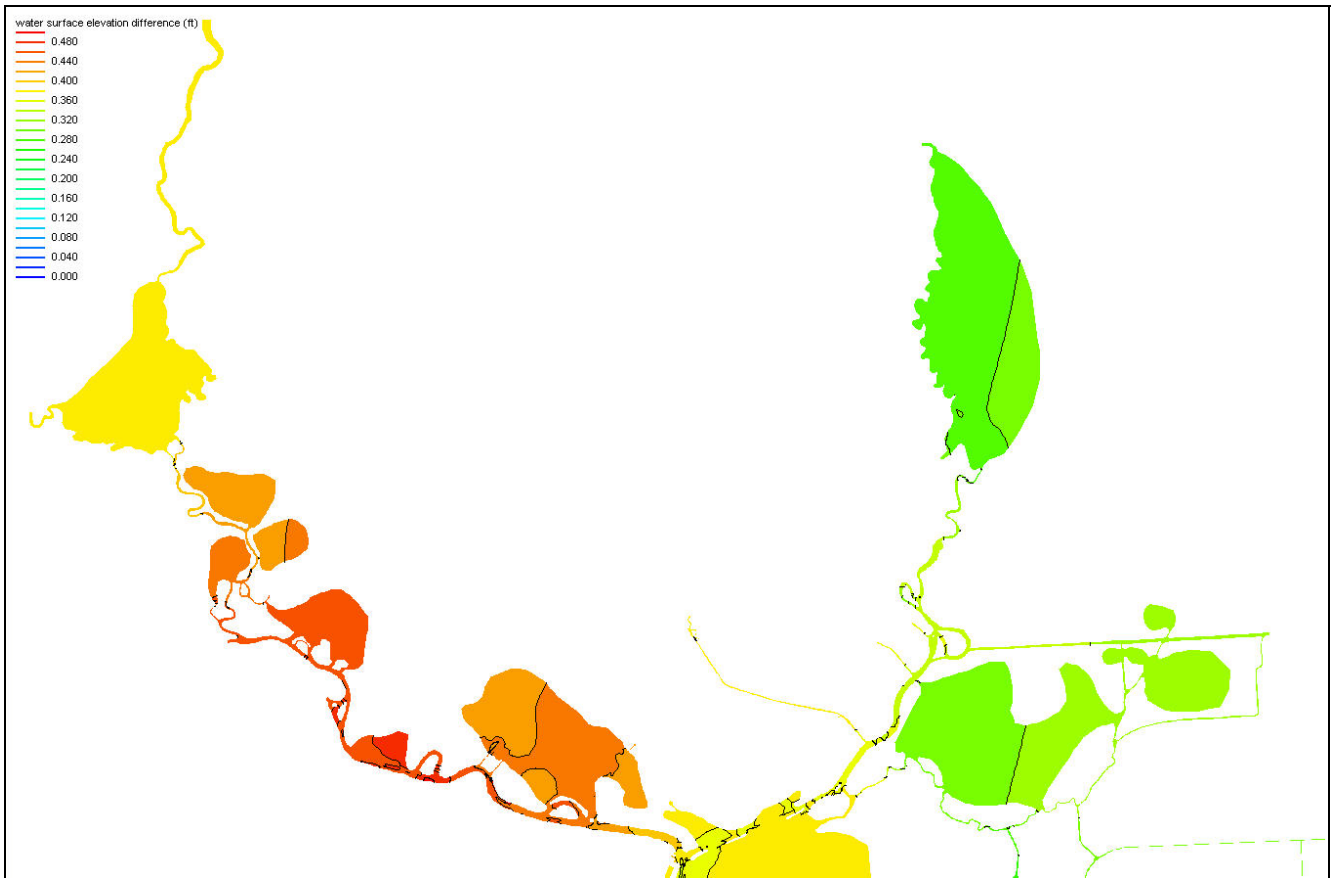


Figure 45: Maximum Water Surface Elevation Difference (Plan Minus Base) Observed at Peak Storm Surge (Contour Interval = 0-0.5 ft)

# Model Analysis of Proposed Salinity Mitigation Alternatives

---

This chapter contains the results of model simulations design to assess the effectiveness of various proposed salinity mitigation measures, and the tools and methods of analysis used to make these assessments.

## Description of Proposed Salinity Mitigation Alternatives

Several options were proposed as potential measures to mitigate the impacts of increased salinity in the study area induced by the implementation of the plan channel. For the purposes of analysis, these mitigation measures were divided into 3 groups.

- Large-scale measures (H-S- Model Runs). These are measures that have the potential to impact the entire system.
- Small-scale measures (Desktop Model). that will have principally localized impacts. Many of these small scale measures represent changes to specific wetlands or inlets that are not resolved in the mesh, except as generalized marsh storage elements.
- Measures that do not require analysis with respect to salinity mitigation (Not Modeled) These are measures were not intended for salinity mitigation or it was not necessary to model them because their effect on salinity was prescribed.

The following table gives a summary of each of these measures:

**Table 4. Proposed Mitigation Measures**

<b>SNWW Mitigation Measures H-S Model Runs</b>
1. Rose City & Bessie Heights West (Rose City West, TX 3-1 and TX 5-1) – low and median conditions; assume entire acreage of both removed from tidal prism by project yr 1. Total area affected – 1840 ac.
2. Rose City, Bessie Heights West, and Bessie Heights East (Rose City West, TX3-1, TX5-1, TX5-2); – low and median flow conditions; assume entire acreage of all removed from tidal prism by project yr 1.) Total area affected – 5019 acres.

3. Rose City, BHW, BHE and Old River Cove (Rose City West, TX3-1, TX5-1, TX5-2, TX6-1, and Old River Cove East); – low and median flow conditions; assume entire acreage of all removed from tidal prism by project yr 1.) Total area affected – 6670 acres.
4. Submerged hard sill at mouth of Sabine Lake (elevation at –10ft MLT). Assume constructed in year 1; low and median conditions.
5. Sensitivity analysis – determine how sensitive the entire system is to a reduction in East Sabine Lake storage from aggregate of channel constriction measures and the reduction in wetted area induced by the construction of marshes (i.e. aggregate effect of small-scale measures).
<b>SNWW Mitigation Measures Desk-top Model</b>
1. TX8-1- assume logging canal plugged but natural Texas Bayou channel remains open. Median condition only since only affects brackish and saline marshes. Total area affected – 5224 ac.
2. TX8-1A - assume one weir at highway bridge that restricts flow to both the natural Texas Bayou channel and the logging canal. Median condition only since only affects brackish and saline marshes. Effective cross sectional area reduced to 40 x 6. Total area affected – 5224 ac.
3. TX8-1B - assume plugging of logging canal, filling behind canal (11 acres marsh), and a rock weir with 40 x 6 ft cross sectional opening in Texas bayou. Median condition only since only affects brackish and saline marshes. Total area effected – 5224 ac.
2. LA2-14 – 2 rock weirs with boat bays at Sabine Lake mouth of Willow Bayou (affects 11,185 ac) and Three Bayou (affects 6,650 ac); low flow condition only; primarily affects intermediate marsh. Total area affected –17835 ac.
3. LA2-15 – 2 rock weirs with boat bays (Greens Bayou and Right Prong of Black Bayou); low flow condition only, primarily affects intermediate marsh. Total area affected –18,332 ac.
4. LA3-2 – rock weir with boat bay at opening of natural trib just east of Raleigh’s ditch on Black Bayou (#2) and plug at small trib opening on west Black Bayou (#6); low flow condition only, primarily affects intermediate marsh. Total area affected – 3056 ac.
5. LA3-3 – Rock liner at mouth of small stream leading south from Black Bayou (#5); low flow condition only, primarily affects intermediate marsh. Total area affected – 1233 ac.
6. LA3-4 – Rock weir with boat bay on small stream leading south from Black Bayou into Sterling Pond (#7); low flow condition only, primarily affects intermediate marsh.

Total area affected – 955 ac.
7. LA3-5 – Rock weir at mouth of stream leading north from Black Bayou (#3); low flow condition only, primarily affects intermediate marsh. Total area affected – 321 ac.
8. LA3-7 – Rock liners at 4 large streams leading north from Black Bayou (#9a-9b); low flow condition only, primarily affects intermediate marsh. Total area affected – 1755 ac.
9. LA3-8 – Plug at oil field canal opening on west side of Black Bayou Cutoff Canal (#11); low flow condition only, primarily affects intermediate marsh. Total area affected – 1552 ac.
<b>SNWW Measures Not Modeled</b>
TX7-1 and 7-2 – North GIWW shoreline restoration
TX8-2 – Texas Point –berm and marsh fill behind jetty (acts as plug)
TX8-3 - Texas Point – filling logging canal
TX8-4 – Texas Point – unconfined marsh restoration behind TX8-2
TX8-5 thru 8-11 – Texas Point shoreline nourishment
TX12-1 – Blue Elbow South – plug of logging canal
LA2-1, 2-2 and 3-14 – marsh creation behind East Sabine Lake foreshore dike
LA2-7 – Willow and Three Bayous – adjustable control structures – assumed managed for specific salinity
LA2-8 – Greens Bayou and Right Prong of Black Bayou - adjustable control structures – assumed managed for specific salinity
LA2-16 thru 2-19, 2-ADD – Willow Bayou terracing or marsh restoration
LA2-11 thru 2-13, Willow Bayou – Unit 7 marsh restoration
LA3-1 – Black Bayou adjustable control structure - assumed managed for specific salinity
LA3-6 – Black Bayou sluice gates
LA3-9 thru 3-10, 3-15 thru 3-18 – Black Bayou marsh restoration
LA5-1/6-1, 5-2/6-2, 5-3 thru 5-6 – Louisiana Gulf shoreline nourishment
LATX1 –Sabine Island – plug pipeline canal
LATX2- Blue Elbow Swamp – plug logging canal

Note that the following mitigation measures were modeled using the 50 ft project mesh, and that

results were reported to the Habitat Workgroup. These results will not be presented in this report because they were eliminated during preliminary screening.

- Purchasing freshwater flows in the Neches and Sabine Rivers
- Marsh islands separating the Sabine Neches Canal B from Sabine Lake
- Marshes constricting flow at the mouth of Sabine Lake
- Marsh constricting flow along the Port Arthur Canal
- Channel islands blocking flow from bayous emptying Rose City and Bessie Heights marshes
- Marsh restoration in Sabine Lake along the east shores of PA 8 and PA 11

## **Modeling Approach: TABS-MDS and DOWSMM**

The large-scale measures were analyzed using the TABS-MDS model described in this report. The small-scale measures were analyzed using a simple desktop model developed for this project: The Desktop Off-channel Wetland Salinity Mitigation Model (DOWSMM). It generates a time-series of data for the spatially averaged salinity of an off-channel wetland, with one primary inlet. The tide and salinity at the inlet are specified as input to the model, as well as a time series of the net precipitation in the wetland. The model is capable of estimating the effects of installing a control structure at the inlet. Hence, the model can be run both with and without the control structure, to predict the salinity impact of the control structure. A complete description of the DOWSMM model can be found in Appendix B.

For some of the small-scale mitigation measures, there are wetlands with multiple inlets. For these cases, the wetlands were subdivided into single inlet wetlands, and the salinity of the entire wetland was estimated by taking a weighted average (by water volume) of the salinity of each sub-wetland, for each time step.

The boundary conditions for the DOWSMM model were taken from the TABS-MDS model runs. Hence, the implicit assumption is that the changes to the hydrodynamics and salinity inside of each wetland (as induced by the implementation of a control structure) do not have a significant effect on the salinity of the overall system.

In order to evaluate this assumption, one of the TABS-MDS model runs (Run 5) is a sensitivity test. In this run, all of the small-scale mitigation measures are implemented into the TABS-MDS mesh in a schematic fashion (i.e. the loss of storage volume and constriction of flow pathways are implemented). Then, the model is run to determine what the overall effect of these aggregate small-scale measures is on the salinity of the entire system.

## **Results**

### **TABS-MDS results: General Observations**

Mitigation Runs 1-3: These runs each feature the reclamation of wetlands in open water areas along the Neches River. The footprint of reclaimed marsh increases from mitigation run 1 to run 3. So it is instructive to consider them together.

Figure 46 is a plot of salinity differences between each of these runs and the salinity in the plan (48-foot channel) run. The contour interval is from -3 to +1: that is, from a 3 ppt decrease to a 1ppt increase in average salinity. Blue represents a 3 ppt decrease (or less), and red represents a 1 ppt increase (or greater).

Note that each of these runs result in a decrease in salinity in the Neches River. Also note that Runs 2 and 3 result in a greater decrease than Run 1. This decrease is due to the fact that the reclamation of the open-water areas along the Neches River effectively reduces the tidal prism that propagates up the river. Hence, the transport of salt water is decreased by decreasing the available storage area for tidal prism. Since there is only one connection to a salt source (the intersection of the Neches River and the Sabine-Neches Canal) the hydraulic behavior of this reach is relatively simple, and can be analyzed in this way.

There is a notable exception to this salinity decrease: a sharp increase in salinity in a portion of Bessie Heights. This is due to the reduction of the power plant discharge area. The power plant discharge is a constant 5000 cfs discharge into Bessie Heights at the ambient salinity of the water (that is, at the salinity of the intake at Old River Cove). Since the flow pathway of this water is constricted by the restored wetlands, the water cannot diffuse as freely and therefore shows a higher salt concentration.

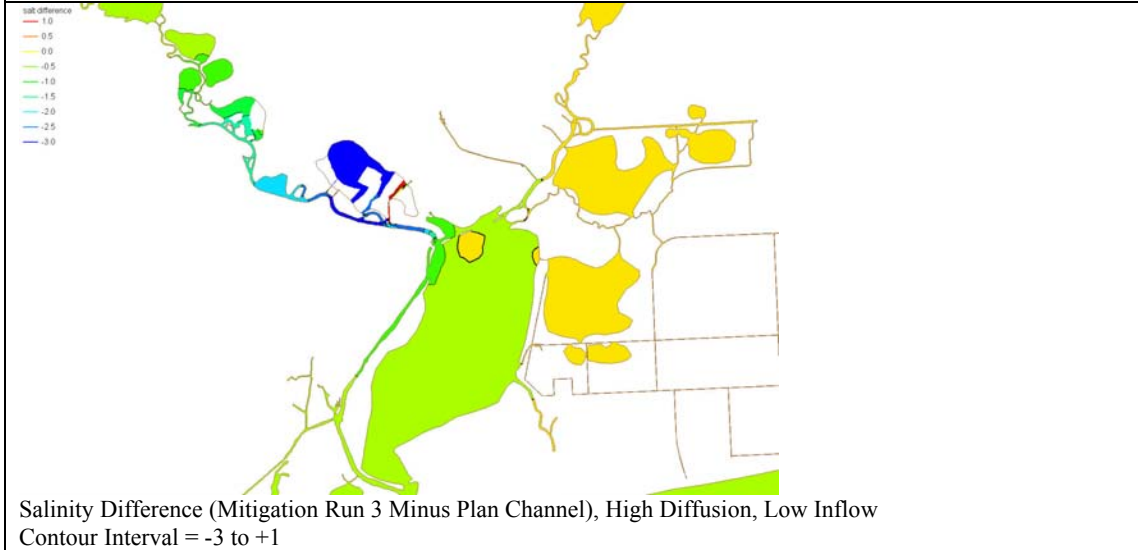
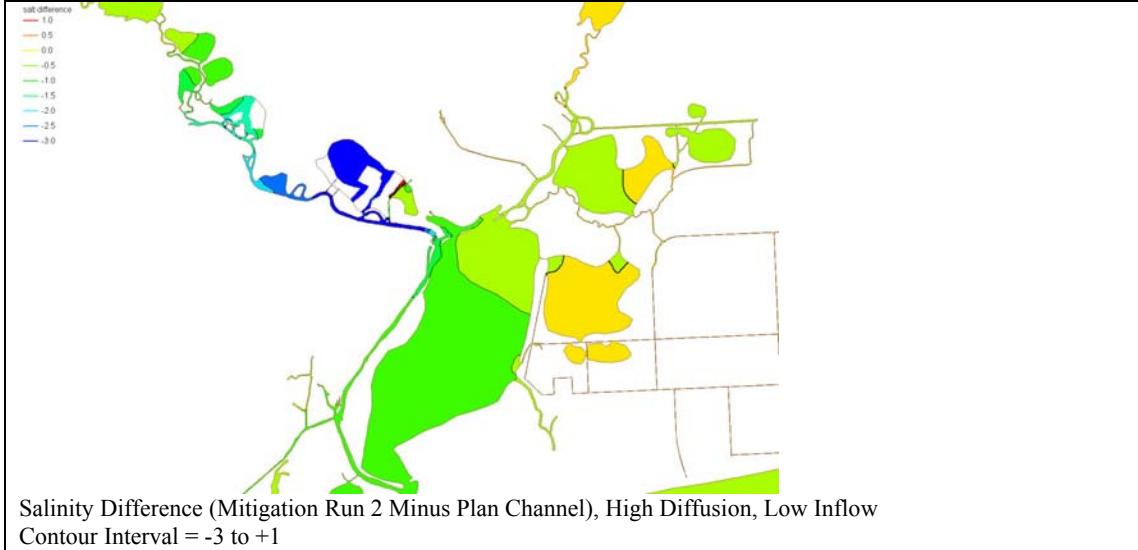
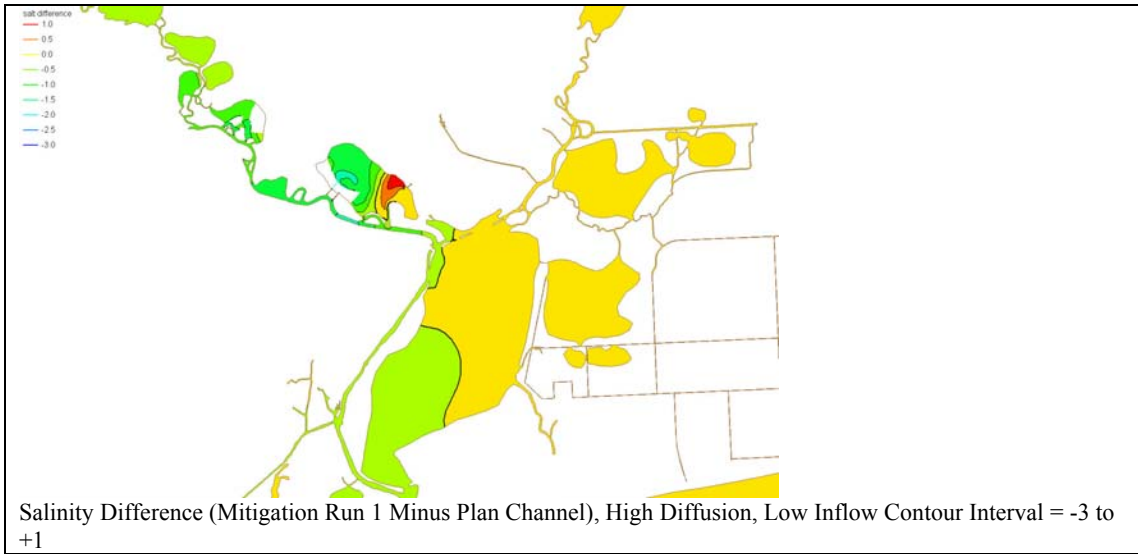


Figure 46: Salinity Difference Comparisons for Mitigation Runs 1-3

Mitigation Run 4: This run is intended to examine the effectiveness (with respect to salinity mitigation) of installing a sill at the downstream end of Sabine Lake, just downstream of the Highway 82 swing bridge. The results are given in Figure 47. This figure only gives the high diffusion results: the low diffusion results show slightly greater salinity mitigation, but since the analysis is based on the most conservative of the runs, the high diffusion results are selected in this case.

Note that the sill provides little if any salinity mitigation, except some reduction in salinity at the southwest end of Sabine Lake. This is likely because the principle pathway for salinity transport into the system is via the Sabine-Neches Canal, which bypasses Sabine Lake. Hence, the sill only mitigates salinity transport directly into the lake from the south, and this transport pathway only advances saline water northward to the midpoint of Sabine Lake, at most.

It is possible that further mitigation could be achieved by further constricting the south end of Sabine Lake, with a higher elevation sill, or a further constriction of the opening. This mitigation would be achieved by effectively constricting the pathways available for tidal current propagation from Sabine Pass, thereby limiting the net tidal prism to the system. However, this constriction would also result in very high velocities across the weir, and could exacerbate flooding in Sabine Lake by retarding drainage of the Lake at the south end.

Figure 48 gives observed peak velocity magnitudes at 3 locations along the weir. Note that, even with the weir set at  $-10\text{ft}$  MLT, the velocity magnitude across the weir increases to almost 9 fps in some locations. Any further constriction would result in hazardous navigation conditions.

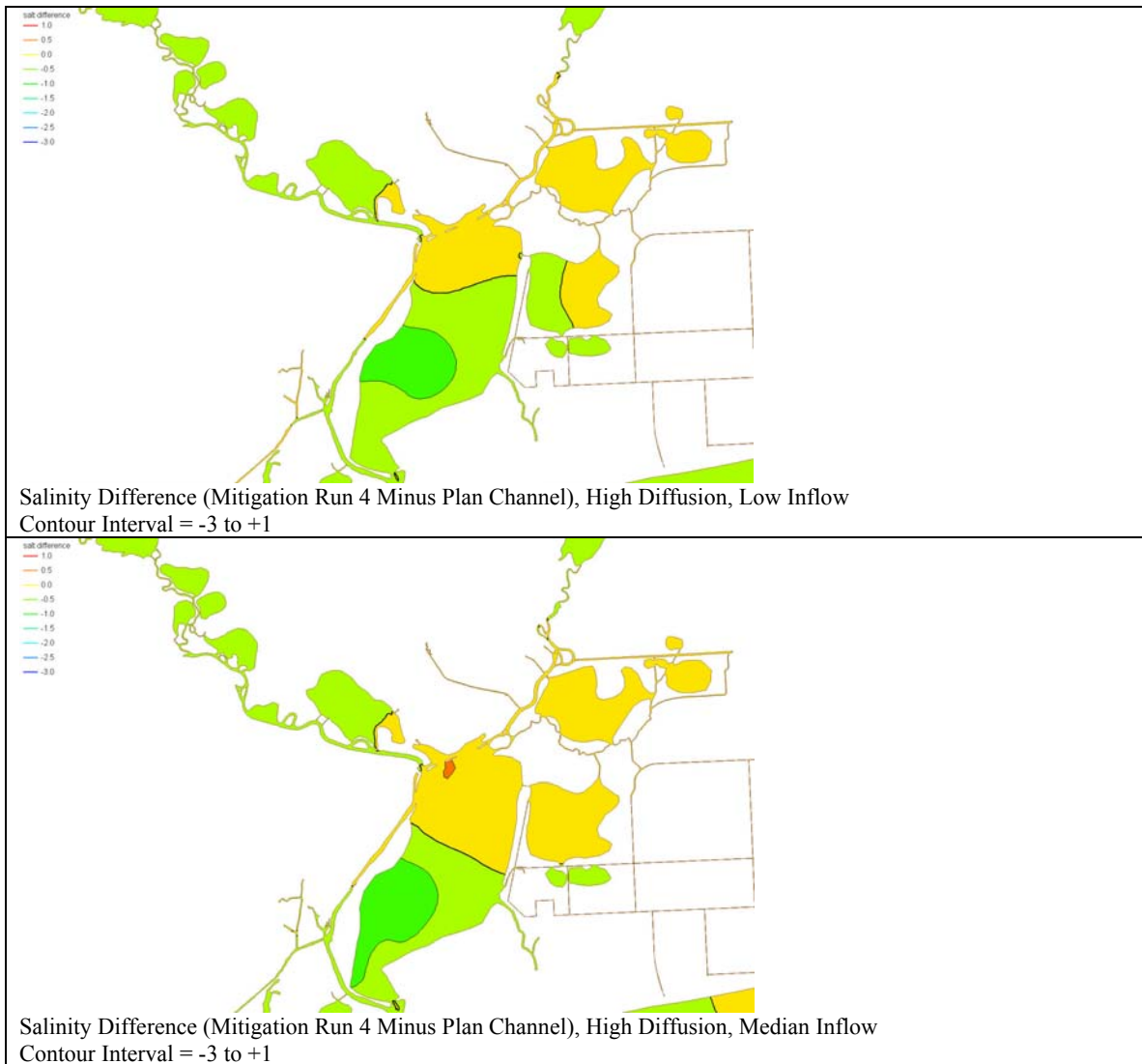
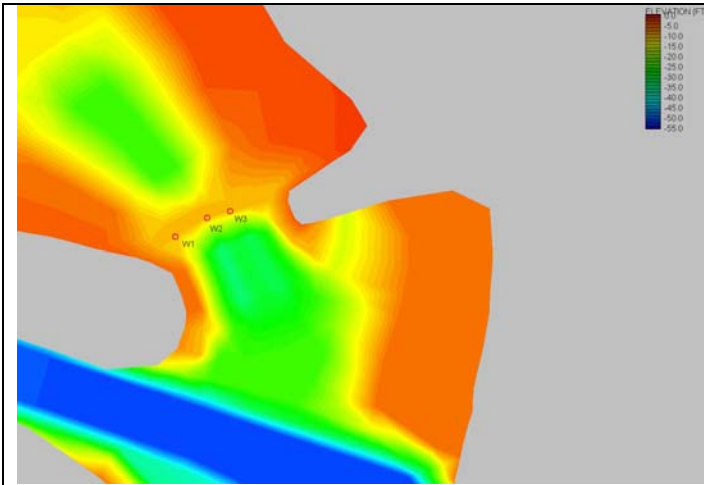
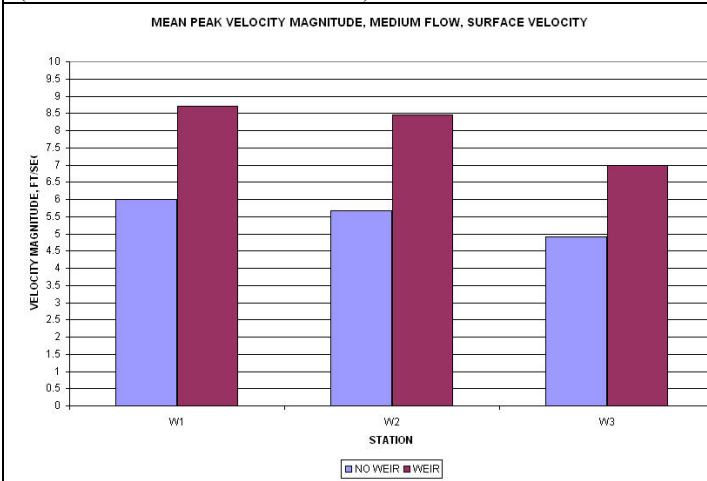


Figure 47: Salinity Difference Comparisons for Mitigation Runs 4



Location of Velocity Magnitude Observations Along Proposed Sabine Lake Weir  
(Weir Elevation = -10.0 Ft MLT)



Peak Velocity Magnitude Observations, Both With and Without the Proposed Weir

Figure 48: Peak Velocity Magnitude Observations at Proposed Sabine Lake Weir

Mitigation Run 5: This run is intended as a gross sensitivity test, to estimate the maximum potential system-wide impact of implementing all of the proposed small-scale mitigation measures. The results are given in Figure 49. Only the low diffusion results are given, since in this case the low diffusion results represent the largest negative impact.

Note that there are some impacts observed, on the order of +0.5 to +1.0 ppt. These are concentrated primarily at the Northeast corner of Sabine Lake, and in the Black Bayou area of the SNWR. The elimination of some of the tidal storage and the constriction of flow pathways in this area results in small changes in the circulation, which in turn result in some localized increases in salinity concentration relative to that observed in the plan condition.

It should be noted that these estimates are worse case estimates, since they assume that all of the small-scale measure are implemented simultaneously.

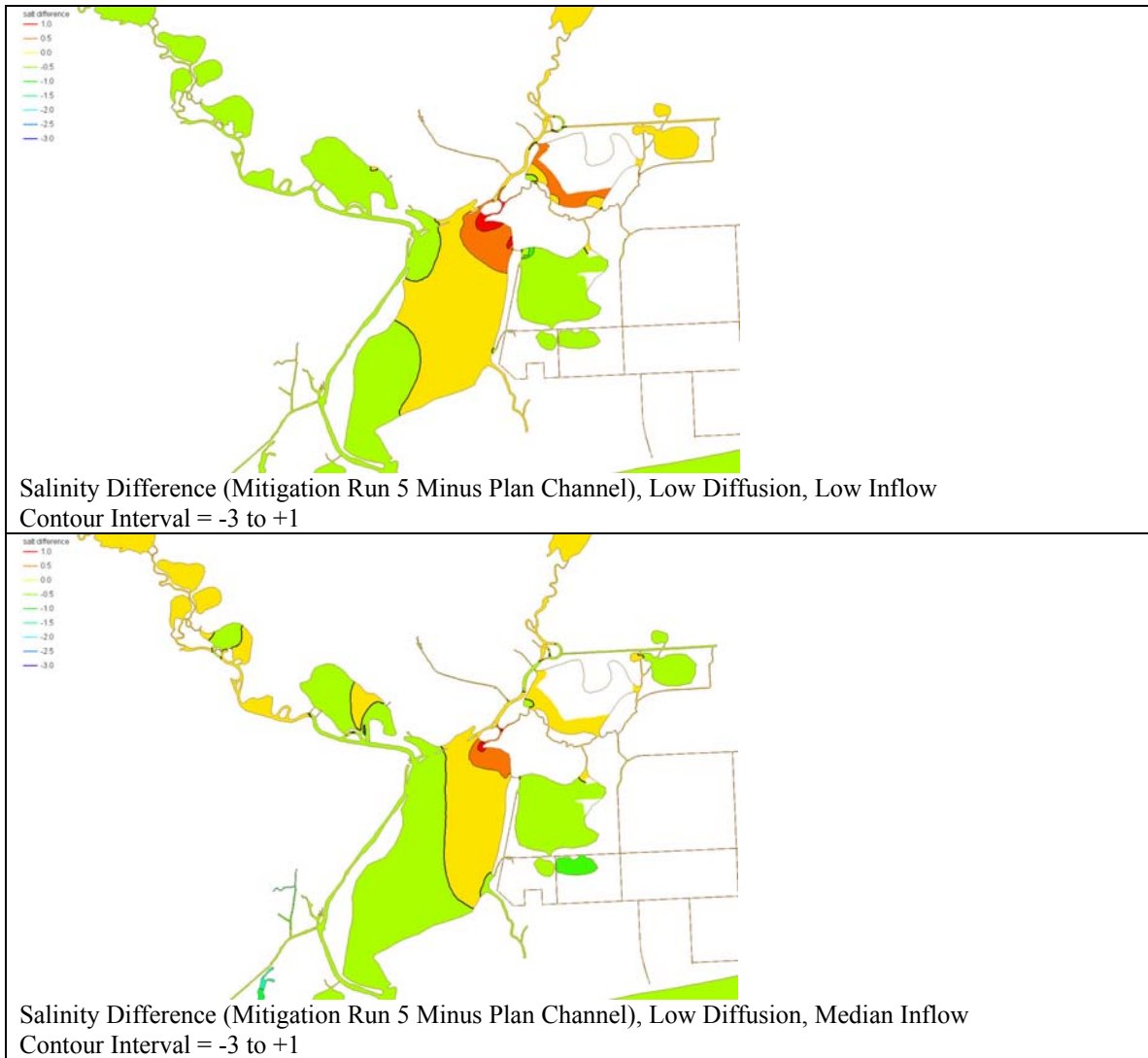


Figure 49: Salinity Difference Comparisons for Mitigation Run 5

### DOWSMM Desktop Modeling Results

The desktop modeling results are given in Figure 50. The figure provides two examples of the time history output from the model. Each of these examples include the time-history of the salinity in the wetland both with and without the mitigation control structure(s) in place, as well as a red line plotting the time-history of the salinity difference. A statistical analysis of all of the desktop scenarios is also given in the figure.

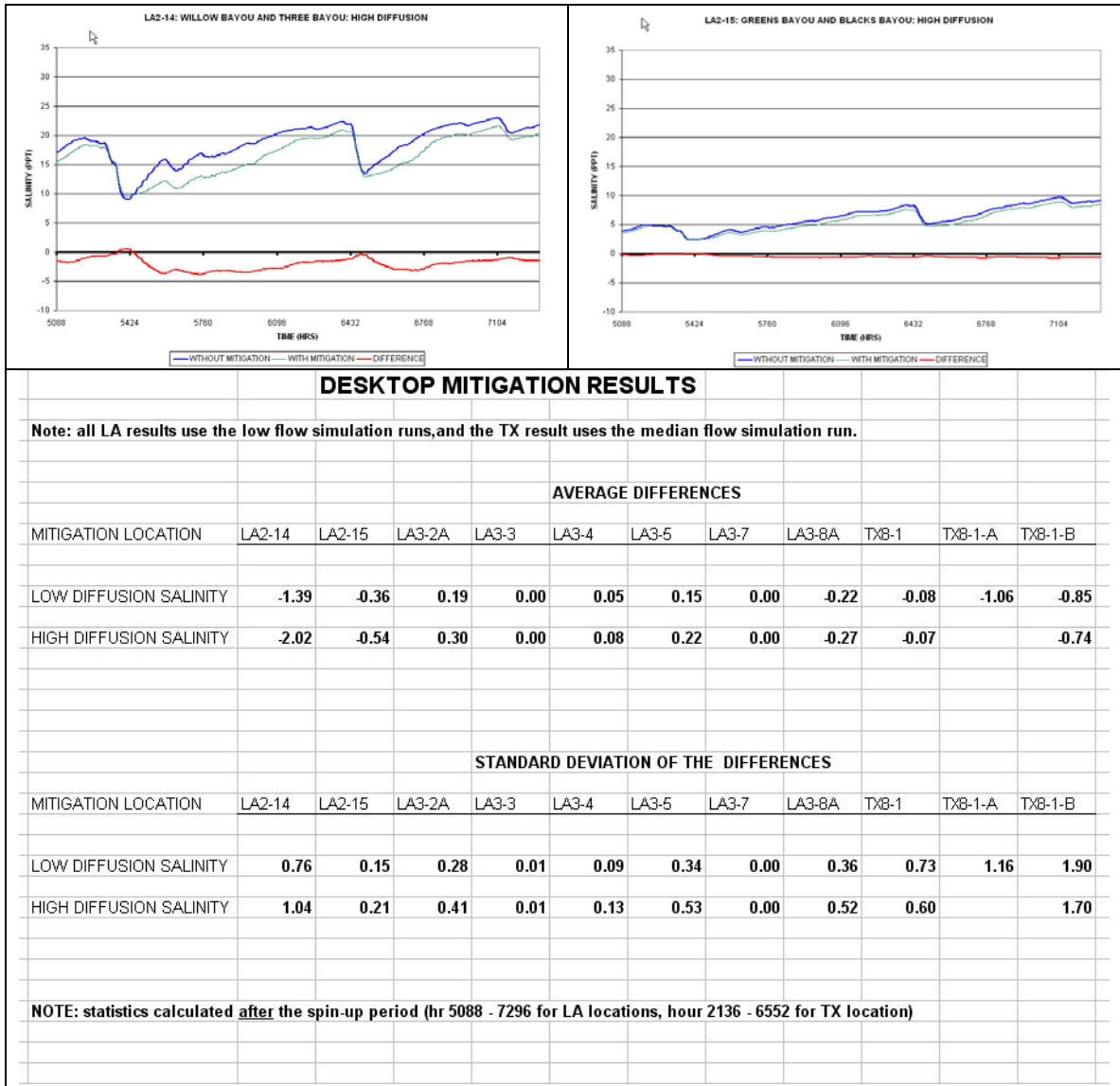


Figure 50: Desktop Analysis Mitigation Results

### Habitat Salinity Analysis

The Habitat Evaluation Workgroup was provided with an extensive quantitative analysis of the model results, for use in evaluating the various mitigation alternatives. These data include the following:

- Time-history plots of salinity (plan salinity, mitigation salinity, and salinity difference) at 34 locations throughout the project area
- Percent exceedance plots of salinity (plan salinity, mitigation salinity, and salinity difference) at 34 locations throughout the project area
- Bar Charts of mean salinity (plan salinity and mitigation salinity) at 34 locations

throughout the project area

- Bar Charts of the mean value of the highest 33% of continuous salinity (plan salinity and mitigation salinity) at 34 locations throughout the project area
- Salinity difference color contour maps of each of the TABS-MDS mitigation model runs
- Bar Charts of mean velocity magnitude (plan velocity magnitude and mitigation magnitude) at 12 locations throughout the project area
- Complete salinity statistics for the spatially averaged salinity for each of the DOWSMM small-scale model runs.
- Complete velocity statistics for the inlet velocity for each of the DOWSMM small-scale model runs.

A sample of both a typical percent exceedance plot and a plot of mean salinity is given in Figure 51. The complete set of mean salinity values and highest 33% continuous salinity values for mitigation runs 1-5 are given in Appendix C.

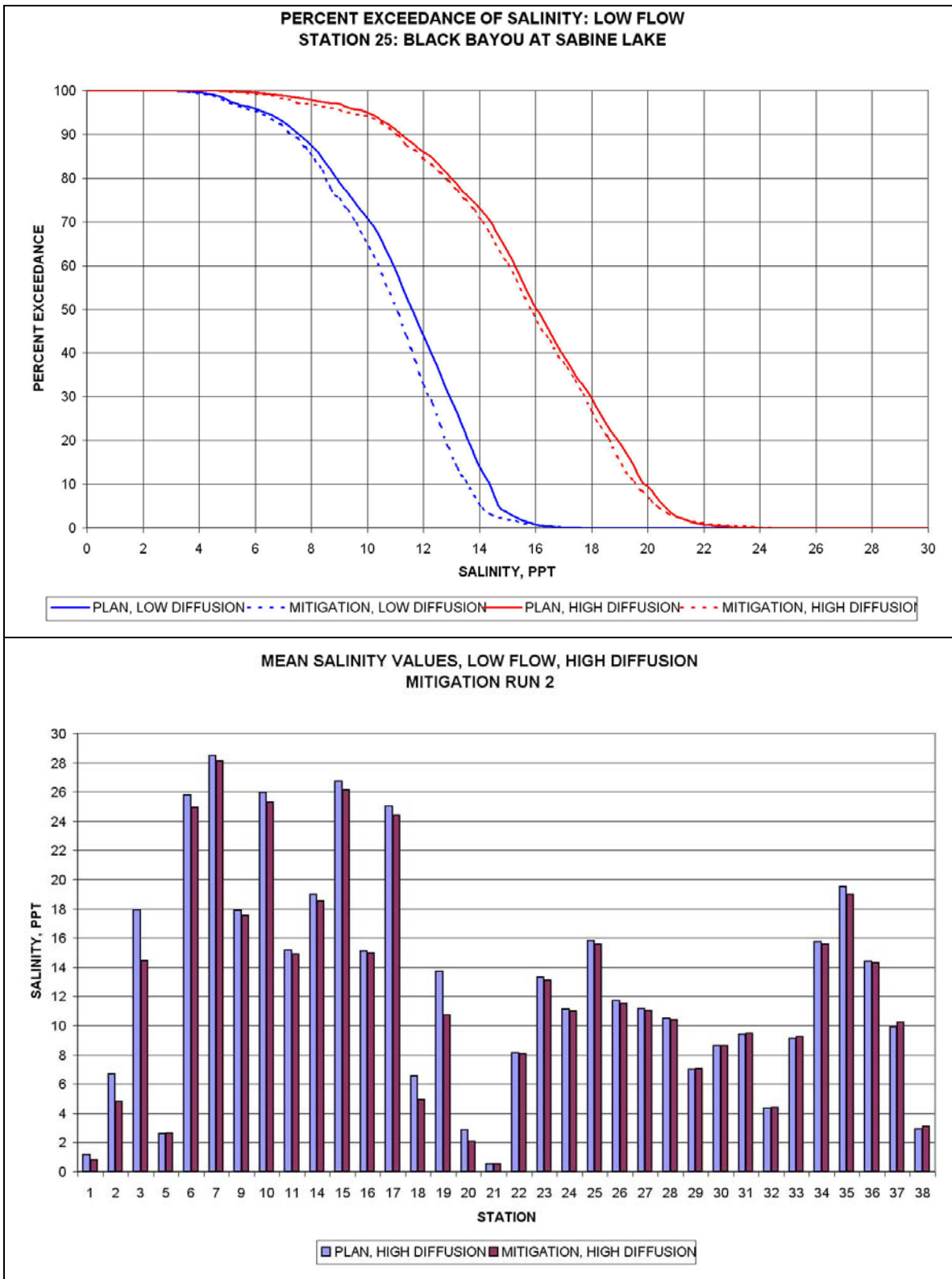


Figure 51: Samples of Habitat Salinity Analysis Data

# Conclusions

---

- The following represents an overview of the conclusions found in this report.
- The TABS-MDS code of ERDC-WES is used for computing hydrodynamics and salinity transport for this study. It is a finite element model, which gives it great flexibility in matching complex geometry. It is capable of both 2D (vertically averaged) and 3D simulation. For this application, 3D resolution was used in the channels and Sabine Lake, and 2D resolution was used in the wetlands and shallow open-water areas.
- The extents of the model domain are given as follows:
  - North to the Neches River at Evadale, TX, and the Sabine River at Ruliff, TX.
  - East to a point approximately mid-way between the Sabine Lake and Calcasieu Lake, including half of the Sabine-Neches Wildlife Refuge
  - South approximately 60 miles into the Gulf of Mexico
  - West to a point approximately mid-way between Sabine Lake and Galveston Bay, including all of the McFaddin National Wildlife Refuge
- The model mesh contains 33,321 surface nodes and 13,035 surface elements.
- The tide comparisons show that the model and field have good agreement with respect to the tidal signal.
- The ADCP discharge comparisons show that the flow split between the Sabine-Neches Canal and Sabine Lake is somewhat different in the model than in the field, with a greater percentage of the total flow passing through the Lake in the model than in the field. However, the total flows at Sabine Pass, at the Neches River, and at the Sabine River match well with the field observations.
- The velocity observations show good agreement at most of the gage locations.
- In order to achieve a satisfactory salinity result in the upper reaches of the system, a non-physical adjustment to the horizontal salinity mixing coefficient was applied to that section of the channel south of the intersection with the Neches River. This adjustment was limited to this southern section of the channel so that the fidelity of the physical description of the system in the Neches and Sabine Rivers is still valid, and hence, changes due to modifications of the plan condition could still be investigated. Since this diffusion adjustment represents a non-physics based contribution to the model, it

introduces an additional uncertainty into the reliability of the model with respect to the evaluation of plan scenarios. Therefore, for all the plan scenarios, the model was run both with and without the high diffusion adjustment, and the run that yielded the largest change at a given location was generally used to define the salinity impact at that location. The high diffusion version yielded the largest change at nearly all locations and it was, therefore, used to define salinity impacts over the vast majority of the study area. However, the low diffusion version was used to predict salinity impacts for areas adjacent to the SNWW south of the GIWW where the low diffusion verification results were closer to field data than high diffusion results. This represents a conservative approach to impact assessment, and is intended to ensure that the additional uncertainty introduced by the artificially elevated horizontal diffusion does not result in assessments that underestimate the potential salinity impacts.

- For the proposed 48-foot plan channel condition, highest salinity impacts are found in the following locations.
  - Low Flow:
    - Neches River, between Bessie Heights and Rose City (approximately 0.5-1.5 ppt)
    - Sabine River (approximately 0-1 ppt)
    - Eastern Shore of Sabine Lake (approximately 2-3 ppt)
  - Median Flow:
    - Keith Lake Fish Pass (approximately 2-4 ppt)
    - Lower Sabine Lake (approximately 2-4 ppt).
    - Sabine-Neches Canal (approximately 2-4 ppt).
- Each of these locations corresponds to sensitive environments. This is especially true of the cypress-tupelo swamps on the Neches and Sabine Rivers; the eastern side of Sabine Lake, where Willow Bayou and Johnson's Bayou link the Lake to the Sabine National Wildlife Refuge (SNWR); and Keith Lake Fish Pass which links the navigation channel to the J.D. Murphree Wildlife Management Area.
- Several options were proposed as potential measures to mitigate the impacts of increased salinity in the study area induced by the implementation of the project channel. For the purposes of analysis, these mitigation measures were divided into 3 groups.
  - Large-scale measures (H-S- Model Runs). These are measures that have the potential to impact the entire system.
  - Small-scale measures (Desktop Model). that will have principally localized impacts. Many of these small scale measures represent changes to specific wetlands or inlets that are not resolved in the mesh, except as generalized marsh storage elements.
  - Measures that do not require analysis with respect to salinity mitigation (Not Modeled) These are measures not expected to affect salinity.
- The large-scale measures were analyzed using the TABS-MDS model described in this

report. The small-scale measures were analyzed using a simple desktop model developed for this project: The Desktop Off-channel Wetland Salinity Mitigation Model (DOWSMM). It generates a time-series of data for the spatially averaged salinity of an off-channel wetland, with one primary inlet. The tide and salinity at the inlet are specified as input to the model, as well as a time series of the net precipitation in the wetland. The model is capable of estimating the effects of installing a control structure at the inlet. Hence, the model can be run both with and without the control structure, to predict the salinity impact of the control structure. A complete description of the DOWMM model can be found in Appendix B.

- Mitigation Runs 1-3 each result in a decrease in salinity in the Neches River. Also note that Runs 2 and 3 result in a greater decrease than Run 1. This decrease is due to the fact that the reclamation of the open-water areas along the Neches River effectively reduces the tidal prism that propagates up the river. Hence, the transport of salt water is decreased by decreasing the available storage area for tidal prism. Since there is only one connection to a salt source (the intersection of the Neches River and the Sabine-Neches Canal) the hydraulic behavior of this reach is relatively simple, and can be analyzed in this way.
- The implementation of a -10 ft MLT sill at the southern end of Sabine Lake (Mitigation run 4) provides little if any salinity mitigation, except some reduction in salinity at the southwest end of Sabine Lake. This is likely because the principle pathway for salinity transport into the system is via the Sabine-Neches Canal, which bypasses Sabine Lake. Hence, the sill only mitigates salinity transport directly into the lake from the south, and this transport pathway only advances saline water northward to the midpoint of Sabine Lake, at most. It is possible that further mitigation could be achieved by further constricting the south end of Sabine Lake, with a higher elevation sill, or a further constriction of the opening. This mitigation would be achieved by effectively constricting the pathways available for tidal current propagation from Sabine Pass, thereby limiting the net tidal prism to the system. However, this constriction would also result in very high velocities across the weir, and could exacerbate flooding in Sabine Lake by retarding drainage of the Lake at the south end.
- There are some negative impacts that result from the implementation of all of the small-scale mitigation alternatives (Mitigation run 5). The impacts are on the order of +0.5 to +1.0 ppt. These are concentrated primarily at the Northeast corner of Sabine Lake, and in the Black Bayou area of the SNWR. The elimination of some of the tidal storage and the constriction of flow pathways in this area results in small changes in the circulation, which in turn result in some localized increases in salinity concentration relative to that observed in the plan condition. It should be noted that these estimates are worse case estimates, since they assume that all of the small-scale measure are implemented simultaneously.
- The Habitat Evaluation Workgroup was provided with an extensive quantitative analysis of the model results, for use in evaluating the various mitigation alternatives.



# References

---

- Chow, V. T. (1959) "Open Channel Hydraulics". McGraw-Hill, New York.
- Cochrane, J. D., and Kelly, F. J. (1986) "Low-frequency circulation on the Texas-Louisiana continental shelf" Journal of Geophysical Research 91(C9), 10645-1659.
- Fagerburg, Tim. (2001) "Field Data Collection Summary Report for the Sabine-Neches Waterway Study" Memorandum For Record, submitted to SWG.
- Gammill, S., Balkum, K., Duffy, K., Meselhe, E., Porthouse, J., Ramsey, E., and Walters, R., (2002) "Hydrologic Investigation of the Louisiana Chenier Plan", report prepared for the Louisiana Coastal Wetlands Conservation and Restoration Task Force, by the Louisiana Department of Natural Resources.
- King, I.P. (1988) "A Finite Element Model for Three-Dimensional Hydrodynamic System", report prepared by Resource Management Associates, Lafayette California, for U.S. Army Corps of Engineers, Waterways Experiment Station, Vicksburg, MS.
- King, I.P. (1993). "RMA-10, a finite element model for three-dimensional density stratified flow," Department of Civil and Environmental Engineering, University of California, Davis.
- Smagorinsky, J. (1963). "General Circulation Experiments with the Primitive Equations." "Monthly Weather Review", Vol. 93, pp 99 – 165.

# Appendix A

---

## TABS-MDS Introduction

TABS-MDS (Multi-Dimensional, Sediment) is a finite element, hydrodynamic model. It is based on RMA10, a model written by Ian King of Resource Management Associates (King, 1993). It is capable of modeling turbulent, sub-critical flows using 1-D, 2-D, and/or 3-D elements. It is also capable of modeling constituent transport. This includes modeling salinity, temperature, and/or fine-grained sediment. The model is capable of coupling the spatial density variation induced by concentration gradients in the constituent field to the hydrodynamic calculations. This enables the model to simulate phenomena such as saline wedges in estuaries. The model has features that permit the simulation of intermittently wetted regions of the domain, such as coastal wetlands.

## TABS-MDS Theoretical Development

### 3-D Equations

We have 6 unknowns (u,v,w,h,s,ρ). Therefore, we require 6 equations.

*The Navier-Stokes Equations (i.e. conservation of fluid momentum)*

$$\begin{aligned} \rho \frac{\partial u}{\partial t} + \rho u \frac{\partial u}{\partial x} + \rho v \frac{\partial u}{\partial y} + \rho w \frac{\partial u}{\partial z} - \frac{\partial}{\partial x} \left( \epsilon_{xx} \frac{\partial u}{\partial x} \right) - \frac{\partial}{\partial y} \left( \epsilon_{xy} \frac{\partial u}{\partial y} \right) - \frac{\partial}{\partial z} \left( \epsilon_{xz} \frac{\partial u}{\partial z} \right) \dots\dots \\ + \frac{\partial p}{\partial x} - \tau_x = 0 \end{aligned} \quad (1)$$

$$\begin{aligned} \rho \frac{\partial v}{\partial t} + \rho u \frac{\partial v}{\partial x} + \rho v \frac{\partial v}{\partial y} + \rho w \frac{\partial v}{\partial z} - \frac{\partial}{\partial x} \left( \epsilon_{yx} \frac{\partial v}{\partial x} \right) - \frac{\partial}{\partial y} \left( \epsilon_{yy} \frac{\partial v}{\partial y} \right) - \frac{\partial}{\partial z} \left( \epsilon_{yz} \frac{\partial v}{\partial z} \right) \dots\dots \\ + \frac{\partial p}{\partial y} - \tau_y = 0 \end{aligned} \quad (2)$$

$$\begin{aligned} \rho \frac{\partial w}{\partial t} + \rho u \frac{\partial w}{\partial x} + \rho v \frac{\partial w}{\partial y} + \rho w \frac{\partial w}{\partial z} - \frac{\partial}{\partial x} \left( \epsilon_{zx} \frac{\partial w}{\partial x} \right) - \frac{\partial}{\partial y} \left( \epsilon_{zy} \frac{\partial w}{\partial y} \right) - \frac{\partial}{\partial z} \left( \epsilon_{zz} \frac{\partial w}{\partial z} \right) \dots\dots \\ + \frac{\partial p}{\partial z} + \rho g - \tau_z = 0 \end{aligned} \quad (3)$$

*The Volume Continuity Equation*

$$\frac{\partial u}{\partial x} + \frac{\partial v}{\partial y} + \frac{\partial w}{\partial z} = 0 \dots\dots\dots (4)$$

*The Advection-Diffusion Equation*

$$\frac{\partial s}{\partial t} + u \frac{\partial s}{\partial x} + v \frac{\partial s}{\partial y} + w \frac{\partial s}{\partial z} - \frac{\partial}{\partial x} \left( D_x \frac{\partial s}{\partial x} \right) - \frac{\partial}{\partial y} \left( D_y \frac{\partial s}{\partial y} \right) - \frac{\partial}{\partial z} \left( D_z \frac{\partial s}{\partial z} \right) \dots\dots\dots (5)$$

$-\theta_s = 0$

*The Equation of State*

$$\rho = F(s, t) \dots\dots\dots (6)$$

where:

$\tau$  = applied forces (e.g. wind stress, bed shear stress, Coriolis force)

$\theta_s$  = salinity source/sink term

Now we reduce the number of unknowns requiring a simultaneous solution from 6 to 3.

Assuming that the influence of vertical momentum on the system is small and may be neglected, equation 3 reduces to the following equation:

$$\frac{\partial p}{\partial z} + \rho g = 0 \dots\dots\dots (7)$$

Equation 7 is a statement that the vertical pressure distribution is hydrostatic.

Equation 4 may then be integrated in the vertical direction to yield the following equation:

$$\int_a^{a+h} \left( \frac{\partial u}{\partial x} + \frac{\partial v}{\partial y} \right) d\eta = - \int_a^{a+h} \frac{\partial w}{\partial z} d\eta = -w_s + w_b \dots\dots\dots (8)$$

where:

$w_s$  = the vertical velocity at the water surface

$w_b$  = the vertical velocity at the bed

The surface velocity can be expressed as follows:

$$w_s = u_s \frac{\partial(z_b + h)}{\partial x} + v_s \frac{\partial(z_b + h)}{\partial y} + \frac{\partial(z_b + h)}{\partial t} \dots\dots\dots (9)$$

Similarly, the bed velocity can be expressed as:

$$w_b = u_b \frac{\partial z_b}{\partial x} + v_b \frac{\partial z_b}{\partial y} + \frac{\partial z_b}{\partial t} \dots\dots\dots (10)$$

where:

$u_s, v_s$  = the surface horizontal velocity components

$u_b, v_b$  = the near bed horizontal velocity components

$z_b$  = the bed elevation

Note that by replacing equations 3 and 4 with 6 and 8, we recast the equations such that  $w$  is present only in the horizontal momentum equations and the advection diffusion equation. It can now be solved in a separate decoupled calculation using the original form of the continuity equation (equation 4). This is done by taking the derivative of equation 4 with respect to  $z$  and solving for  $w$ , applying  $w_s$  and  $w_b$  as boundary conditions.

We can further eliminate  $\rho$  from the list of unknowns requiring a simultaneous solution by solving the equation of state (equation 6) in a decoupled step.

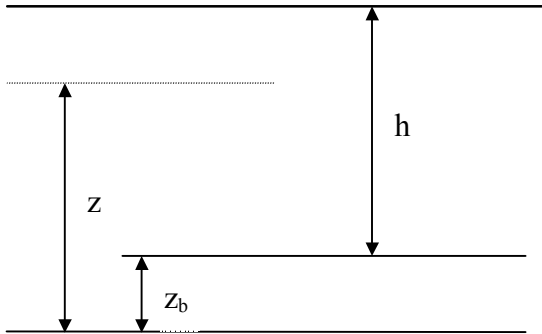
Thus, we are left with 4 equations (1,2,8 and 5) and 4 unknowns ( $u,v,h$  and  $s$ ) to be solved simultaneously. In practice, however, the solution is broken up into 2 steps: First the velocities and depth are solved simultaneously, and then the constituent concentration is solved. This method improves solution efficiency dramatically over the simultaneous solution of all 4 equations and unknowns.

Hence, the solution of a system of 4 equations and 4 unknowns becomes the solution of a system of 3 equations (1,2, and 8) and 3 unknowns ( $u,v$ , and  $h$ ), followed by the solution of 1 equation (5) and 1 unknown ( $s$ ).

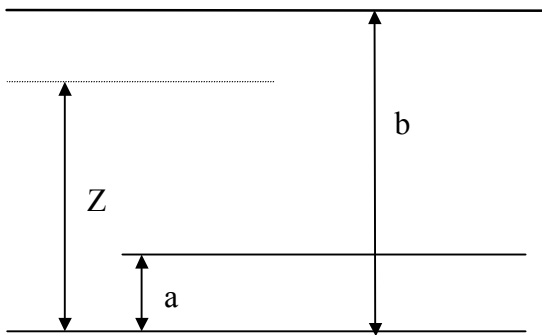
*Geometric transform*

In order to use a fixed geometry to model a system with a time varying vertical dimension (depth) it is convenient to use a geometric transformation to map the system to a fixed geometry.

*Time varying system*



*Fixed grid system*



The transformation is based on the following relation:

$$\frac{h}{(z - z_b)} = \frac{(b - a)}{(Z - a)} \dots\dots\dots (11)$$

$$z = \frac{(Z - a)}{(b - a)} h + z_b \dots\dots\dots (12)$$

Hence:

$$U(x, y, z) = u(X, Y, \left( \left( \frac{Z - a}{b - a} \right) h + z_b \right)) \dots\dots\dots (13)$$

After completing the transformation of the terms and simplifying, we arrive at the following transformed equations:

*The Momentum Equations*

$$\left\{ \begin{array}{l} \rho \left[ h \frac{\partial u}{\partial t} + hu \frac{\partial u}{\partial x} + hv \frac{\partial u}{\partial y} + \frac{\partial u}{\partial z} (b - a) \left( w - uT_x - vT_y - \frac{(z - a)}{(b - a)} \frac{\partial h}{\partial t} - \frac{\partial z_b}{\partial t} \right) \right] \\ - h \frac{\partial}{\partial x} \left( \varepsilon_{xx} \frac{\partial u}{\partial x} \right) - h \frac{\partial}{\partial y} \left( \varepsilon_{xy} \frac{\partial u}{\partial y} \right) - (b - a) \frac{\partial}{\partial z} \left( \varepsilon_{xz} \left( \frac{(b - a)}{h} \right) \frac{\partial u}{\partial z} \right) \\ + \rho gh \frac{\partial z_b}{\partial x} + \rho gh \frac{\partial h}{\partial x} + h \frac{\partial p}{\partial x} + \rho gh \frac{\partial h_D}{\partial x} - h\tau_x \end{array} \right\} \frac{1}{(b - a)} = 0 \quad (14)$$

$$\left\{ \begin{array}{l} \rho \left[ h \frac{\partial v}{\partial t} + hu \frac{\partial v}{\partial x} + hv \frac{\partial v}{\partial y} + \frac{\partial v}{\partial z} (b - a) \left( w - uT_x - vT_y - \frac{(z - a)}{(b - a)} \frac{\partial h}{\partial t} - \frac{\partial z_b}{\partial t} \right) \right] \\ - h \frac{\partial}{\partial x} \left( \varepsilon_{yx} \frac{\partial v}{\partial x} \right) - h \frac{\partial}{\partial y} \left( \varepsilon_{yy} \frac{\partial v}{\partial y} \right) - (b - a) \frac{\partial}{\partial z} \left( \varepsilon_{yz} \left( \frac{(b - a)}{h} \right) \frac{\partial v}{\partial z} \right) \\ + \rho gh \frac{\partial z_b}{\partial y} + \rho gh \frac{\partial h}{\partial y} + h \frac{\partial p}{\partial y} + \rho gh \frac{\partial h_D}{\partial y} - h\tau_y \end{array} \right\} \frac{1}{(b - a)} = 0 \quad (15)$$

*Volume Continuity*

$$\int_a^b \left[ \frac{h}{(b-a)} \left( \frac{\partial u}{\partial x} + \frac{\partial v}{\partial y} \right) - \frac{\partial u}{\partial z} T_x - \frac{\partial v}{\partial z} T_y \right] dz + u_s \frac{\partial(z_b + h)}{\partial x} + v_s \frac{\partial(z_b + h)}{\partial y} + \frac{\partial(z_b + h)}{\partial t} - u_b \frac{\partial z_b}{\partial x} - v_b \frac{\partial z_b}{\partial y} - \frac{\partial z_b}{\partial t} = 0 \dots\dots (16)$$

*Advection-Diffusion Equation*

$$\left\{ \begin{array}{l} h \frac{\partial s}{\partial t} + hu \frac{\partial s}{\partial x} + hv \frac{\partial s}{\partial y} + \frac{\partial s}{\partial z} (b-a) \left( w - uT_x - vT_y - \frac{(z-a)}{(b-a)} \frac{\partial h}{\partial t} - \frac{\partial z_b}{\partial t} \right) \\ -h \frac{\partial}{\partial x} \left( D_x \frac{\partial s}{\partial x} \right) - h \frac{\partial}{\partial y} \left( D_y \frac{\partial s}{\partial y} \right) - (b-a) \frac{\partial}{\partial z} \left( D_z \left( \frac{(b-a)}{h} \right) \frac{\partial s}{\partial z} \right) - h\theta_s \end{array} \right\} \frac{1}{(b-a)} = 0 \quad (17)$$

where:

$$T_x = \frac{\partial z_b}{\partial x} + \frac{(z-a)}{(b-a)} \frac{\partial h}{\partial x} - \frac{h}{(b-a)} \frac{\partial a}{\partial x} + \frac{(z-a)}{(b-a)^2} h \frac{\partial a}{\partial x} \dots\dots\dots (18)$$

$$T_y = \frac{\partial z_b}{\partial y} + \frac{(z-a)}{(b-a)} \frac{\partial h}{\partial y} - \frac{h}{(b-a)} \frac{\partial a}{\partial y} + \frac{(z-a)}{(b-a)^2} h \frac{\partial a}{\partial y} \dots\dots\dots (19)$$

$$h_D = -\frac{(b-z)}{(b-a)} h \dots\dots\dots (20)$$

2-D Vertically Averaged Equations

If  $u, v,$  and  $s$  are assumed constant with respect to elevation ( $z$ ), the 3-D equations can be integrated over depth to yield 2-D vertically averaged equations. For example, the X-momentum equation reduces to the following:

$$\left\{ \begin{array}{l} \rho(b-a) \left[ h \frac{\partial u}{\partial x} + hu \frac{\partial u}{\partial x} + hv \frac{\partial u}{\partial y} \right] \\ -h(b-a) \frac{\partial}{\partial x} \left( \epsilon_{xx} \frac{\partial u}{\partial x} \right) - h(b-a) \frac{\partial}{\partial y} \left( \epsilon_{xy} \frac{\partial u}{\partial y} \right) \\ + \rho gh(b-a) \left( \frac{\partial z_b}{\partial x} + \frac{\partial h}{\partial x} \right) + (b-a) \frac{gh^2}{2} \frac{\partial \rho}{\partial x} - h(b-a)\tau_x \end{array} \right\} \frac{1}{(b-a)} = 0 \dots\dots\dots (21)$$

Similarly, the continuity equation reduces to:

$$h \left( \frac{\partial u}{\partial x} + \frac{\partial v}{\partial y} \right) + u \frac{\partial h}{\partial x} + v \frac{\partial h}{\partial y} + \frac{\partial h}{\partial t} = 0 \dots\dots\dots (22)$$

And the advection-diffusion equation reduces to:

$$\left\{ \begin{array}{l} h(b-a) \frac{\partial s}{\partial t} + h(b-a)u \frac{\partial s}{\partial x} + h(b-a)v \frac{\partial s}{\partial y} \\ -h(b-a) \frac{\partial}{\partial x} \left( D_x \frac{\partial s}{\partial x} \right) - h(b-a) \frac{\partial}{\partial y} \left( D_y \frac{\partial s}{\partial y} \right) - h(b-a)\theta_s \end{array} \right\} \frac{1}{(b-a)} = 0 \dots\dots\dots (23)$$

## 2-D Laterally Averaged Equations

Lateral averaging eliminates the momentum equation in the direction normal to the dominant flow direction. The equations are integrated across the width of the channel. This operation requires that the channel width  $c$  is specified. For the purposes of TABS-MDS, the channel width in laterally averaged elements is constrained such that it is constant with respect to depth, but can vary with respect to  $x$  and  $y$  (i.e. along the channel length). For example, the X-momentum equation reduces to the following.

$$\left\{ \begin{array}{l} \rho \left[ h \frac{\partial u}{\partial t} + hu \frac{\partial u}{\partial x} + \frac{\partial u}{\partial z} (b-a) \left( w - uT_x - \frac{(z-a)}{(b-a)} \frac{\partial h}{\partial t} - \frac{\partial z_b}{\partial t} \right) \right] \\ - h \frac{\partial}{\partial x} \left( \epsilon_{xx} \frac{\partial u}{\partial x} \right) - (b-a) \frac{\partial}{\partial z} \left( \epsilon_{xz} \left( \frac{(b-a)}{h} \right) \frac{\partial u}{\partial z} \right) \\ + \rho gh \frac{\partial z_b}{\partial x} + \rho gh \frac{\partial h}{\partial x} + h \frac{\partial p}{\partial x} + \rho gh \frac{\partial h_D}{\partial x} - h\tau_x \end{array} \right\} \frac{c}{(b-a)} = 0 \dots\dots\dots (24)$$

Similarly, the continuity equation reduces to:

$$\int_a^b \left[ \frac{h}{(b-a)} \left( c \frac{\partial u}{\partial x} + u \frac{\partial c}{\partial x} \right) - c \frac{\partial u}{\partial z} T_x \right] dz + cu_s \frac{\partial (z_b + h)}{\partial x} + \frac{\partial (z_b + h)}{\partial t} - cu_b \frac{\partial a}{\partial x} - \frac{\partial z_b}{\partial t} = 0 \dots\dots\dots (25)$$

And the advection-diffusion equation reduces to:

$$\left\{ \begin{array}{l} h \frac{\partial s}{\partial t} + hu \frac{\partial s}{\partial x} + \frac{\partial s}{\partial z} (b-a) \left( w - uT_x - \frac{(z-a)}{(b-a)} \frac{\partial h}{\partial t} - \frac{\partial z_b}{\partial t} \right) \\ - h \frac{\partial}{\partial x} \left( D_x \frac{\partial s}{\partial x} \right) - (b-a) \frac{\partial}{\partial z} \left( D_z \left( \frac{(b-a)}{h} \right) \frac{\partial s}{\partial z} \right) - h\theta_s \end{array} \right\} \frac{c}{(b-a)} = 0 \dots\dots\dots (26)$$

## 1-D Equations

Under this approximation both vertical and lateral integration are applied. Hence, the form of the cross-section must be defined. In TABS-MDS, the cross section is assumed trapezoidal, with allowance made for off-channel storage.

For example, the X-momentum equation reduces to the following:

$$\left\{ \begin{array}{l} \rho \left[ A \frac{\partial u}{\partial t} + Au \frac{\partial u}{\partial x} \right] \\ - A \frac{\partial}{\partial x} \left( \varepsilon_{xx} \frac{\partial u}{\partial x} \right) \\ + \rho g A \frac{\partial z_b}{\partial x} + \rho g A \frac{\partial h}{\partial x} + \frac{gAh}{2} \frac{\partial \rho}{\partial x} - A \tau_x \end{array} \right\} = 0 \dots\dots\dots (27)$$

Similarly, the continuity equation reduces to:

$$A \left( \frac{\partial u}{\partial x} \right) + u \frac{\partial A}{\partial x} + \frac{\partial (A + A_{oc})}{\partial t} = 0 \dots\dots\dots (28)$$

And the advection diffusion equation reduces to:

$$\left\{ (A + A_{oc}) \frac{\partial s}{\partial t} + A \frac{\partial s}{\partial x} - A \frac{\partial}{\partial x} \left( D_x \frac{\partial s}{\partial x} \right) - A \theta_s \right\} = 0 \dots\dots\dots (29)$$

where:

A = The main channel cross-sectional area

A<sub>oc</sub>= The off-channel storage cross-sectional area

Finite Element Formulation

In order to generate the finite element equations, we must integrate each of the equations over the element volume (for 3-D), area (for 2-D), or length (for 1-D), remembering to include the weight function in the integration (which, for the Galerkin method, is the same as the basis function).

In addition, we must recast the higher-order terms using integration by parts. This causes the boundary terms to drop out of the equations. For example,

Take the following pressure term, multiplied through by a weight function N.

$$N \frac{\rho g h}{(b-a)} \frac{\partial h}{\partial x} \dots\dots\dots (30)$$

This can be rewritten as:

$$N \frac{\rho g}{2(b-a)} \frac{\partial h^2}{\partial x} \dots\dots\dots (31)$$

Then , it can be integrated by parts:

$$N \frac{\rho g}{2(b-a)} \frac{\partial h^2}{\partial x} = \frac{\partial}{\partial x} \left( N \frac{\rho g h^2}{2(b-a)} \right) - \frac{\partial N}{\partial x} \left( \frac{\rho g h^2}{2(b-a)} \right) \dots\dots\dots (32)$$

$$- N \frac{g h^2}{2(b-a)} \frac{\partial \rho}{\partial x} - N \frac{\rho g h^2}{2(b-a)^2} \frac{\partial a}{\partial x}$$

Note that the first term on the right hand side of the equation can be evaluated as an area integral via the Gauss Divergence Theorem. Hence, it becomes a boundary term.

### Time Derivative Solution Method

The time derivative is approximated with a simple, fully-implicit finite difference formulation. I.e.,

$$\frac{\partial \beta_t}{\partial t} = \frac{(\beta_t - \beta_{t-\Delta t})}{\Delta t} \dots\dots\dots (33)$$

where:

$\beta_t$  = any of the unknown variables at time t.

$\Delta t$  = the time step

### Newton-Rhapson Implementation

Once the finite element equations are built, they are solved using the Newton-Rhapson iterative method. In order to do this, partial derivatives with respect to each of the unknown variables must be derived for each system equation. These derivatives compose the stiffness matrix, and are used to drive the residual (i.e. the integral of each equation across an element) to 0.

$$\begin{bmatrix} X_u & Y_u & Z_u \\ X_v & Y_v & Z_v \\ X_h & Y_h & Z_h \end{bmatrix} \begin{bmatrix} u \\ v \\ h \end{bmatrix} = \begin{bmatrix} X \\ Y \\ Z \end{bmatrix} \dots\dots\dots (34)$$

## Expressions for Applied Loads and Turbulent Mixing

### Bed Shear Stress

The bed shear stress is given by a modified form of Manning's Equation, as given by Christensen (1970). Any of 3 expressions can be used, depending on the instantaneous value of the depth/roughness height ratio ( $\frac{d}{k}$ ). The expressions are as follows (given for the X-direction only):

$$\text{for } \frac{d}{k} < 4.32 \quad \tau_x = \frac{\rho g}{L^2} \frac{|v|v_x}{d^{2/3}} \quad \text{where } L = \frac{6.46\sqrt{g}}{k^{1/3}} \dots\dots\dots (35)$$

$$\text{for } 4.32 < \frac{d}{k} < 276 \quad \tau_x = \frac{\rho g}{M^2} \frac{|v|v_x}{d^{1/3}} \quad \text{where } M = \frac{8.25\sqrt{g}}{k^{1/6}} \dots\dots\dots (36)$$

$$\text{for } \frac{d}{k} > 276 \quad \tau_x = \frac{\rho g}{N^2} \frac{|v|v_x}{d^{1/6}} \quad \text{where } N = \frac{13.18\sqrt{g}}{k^{1/12}} \dots\dots\dots (37)$$

where:

$\tau_x$  = the bed shear in the X-direction

$k$  = the roughness height

$d$  = the local depth

$v$  = the local velocity

$g$  = the gravitational constant

$\rho$  = the density of water

$k$  is found as a function of Manning's  $n$  from the following expression:

$$k = \left( \frac{8.25\sqrt{\text{g n}}}{1.486} \right)^6 \dots\dots\dots (38)$$

The Wind Stress

The wind stress is given by the following expression (given for the X-direction only):

$$\tau_{wx} = \rho_a C_w V_w^2 \cos\theta_w \dots\dots\dots (39)$$

where:

$\tau_{wx}$  = the wind stress in the X-direction

$\rho_a$  = the density of air

$V_w$  = the wind velocity

$\theta_w$  = the direction from which the wind is blowing, measured counterclockwise from the positive X- axis.

$C_w$  = the wind stress coefficient

For deep water, the wind stress coefficient is given by Wu (1980).

$$C_w = \frac{0.8 + 0.065 \times V_w}{1000} \dots\dots\dots (40)$$

For shallow water, the wind stress is given by Teeter et. al., (2001)

$$C_w = \left( \frac{0.4}{16.11 - 0.5 \ln(d) - 2.48 \ln(V_w)} \right)^2 \times \left( 1 - \frac{1.118}{\sqrt{V_{w1}}} e^{-6(d_1-2)} \right) \dots\dots\dots (41)$$

where:

d = the local water depth (in meters)

$d_1$  = the maximum of the local water depth (in meters) and 2 meters

$V_{w1}$  = the maximum of the wind velocity (in m/s) and 5.063 m/s

Horizontal Turbulent Mixing and Diffusion

Horizontal Turbulent mixing can be specified directly, or it can be controlled by the method of Smagorinsky (1963). A description of this method follows.

The Smagorinsky method of describing horizontal eddy viscosities and diffusion coefficients is a “tensorially invariant generalization of the mixing length type representation” (Speziale, 1998). The Smagorinsky description of the turbulent mixing terms in the Navier-Stokes Equations are given as follows. For the x-momentum equation

$$\rho h \frac{\partial}{\partial x} \left( 2S \frac{\partial u}{\partial x} \right) + \rho h \frac{\partial}{\partial y} \left( S \left( \frac{\partial u}{\partial y} + \frac{\partial v}{\partial x} \right) \right) \dots\dots\dots (42)$$

For the y momentum equation

$$\rho h \frac{\partial}{\partial y} \left( 2S \frac{\partial v}{\partial y} \right) + \rho h \frac{\partial}{\partial x} \left( S \left( \frac{\partial u}{\partial y} + \frac{\partial v}{\partial x} \right) \right) \dots\dots\dots (43)$$

where:

$$\dots\dots\dots S = kA \left[ \left( \frac{\partial u}{\partial x} \right)^2 + \left( \frac{\partial v}{\partial y} \right)^2 + \frac{1}{2} \left( \frac{\partial u}{\partial y} + \frac{\partial v}{\partial x} \right)^2 \right]^{\frac{1}{2}} \quad (44)$$

k = Smagorinsky coefficient, usually given a value ranging from approximately 0.005 for rivers to 0.05 for estuaries and lakes (Speziale, 1998; Thomas et al, 1995)

A = the surface area of the element

The Smagorinsky description of the turbulent diffusion terms in the advection-diffusion equation is given as follows:

$$h \frac{\partial}{\partial x} \left( 2S \frac{\partial C}{\partial x} \right) + h \frac{\partial}{\partial y} \left( 2S \frac{\partial C}{\partial y} \right) \dots\dots\dots (45)$$

In order to promote numerical stability, TABS-MDS provides a means of establishing minimum values of turbulent mixing and turbulent diffusion. These values are used in place of the Smagorinsky term (S) when they are found to exceed the value of that term. The minimum turbulent mixing value is given by the following equation:

$$S_{Emin} = TBMINF \times \rho \alpha \sqrt{A} \dots\dots\dots (46)$$

The minimum turbulent diffusion value is given by the following equation:

$$S_{Dmin} = TBMINFS \times \alpha \sqrt{A} \dots\dots\dots (47)$$

where

TBMINF = minimum turbulent mixing factor (default = 1.0)

TBMINFS = minimum diffusion factor (default = 1.0)

$\alpha$  = a coefficient, given as  $5.00 \times 10^{-3}$  ft/sec or  $1.52 \times 10^{-3}$  m/s, depending on the unit system being used in the simulation. This value is an arbitrary estimate of the minimum turbulent mixing needed to ensure model stability. It equals the value of eddy viscosity/diffusion which corresponds to a Peclet number of 40 and a velocity magnitude of 0.2 ft/sec.

Also, if  $|V| < TBMINF \times V_{min}$ ,  $S_{Emin}$  is applied, regardless of the turbulent mixing as given by the Smagorinsky calculation. This is done to inhibit numerical instability in areas with both extremely small velocities and high velocity gradients.

Vertical Turbulent Mixing and Diffusion

Vertical turbulent mixing and diffusion are given by the method of Mellor-Yamada (1982) with a modification according to Hendersen-Sellers (1984).

The Mellor-Yamada expressions for vertical eddy viscosity and diffusion are given as follows:

$$E_{xz} = E_{yz} = \rho S_m l_m q \dots\dots\dots (48)$$

$$D_z = S_h l_m q \dots\dots\dots (49)$$

where:

$$l_m = 0.4(z - a) \left| 1 - \frac{(z - a)}{h} \right|^{\frac{1}{2}} \dots\dots\dots (50)$$

$$q = \left\{ b_1 l_m^2 S_m \left[ \left| \frac{\partial u}{\partial z} \right|^2 + \left| \frac{\partial v}{\partial z} \right|^2 \right] \right\}^{\frac{1}{2}} \dots\dots\dots (51)$$

$$S_m = 0.393$$

$$S_h = 0.494$$

$$b_1 = 16.6$$

The Henderson-Sellers adjustment is a factor that accounts for the dampening affect on turbulence induced by stable stratification. The factor is expressed in terms of the Richardson Number:

$$R_i = \frac{-g(\partial\rho/\partial z)}{\rho \left[ \left( \frac{\partial u}{\partial z} \right)^2 + \left( \frac{\partial v}{\partial z} \right)^2 \right]} \dots\dots\dots (52)$$

For vertical diffusion of momentum (i.e. vertical eddy viscosity) the expression is given as follows:

$$E_z = \frac{E_{z0}}{(1 + 0.74R_i)} \dots\dots\dots (53)$$

Where  $E_z$  is the vertical eddy viscosity, and  $E_{z0}$  is the vertical eddy viscosity assuming no stratification influence on the turbulence (i.e. the value taken from Mellor-Yamada).

For vertical diffusion of salinity (i.e. vertical diffusion coefficient) the expression is given as follows:

$$D_z = \frac{D_{z0}}{(1 + 37R_i^2)} \dots\dots\dots (54)$$

Where  $D_z$  is the vertical diffusion coefficient, and  $D_{z0}$  is the vertical diffusion coefficient assuming no stratification influence on the turbulence (i.e. the value taken from Mellor-Yamada).

## References

Christensen, B. A. (1970) *Manning's n For Cast-In-Place Concrete Pipe; Discussions by Bent A. Christensen, and R. Sakthivadivel, S. Seetharaman and M.V. Somasundaram*, Journal of the Hydraulics Division, Proceedings of the American Society of Civil Engineers, Vol. 96, No. HY3.

Henderson-Sellers, B. (1984) *Engineering Limnology*, Pitman Advanced Publishing, Boston, pp 81-91.

King, I.P. (1988) *A Finite Element Model for Three Dimensional Hydrodynamic Systems*, Report prepared by Resource Management Associates, Lafayette California, for U.S. Army Corps of Engineers, Waterways Experiment Station, Vicksburg, Mississippi.

Mellor, G.L. and Yamada, T. (1982) *Development of a Turbulence Closure Model for Geophysical Fluid Problems*, Reviews of Geophysics and Space Physics, Vol20, No.4, pp 851-875.

Smagorinsky, J. (1963) *General Circulation Experiments with the Primitive Equations, I. The Basic Experiment*, Monthly Weather Review, 91, 99-164.

Speziale, Charles G. (1998) *Turbulence Modeling for Time-Dependent RANS and VLES: A Review*, AIAA Journal, Vol 36, No 2, pp 173-184.

Teeter, A. M., Johnson, B. H., Berger, C., Stelling, G., Scheffner, N. W., Garcia, M. H., Parchure, T. M., (2001) *Hydrodynamic and Sediment Transport Modeling With Emphasis on Shallow-water, Vegetated Areas (Lakes, Reservoirs, Estuaries, and Lagoons)*. Hydrobiologia 444: 1-23.

Thomas, T.G., Williams, J.R.R. (1995) *Large Eddy Simulation of a Symmetric Trapezoidal Channel at a Reynolds Number of 430,000*, Journal of Hydraulic Research, Vol 33, No 6, pp 825-830.

# Appendix B

---

## **Desktop Off-Channel Wetland Salinity Mitigation Model (DOWSMM)**

### **Theoretical Development and User's Manual DRAFT**

Gary L. Brown and Trimbak Parchure

USACE-ERDC-CHL

**July, 2005**

## Desktop Off-Channel Wetland Salinity Mitigation Model (DOWSMM)

The following gives the theoretical development of the Desktop Off-Channel Wetland Salinity Mitigation Model (DOWSMM). Included are the desktop model equations, the solution method, the input and output parameters, the simplifying assumptions used in the model and the limitations of the model.

This desktop model is intended to yield a time-history of the approximate predicted salinity values in an off-channel wetland, either with or without an inlet structure applied to mitigate salinity impacts. This enables the user to ascertain the effectiveness of a given salinity mitigation structure.

This desktop model is derived with many simplifying assumptions. Therefore, the model should only be used with sound engineering judgment, and with a full understanding of the assumptions and limitations involved, and the impact of those assumptions and limitations on the uncertainty of the results.

### **Introduction**

Assume there is a wetland connected via a single primary inlet to a large main channel or estuary (Figure 1). Assume also that salinity mitigation in the wetland is desired, and that a submerged weir structure is proposed for the inlet (Figure 2). DOWSMM is designed to evaluate this scenario, and to determine the effectiveness of the structure in achieving the salinity mitigation.

The user supplies the DOWSMM model with time-history tables of the salinity and water surface elevation at the inlet, as well as a time-history table of the net precipitation in the wetland (rainfall minus evaporation). The user also supplies the model with pertinent information to define the dimensions of the wetland, the inlet, and the mitigation structure. The model output yields time-history tables of the velocity in the inlet and the salinity in the wetland. Comparison of the salinity output results both with and without the proposed mitigation structure yield the necessary information to evaluate the effectiveness of the structure at mitigating the salinity in the wetland.

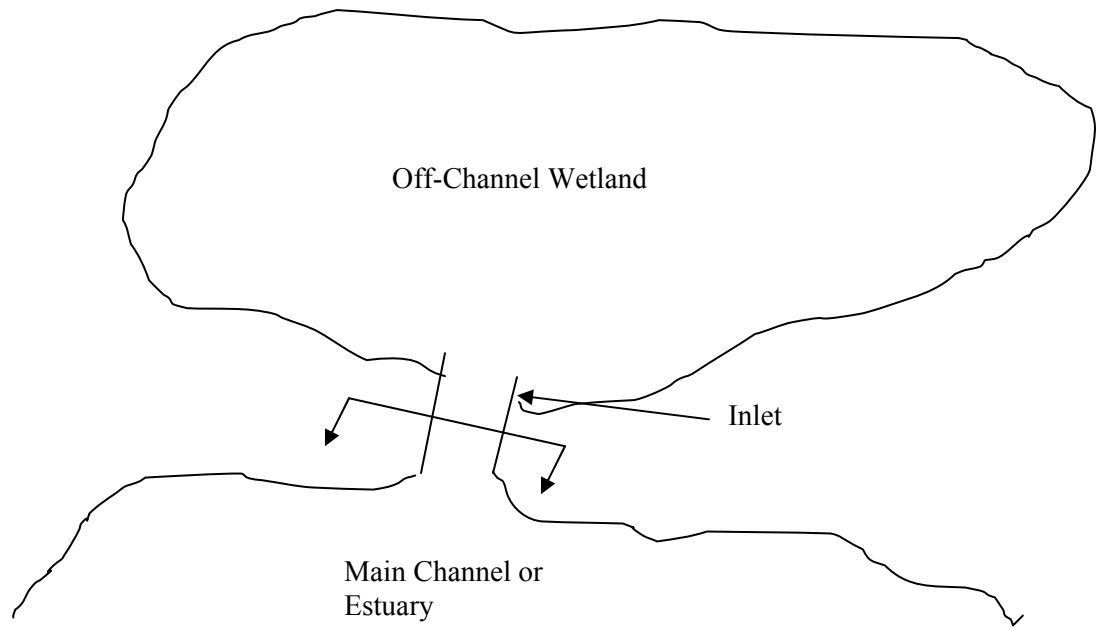


Figure 1: Schematic Diagram of an Off-Channel Wetland with a Single Inlet

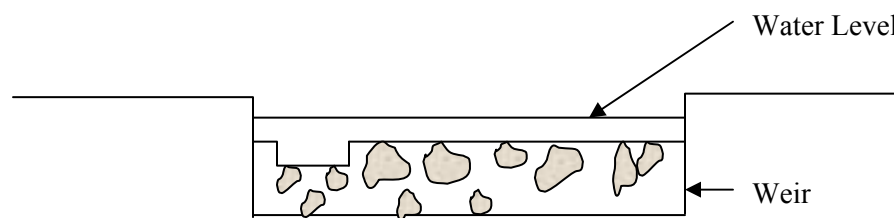


Figure 2: Schematic Diagram of a Submerged Weir with a Boat Bay

**Desktop Model Equations**

Applying the conservation of energy across the inlet yields the following (assuming quasi-steady flow):

$$\eta_I - \eta_W = \zeta_T \frac{v_I^2}{2g} \dots\dots\dots$$

(1)

The velocity in the inlet is given as follows:

$$v_I = \frac{Q_I}{W_I(\eta_I - z_I)} \dots\dots\dots$$

(2)

The discharge through the inlet can be derived from the conservation of water mass:

$$Q_I = \frac{A_{S,W} \alpha_{WS,W} (\eta_W - \eta_{W,o})}{\Delta t} - Q_{RE} \dots\dots\dots$$

(3)

Where the volumetric rainfall rate is given as follows:

if  $q_{RE} > 0$ ,  $Q_{RE} = q_{RE} A_{S,W} \dots\dots\dots$  (4)

if  $q_{RE} < 0$ ,  $Q_{RE} = q_{RE} A_{S,W} \alpha_{WS,W} \dots\dots\dots$  (5)

Combining Equations 1-5 and solving for  $\eta_W$  yields the following equation.

$$\eta_W = \frac{-b + \sqrt{b^2 - 4ac}}{2a} \dots\dots\dots$$

(6)

Where:

$$a = K_{TE} \dots\dots\dots$$

(7)

$$b = 1 - 2K_{TE} \eta_{W,o} - 2K_{TRE} \dots\dots\dots$$

(8)

$$c = K_{TE} \eta_{W,o}^2 + K_{RE} + 2K_{TRE} \eta_{W,o} - \eta_I \dots\dots\dots$$

(9)

The constants  $K_{TE}$  and  $K_{RE}$  are given as:

$$K_{TE} = \frac{\zeta_T A_{S,W}^2}{2gW_I^2 (\eta_I - z_I)^2 \Delta t^2} \dots\dots\dots$$

(10)

$$K_{TRE} = \frac{\zeta_T A_{S,W} Q_{RE}}{2gW_I^2 (\eta_I - z_I)^2 \Delta t} \dots\dots\dots$$

(11)

$$K_{RE} = \frac{\zeta_T Q_{RE}^2}{2gW_I^2 (\eta_I - z_I)^2} \dots\dots\dots$$

(12)

Note that  $K_{TE}$ ,  $K_{TRE}$  and  $K_{RE}$  need to be multiplied by  $-1$  when the flow is out of the wetland ( $Q_I < 0$  from Equation 3). This ensures that friction is always included as a net loss of energy.

Since the direction of the flow is unknown, the quantities in Equations 10-12 are initially assumed positive, and a solution is obtained for Equation 6. Note, however, that if the quantity  $(b^2 - 4ac)$  in Equation 6 is less than 0, the signs of the quantities in equations 10-12 must be changed before Equation 6 can be solved.

The result of the solution of Equation 6 is then used to find the inlet discharge from Equation 3. If the sign of the discharge that results from the solution of Equation 3 is not the same as the signs of the quantities in Equations 10-12, the signs of these quantities are changed and Equation 6 is resolved.

The total friction loss is equal to the local loss as the inlet plus the loss due to friction in the wetland, or:

$$\zeta_T = \zeta_L + \zeta_F \dots\dots\dots$$

(13)

The local loss as the inlet is equal to the sum of the inlet and exit losses (approximated as 1.06), as well as the loss due to the presence of the structure. The loss due to the presence of the structure is approximated by summing Borda's expression for a sudden enlargement loss, and Brighmore's expression for a contraction loss. These expressions can be found in the following source:

Brater, E. F., and King, H. W.(1976) *Handbook of Hydraulics*, Sixth Edition, McGraw-Hill., pp 6-21, 6-23.

The final equation is given as follows:

$$\zeta_L = 1.06 + 1.7 \left( \frac{\eta_I - z_I}{\eta_I - z_S} - 1 \right)^2 \dots\dots\dots (14)$$

Note that the quantity  $(\eta_I - z_S)$  in Equation 14 is not permitted to be less than 0.1ft. Also, note that only a single value for the elevation of the sill is permitted. Therefore, sills that have a variable elevation across the inlet (such as sills designed with a boat bay) are assigned a sill elevation value equal to the average sill elevation across the inlet.

The friction loss in the wetland is approximated with the following equation:

$$\zeta_F = \sqrt{A_{S,W}} \frac{k_S^{1/3}}{34.03(\eta_W - z_W)^{4/3}} \left( \frac{W_I(\eta_I - z_I)}{\sqrt{A_{S,W}} \alpha_{WS,W} (\eta_W - z_W)} \right)^2 \dots\dots\dots (15)$$

Where, for English Units,:

$$k_S = (31.512 n)^6 \dots\dots\dots (16)$$

By applying both the conservation of water mass and of salt mass, the following equations for the salinity in the wetland are derived:

$$\text{if } Q_I > 0, s_W = \frac{s_I Q_I \Delta t + s_{W,o} A_{S,W} \alpha_{WS,W} (\eta_{W,o} - z_W)}{(Q_I + Q_{RE}) \Delta t + A_{S,W} \alpha_{WS,W} (\eta_{W,o} - z_W)} \dots\dots\dots (17)$$

$$\text{if } Q_I \leq 0, s_W = \frac{s_{W,o} A_{S,W} \alpha_{WS,W} (\eta_{W,o} - z_W)}{Q_{RE} \Delta t + A_{S,W} \alpha_{WS,W} (\eta_{W,o} - z_W)} \dots\dots\dots (18)$$

Note that the quantity  $(\eta_{W,o} - z_W)$  in Equations 17 and 18 is not permitted to be less than 0.01ft.

## Solution Method

The model solution proceeds as follows:

- 1) Step forward one time step
- 2) Set  $\eta_{W,o} = \eta_W$  and set  $s_{W,o} = s_W$ .
- 3) Read in the new values of  $\eta_I$ ,  $s_I$ , and,  $q_{RE}$  from the input files

- 4) Solve Equation (4) or (5) to obtain  $Q_{RE}$ .
- 5) Solve Equation (6) to obtain  $\eta_w$ . If the quantity  $(b^2-4ac)$  in Equation 6 is less than zero, change the signs of the quantities  $K_{TE}$ ,  $K_{TRE}$  and  $K_{RE}$  in Equations 10 –12 before solving Equation 6.
- 6) Solve Equations (2) and (3) to obtain  $v_I$  and  $Q_I$ .
- 7) If the sign of  $Q_I$  is not the same as the signs of the quantities  $K_{TE}$ ,  $K_{TRE}$  and  $K_{RE}$  (from Equations 10-12), change the signs of these quantities and repeat from step 5.
- 8) Solve Equation 17 or 18 to obtain  $s_w$ .
- 9) Repeat Step 1

For the first time step in the series, it is assumed that the initial conditions of the wetland are given as follows:  $\eta_{w,0} = \eta_I$  and set  $s_{w,0} = s_I$ .

## Input and Output Parameters

The input parameters are as follows:

- The filename for the time-history file with the water surface elevation data at the inlet
- The filename for the time-history file with the salinity data at the inlet
- The filename for the time-history file with the net precipitation data for the wetland.
- The filename for the output results file.
- The surface area of the wetland,  $A_{S,W}$
- The wetted surface area factor,  $\alpha_{WS,W}$  (between 0 and 1)
- Manning's  $n$  for the wetland,  $n$
- The width of the inlet,  $W_I$
- The elevation of the bed of the inlet,  $z_I$
- The elevation of the top of the sill in the inlet,  $z_S$
- The elevation of the bed in the wetland,  $z_W$

The time history files consist of two columns of data. The first column is the time (in hours), and the second column is the data value. The first line of each time-history file is assumed to be a text header.

The following is a sample of model input.

```
t-mf-7.txt
s-mfhd-7.txt
dt-mf-rainevap.txt
tx-81-B-st-hd-out.txt
227078280.
.75
```

0.08  
 40.  
 -5.8  
 -0.1  
 0.0

Note that, if there is no structure in the inlet, the sill elevation can just be set equal to the bed elevation in the inlet.

The output parameters are as follows:

- Time,  $t$ , (hours)
- The water surface elevation in the inlet,  $\eta_I$ , (ft)
- The water surface elevation in the wetland,  $\eta_W$ , (ft)
- The discharge through the inlet,  $Q_I$ , (cfs)
- The velocity in the inlet,  $v_I$ , (ft/sec)
- The salinity in the inlet,  $s_I$ , (ppt)
- The salinity in the wetland,  $s_W$ , (ppt)

The discharge and velocity are both defined as positive quantities for flow into the wetland (flood-tide).

The following is a sample of model output:

Time	z-inlet	z-wetland	q	vel	s-inlet	s-wetland
3648.000	1.200	1.200	10.6	0.050	1.500	1.501
3649.000	1.200	1.200	7.9	0.037	1.500	1.503
3650.000	1.190	1.194	-57.1	-0.271	1.500	1.504
3651.000	1.190	1.191	-23.6	-0.112	1.500	1.505
3652.000	1.190	1.190	-0.3	-0.002	1.500	1.507
3653.000	1.200	1.196	77.1	0.365	1.500	1.508
3654.000	1.220	1.207	131.6	0.619	1.500	1.509
3655.000	1.230	1.218	129.9	0.610	1.500	1.511
3656.000	1.240	1.228	128.5	0.602	1.500	1.512

## Assumptions and Limitations

- Exchange of water between the wetland and the main channel or estuary takes place through only one connection, which has a well-defined and stable geometry. If multiple inlets exist, the wetland must be divided into subdomains, and each subdomain must be computed independently. The salinity for the entire wetland can be estimated by calculating a weighted average (weighted by wetland subdomain volume) of the salinity in each subdomain.
- Salt water added to the wetland during flood tidal phase mixes instantly and completely over the entire wetland volume throughout the water depth.
- Ebb volume coming out from the wetland has no effect on the salinity of the main channel or estuary.
- Fresh water added to the wetland by rainfall is applied over the entire wetland surface area, and mixes instantly and completely over the entire wetland volume throughout the water depth.
- Evaporation in the wetland removes freshwater uniformly over the entire wetted wetland surface area.
- The salinity in the main channel or estuary is dominantly influenced by tidal salt flux and riverine freshwater flux. Rainfall and evaporation are secondary influences.
- The length to width ratio of the wetland is close to unity.
- The bed elevation of the wetland is uniform, and is defined by only one value.
- The wetted surface area of the wetland is constant with respect to time.
- The hydraulic roughness of the wetland is uniform, and is defined by only one value.
- The elevation of the sill associated with the inlet structure is uniform, and is defined by only one value. Sills that have a variable elevation across the inlet (such as sills designed with a boat bay) are assigned a sill elevation value equal to the average sill elevation across the inlet.
- The flow in the inlet is assumed to be quasi-steady (i.e. forces due to unsteady flow are assumed to be small relative to steady flow forcing terms).
- The cross-section of the inlet is assumed to be rectangular.

## Definitions of Symbols

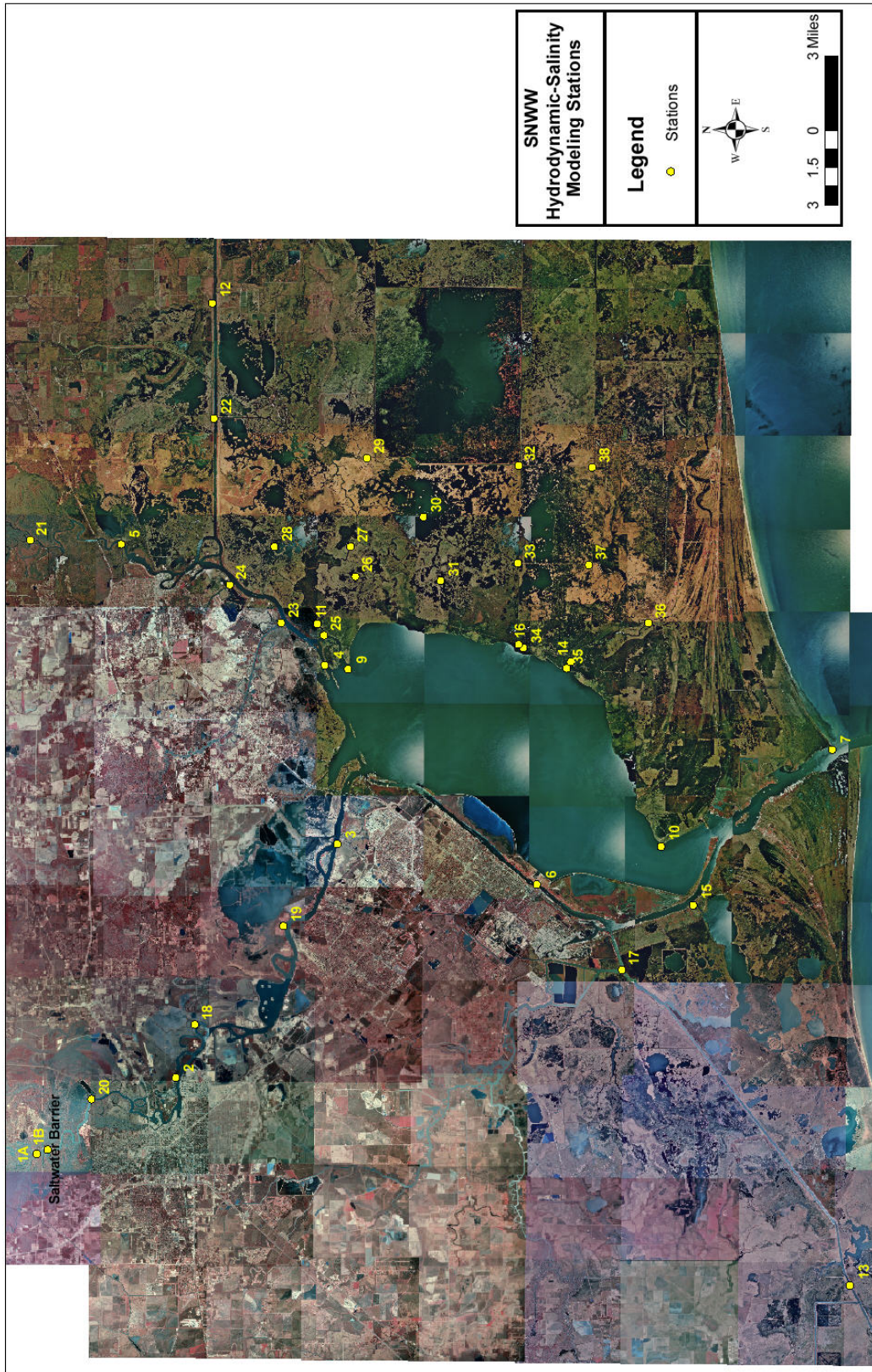
- $A_{S,W}$  = ..... the surface area of the wetland (ft<sup>2</sup>)  
 $a$  = a constant  
 $b$  = a constant  
 $c$  = a constant  
 $g$  = the acceleration due to gravity (ft/s<sup>2</sup>)  
 $k_S$  = the hydraulic roughness height in the wetland (ft)  
 $K_{RE}$  = ..... a constant (ft)  
 $K_{TE}$  = ..... a constant (1/ft)  
 $K_{TRE}$  = ..... a constant  
 $n$  = Manning's n for the wetland  
 $Q_I$  = the discharge in the inlet, defined as flood-tide positive (cfs)  
 $Q_{RE}$  = ..... the volumetric flux of the net precipitation (cfs)  
 $q_{RE}$  = the unit surface area flux of the net precipitation (ft/sec)  
 $v_I$  = the velocity in the inlet, defined as flood-tide positive (ft/s)  
 $W_I$  = the width of the inlet (ft)  
 $s_I$  = the salinity in the inlet (ppt)  
 $s_W$  = the salinity in the wetland (ppt)  
 $s_{W,o}$  = the salinity in the wetland at the previous time step (ppt)  
 $t$  = the total elapsed time  
 $z_I$  = the bed elevation in the inlet (ft)  
 $z_S$  = the sill elevation in the inlet (ft)  
 $z_W$  = the bed elevation in the wetland (ft)  
 $\alpha_{WS,W}$  = .. the wetted surface area factor, defined as the ratio of the wetted surface area of the wetland to the total surface area of the wetland  
 $\Delta t$  = the time step (seconds)  
 $\eta_I$  = the water surface elevation in the inlet (ft)  
 $\eta_W$  = the water surface elevation in the wetland (ft)  
 $\eta_{W,o}$  = ... the water surface elevation in the wetland at the previous time step (ft)  
 $\zeta_F$  = the head loss coefficient associated with friction losses in the wetland  
 $\zeta_L$  = the head loss coefficient associated with local losses in the inlet  
 $\zeta_T$  = the total head loss coefficient

# Appendix C

---

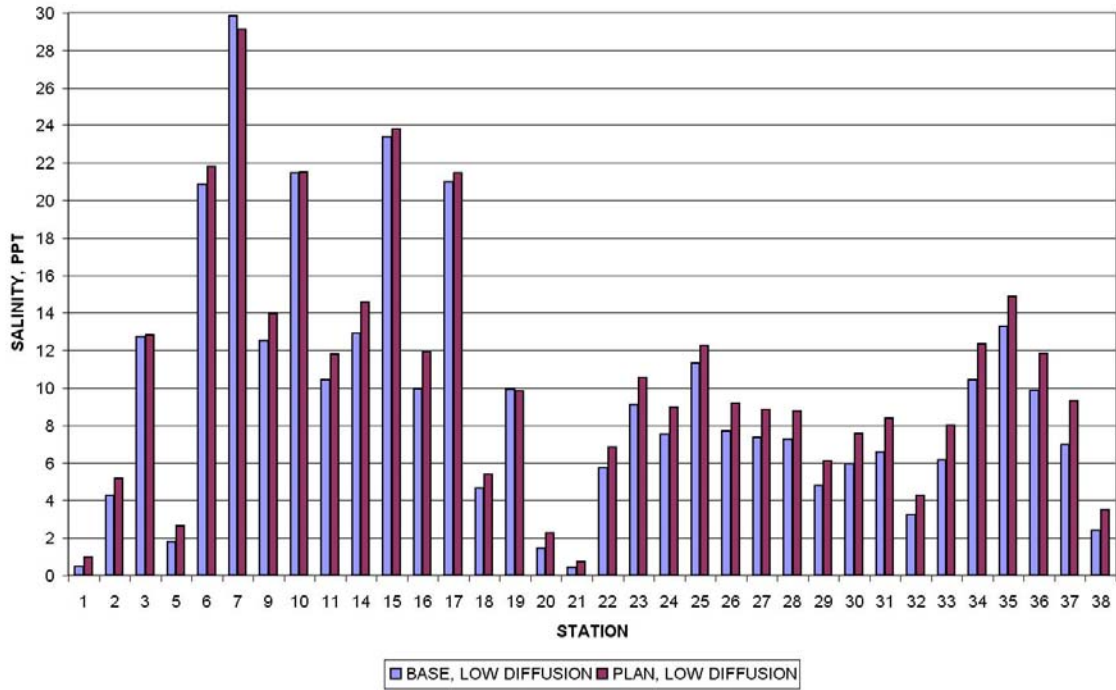
## **Mean and Highest 33% Salinity Differences for Base Conditions, Plan Channel Conditions, and Mitigation Scenarios 1-5**

# Observation Station Locations

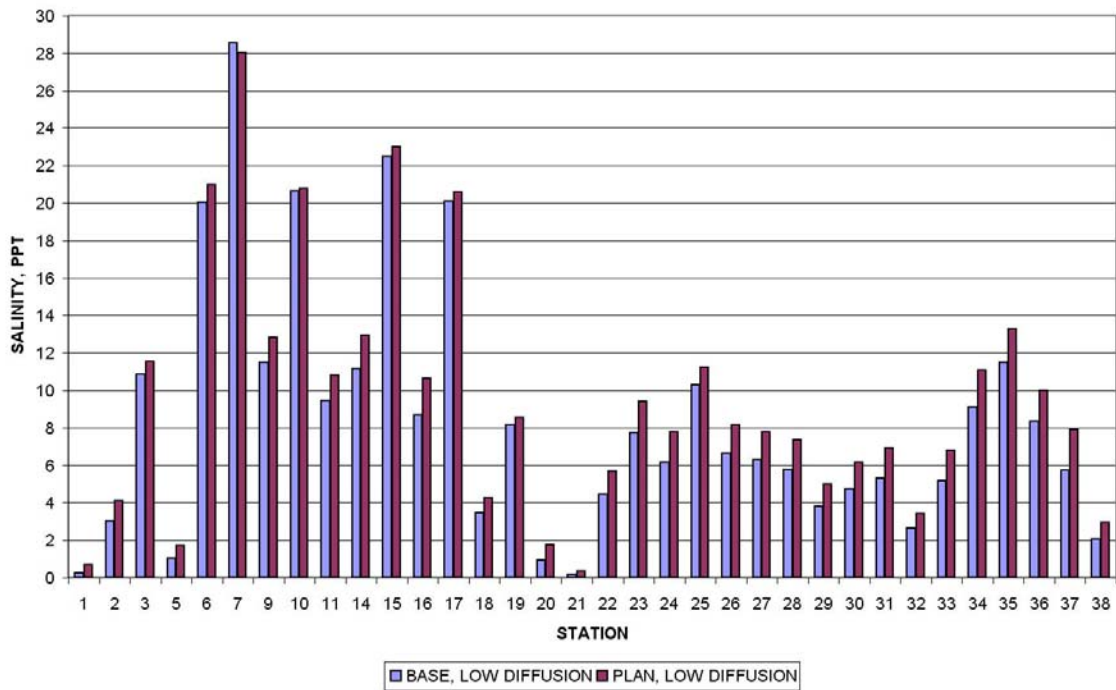


# Base and Plan Conditions

HIGHEST 33% CONTINUOUS SALINITY, LOW FLOW, LOW DIFFUSION

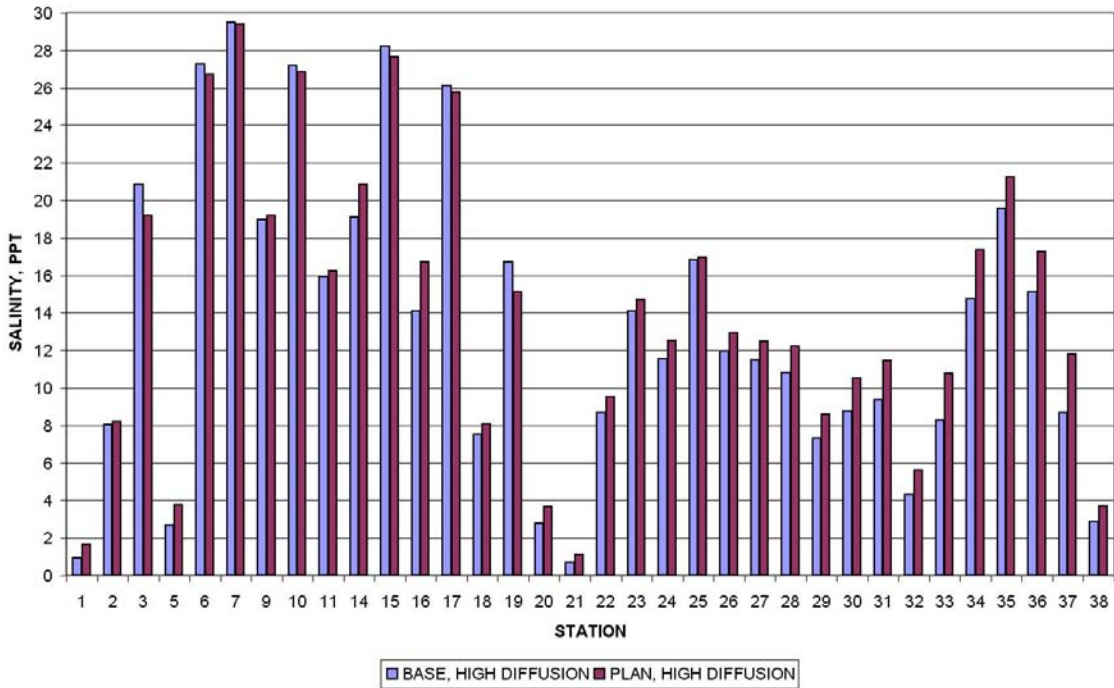


MEAN SALINITY VALUES, LOW FLOW, LOW DIFFUSION

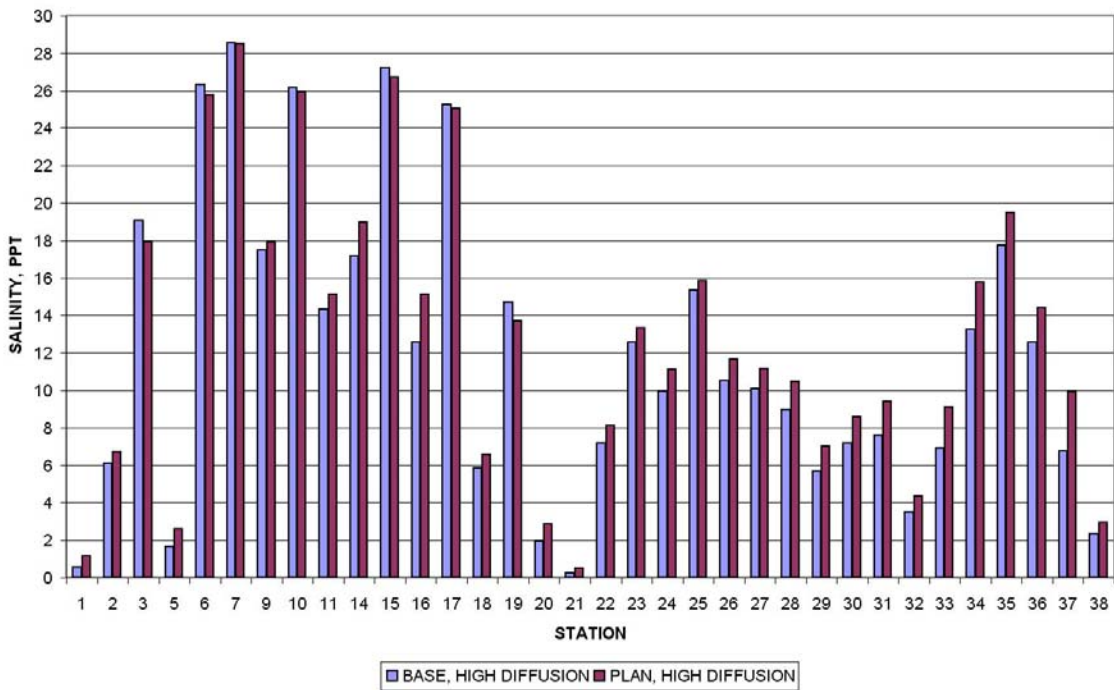


# Base and Plan Conditions

HIGHEST 33% CONTINUOUS SALINITY, LOW FLOW, HIGH DIFFUSION

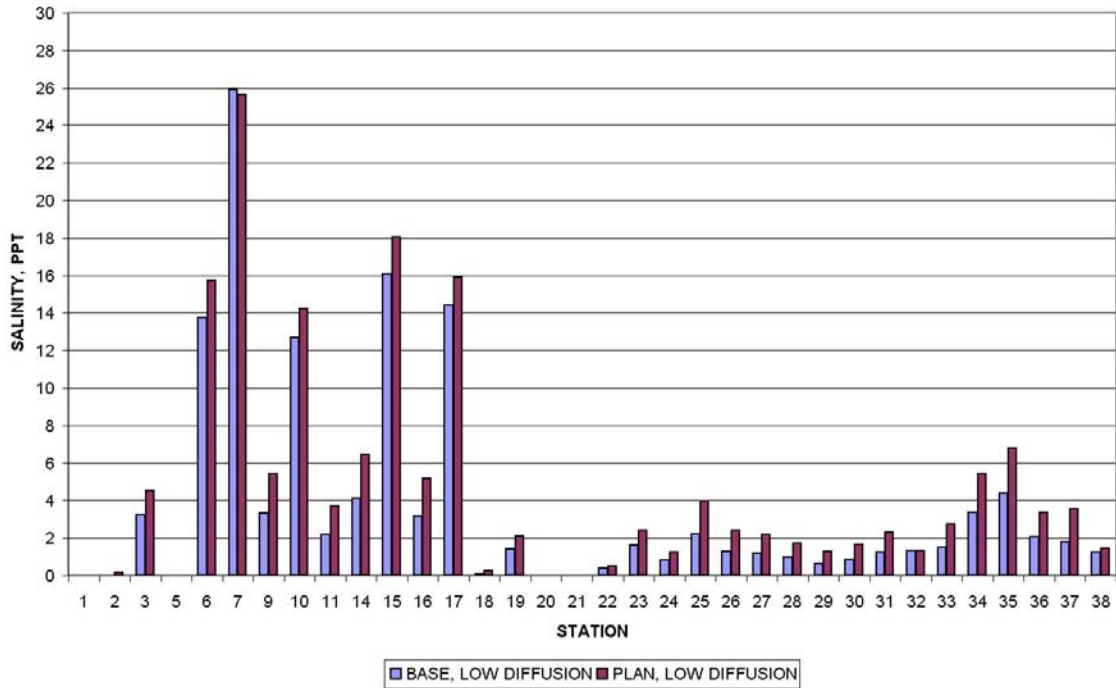


MEAN SALINITY VALUES, LOW FLOW, HIGH DIFFUSION

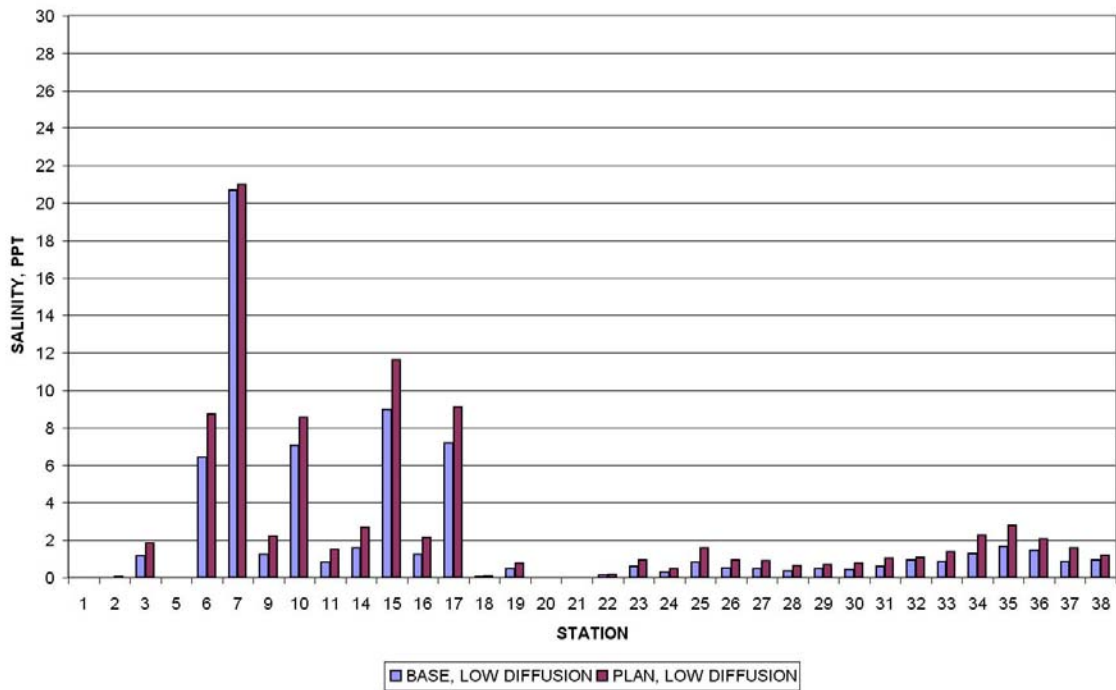


# Base and Plan Conditions

HIGHEST 33% CONTINUOUS SALINITY, MEDIAN FLOW, LOW DIFFUSION

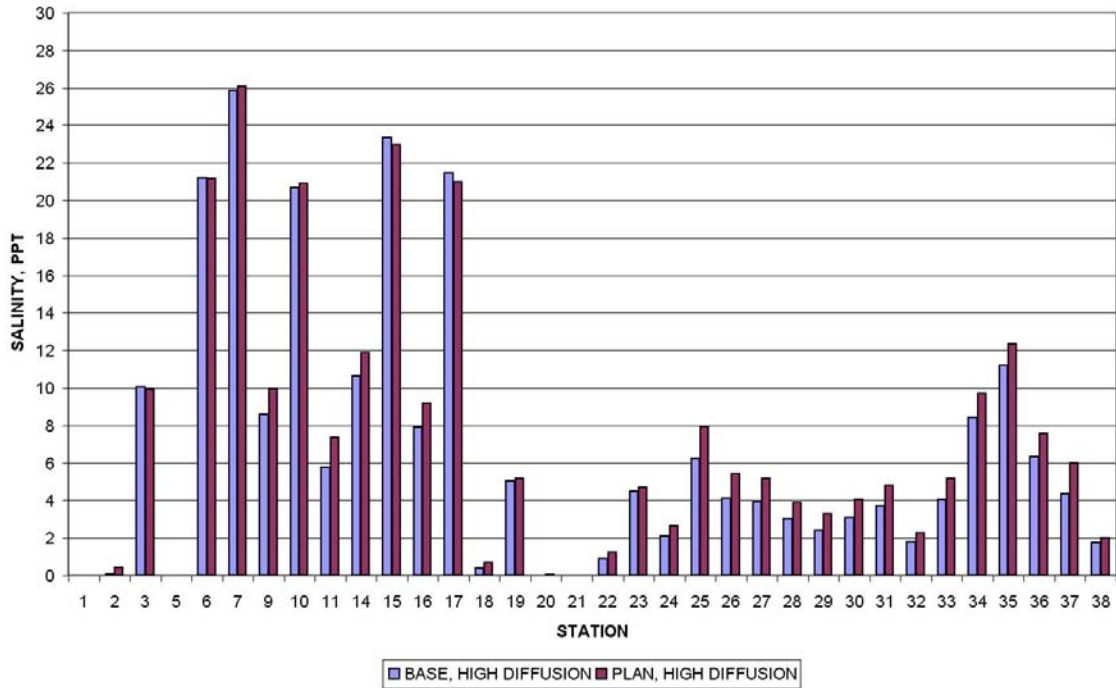


MEAN SALINITY VALUES, MEDIAN FLOW, LOW DIFFUSION

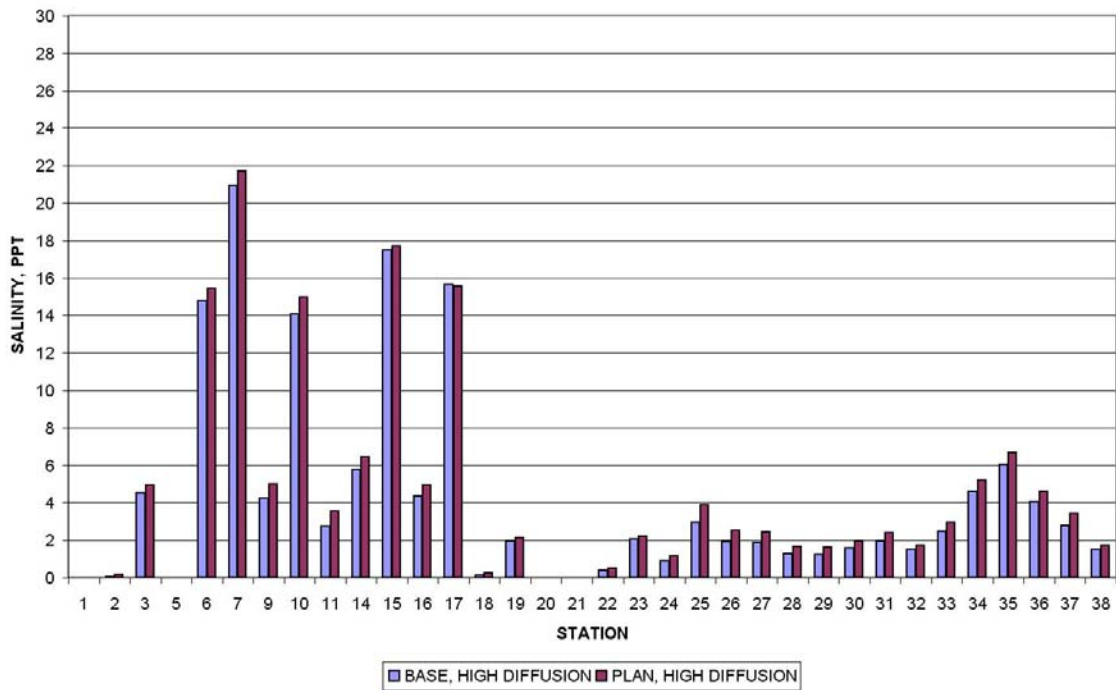


# Base and Plan Conditions

HIGHEST 33% CONTINUOUS SALINITY, MEDIAN FLOW, HIGH DIFFUSION

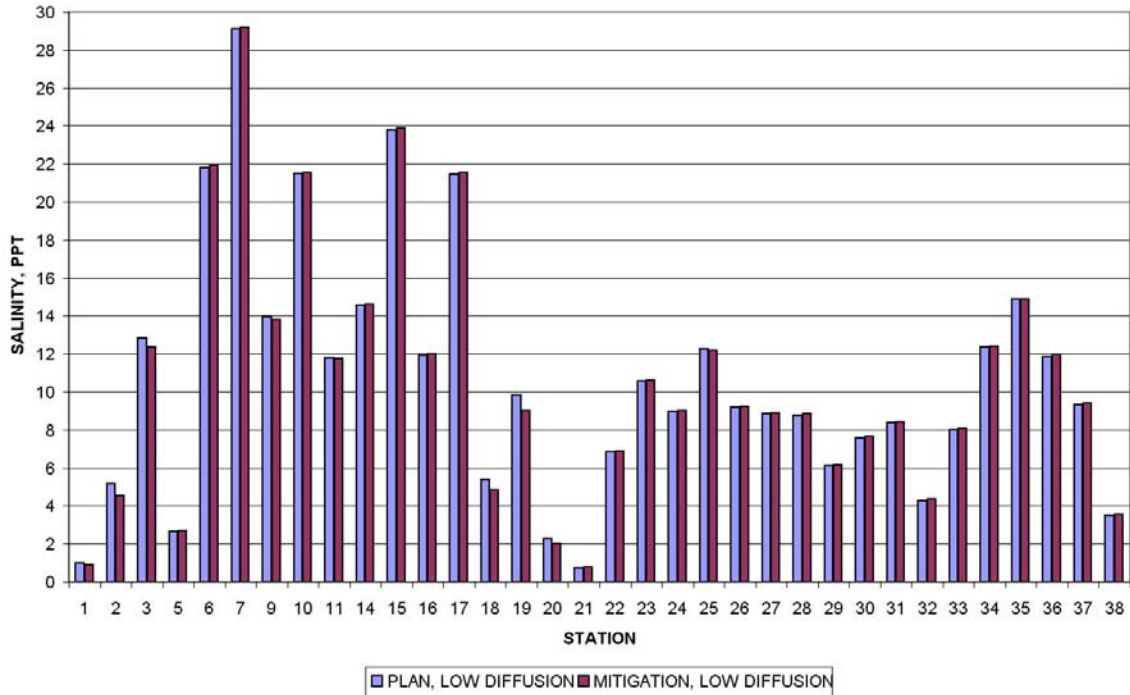


MEAN SALINITY VALUES, MEDIAN FLOW, HIGH DIFFUSION

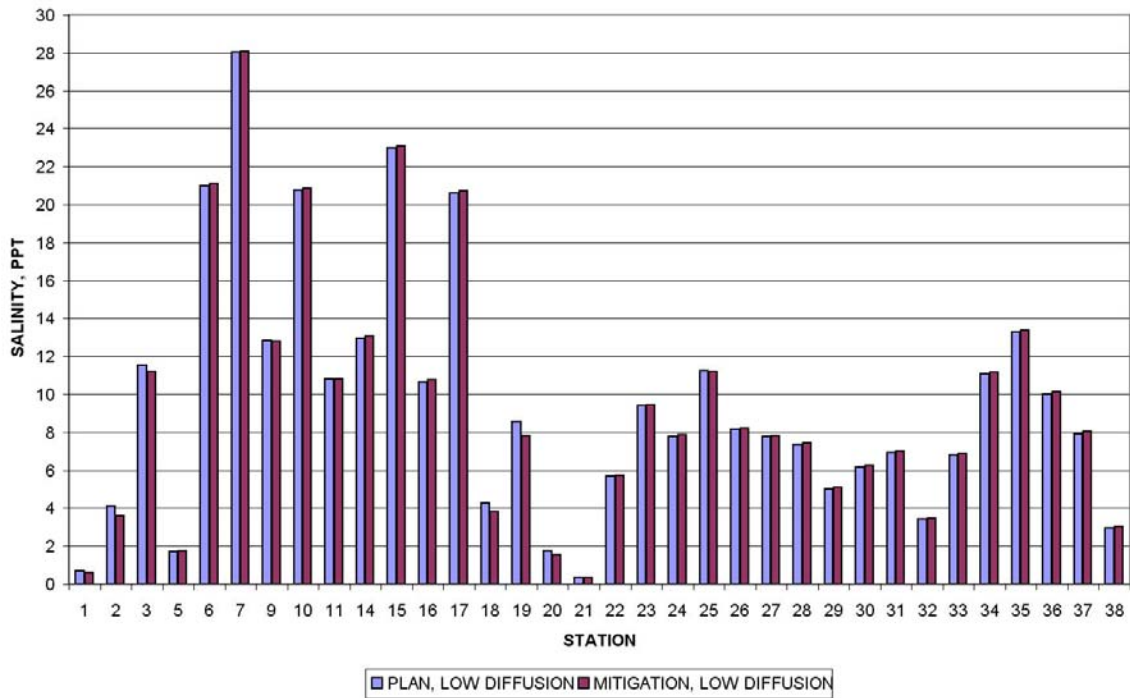


# Mitigation Scenario 1

HIGHEST 33% CONTINUOUS SALINITY, LOW FLOW, LOW DIFFUSION

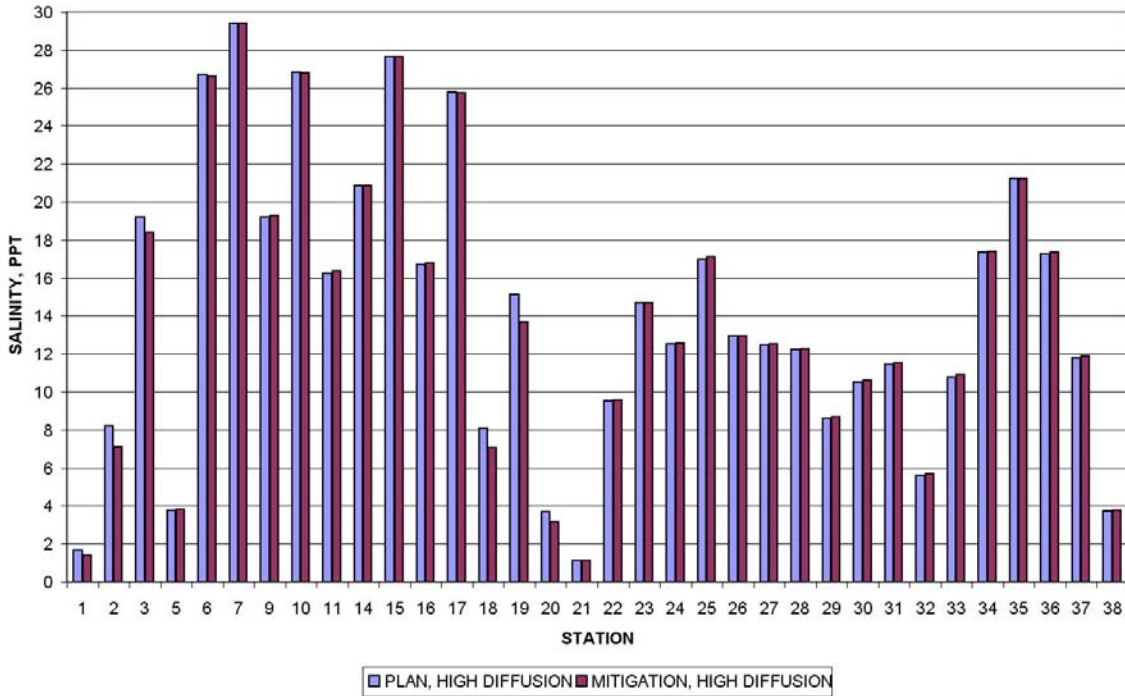


MEAN SALINITY VALUES, LOW FLOW, LOW DIFFUSION

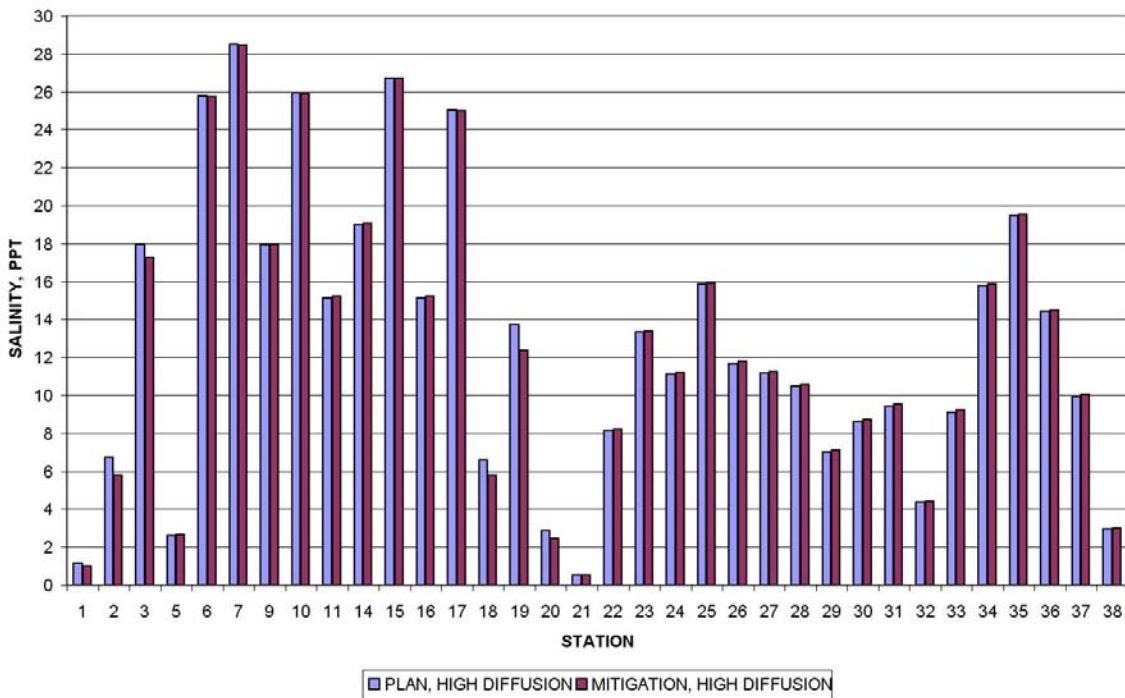


# Mitigation Scenario 1

HIGHEST 33% CONTINUOUS SALINITY, LOW FLOW, HIGH DIFFUSION

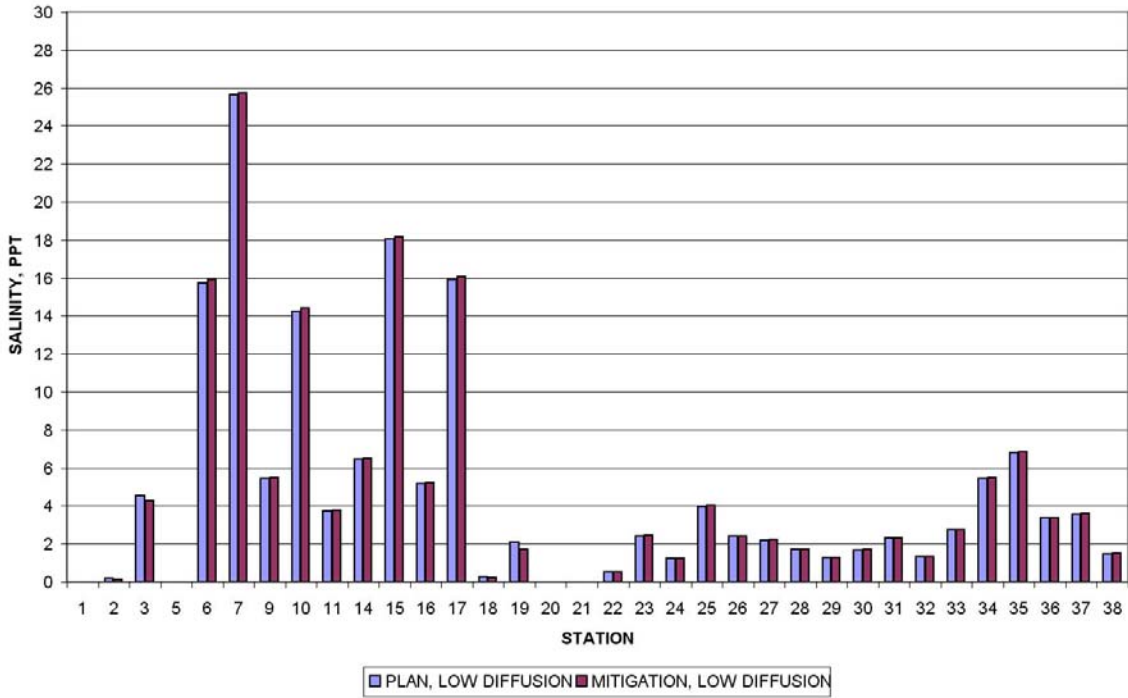


MEAN SALINITY VALUES, LOW FLOW, HIGH DIFFUSION

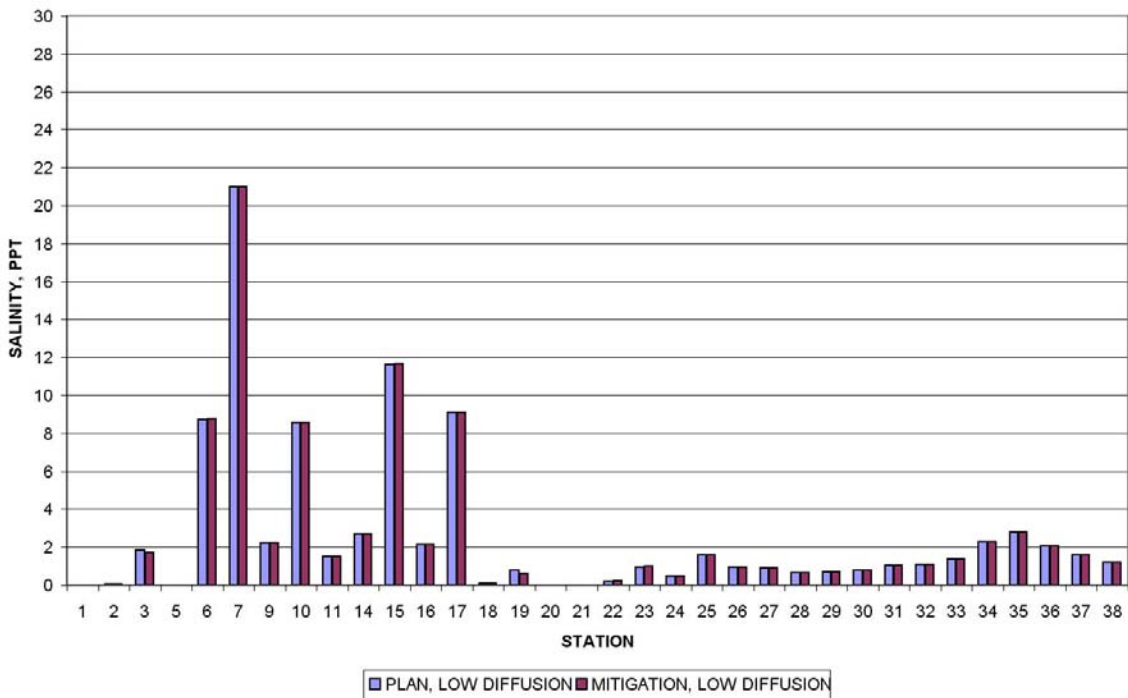


# Mitigation Scenario 1

HIGHEST 33% CONTINUOUS SALINITY, MEDIAN FLOW, LOW DIFFUSION

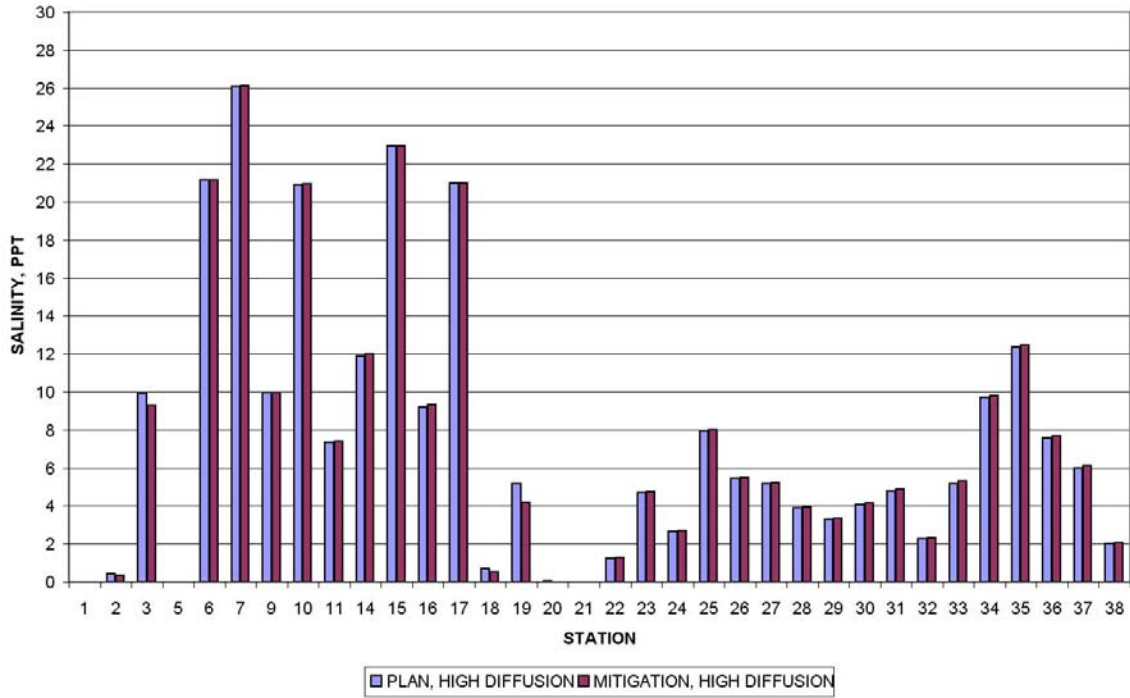


MEAN SALINITY VALUES, MEDIAN FLOW, LOW DIFFUSION

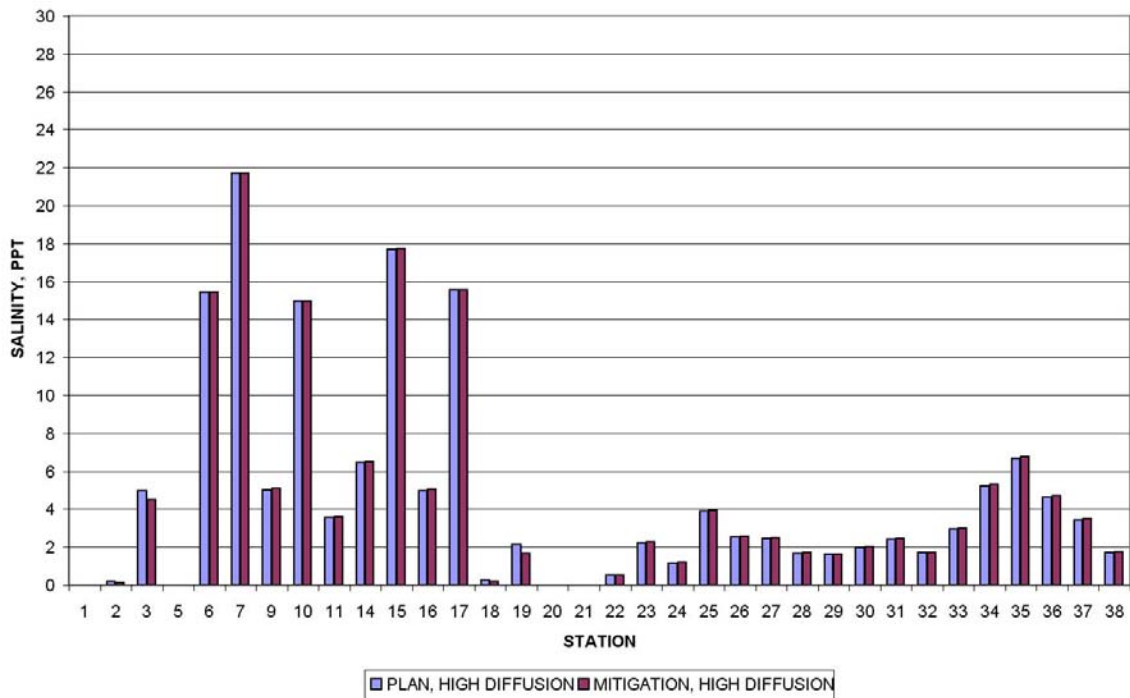


# Mitigation Scenario 1

HIGHEST 33% CONTINUOUS SALINITY, MEDIAN FLOW, HIGH DIFFUSION

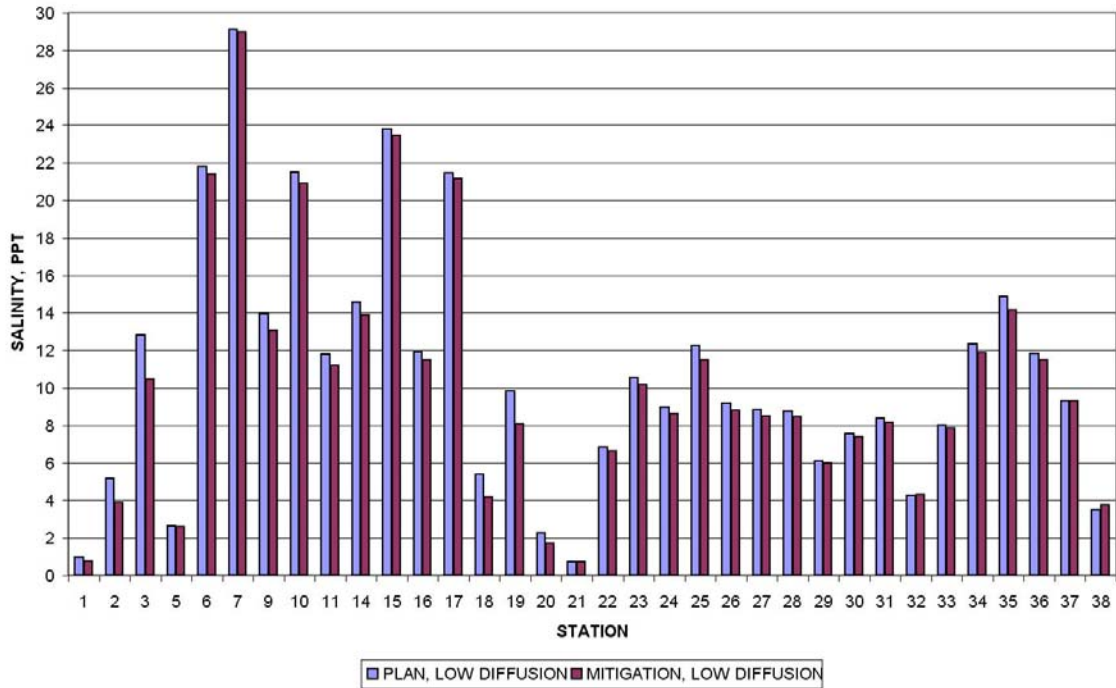


MEAN SALINITY VALUES, MEDIAN FLOW, HIGH DIFFUSION

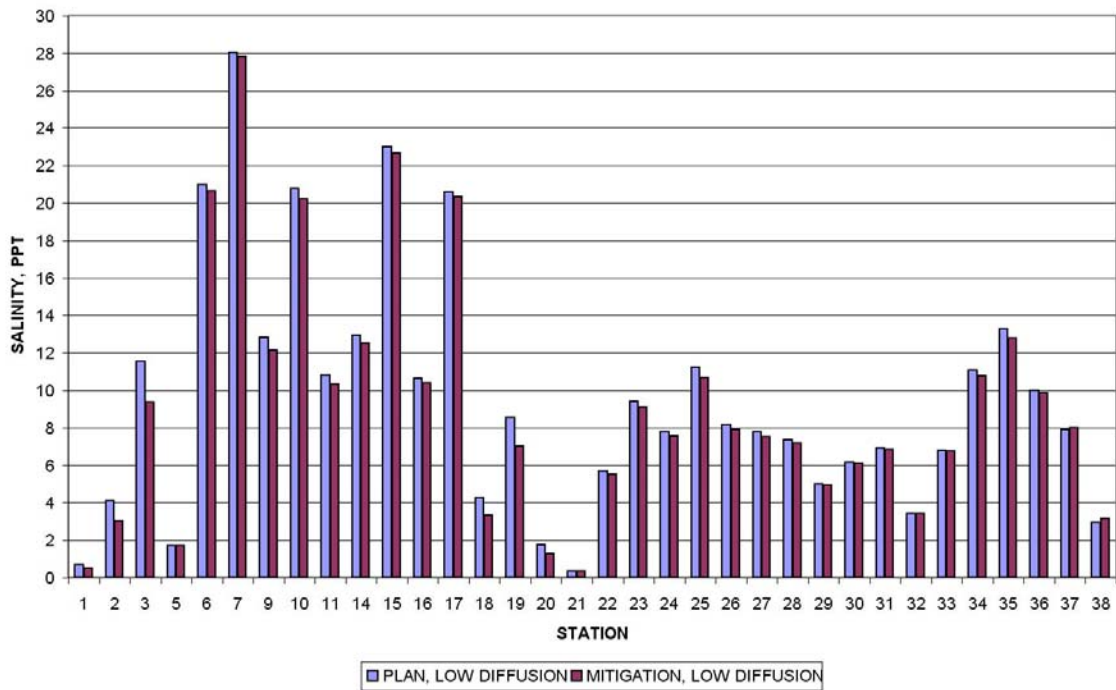


# Mitigation Scenario 2

HIGHEST 33% CONTINUOUS SALINITY, LOW FLOW, LOW DIFFUSION

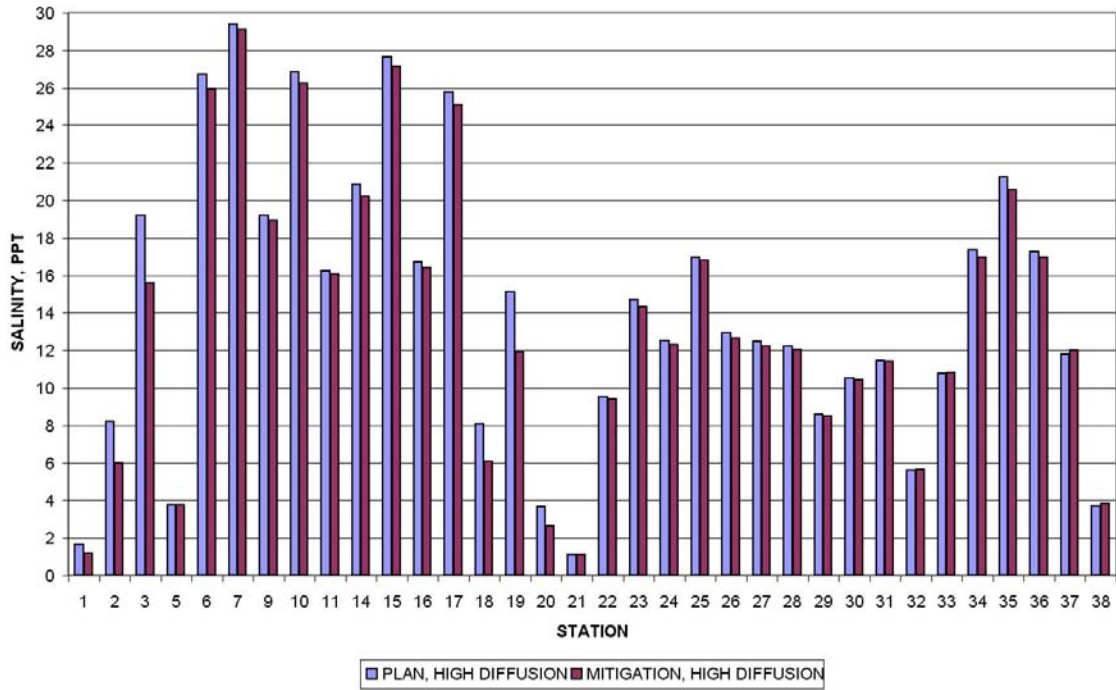


MEAN SALINITY VALUES, LOW FLOW, LOW DIFFUSION

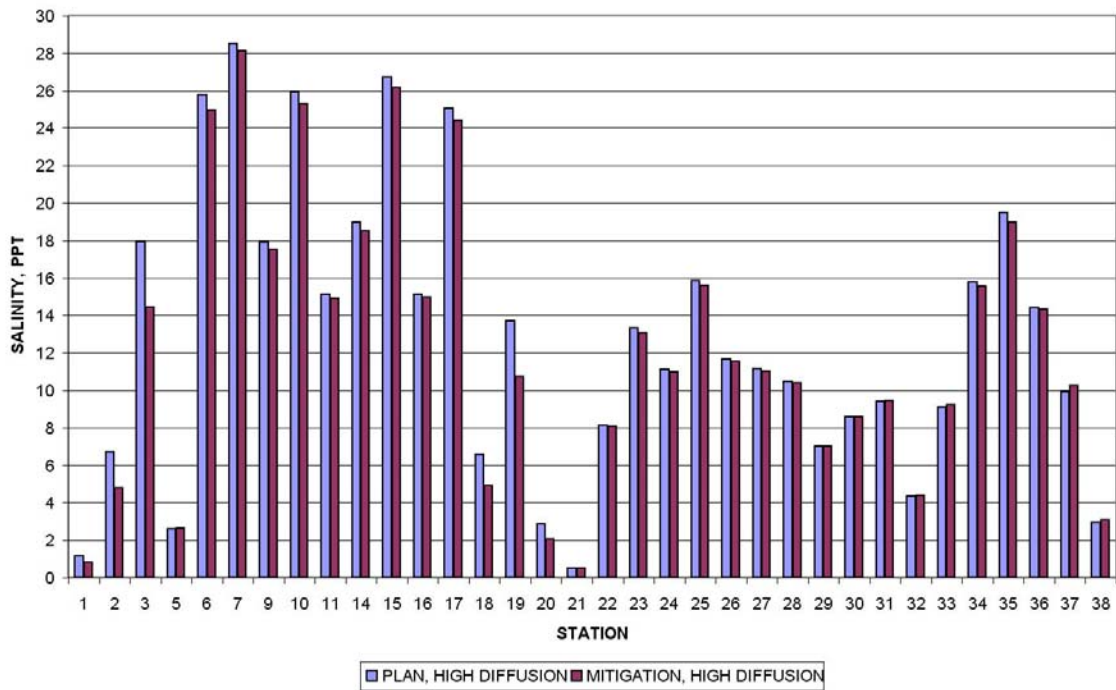


# Mitigation Scenario 2

HIGHEST 33% CONTINUOUS SALINITY, LOW FLOW, HIGH DIFFUSION

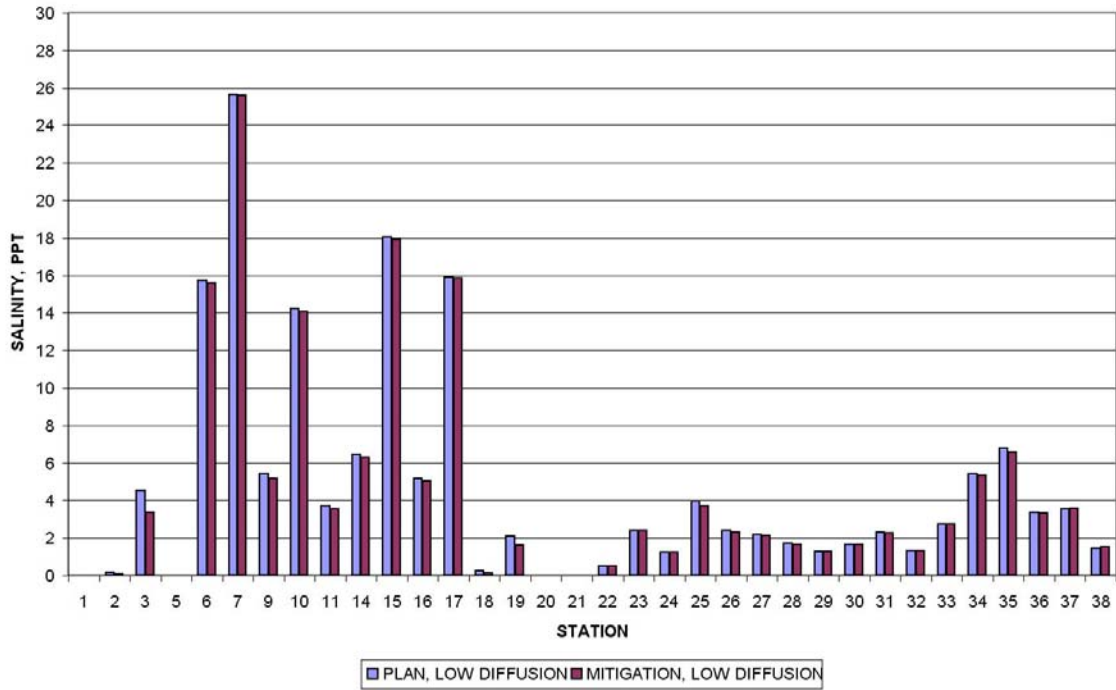


MEAN SALINITY VALUES, LOW FLOW, HIGH DIFFUSION

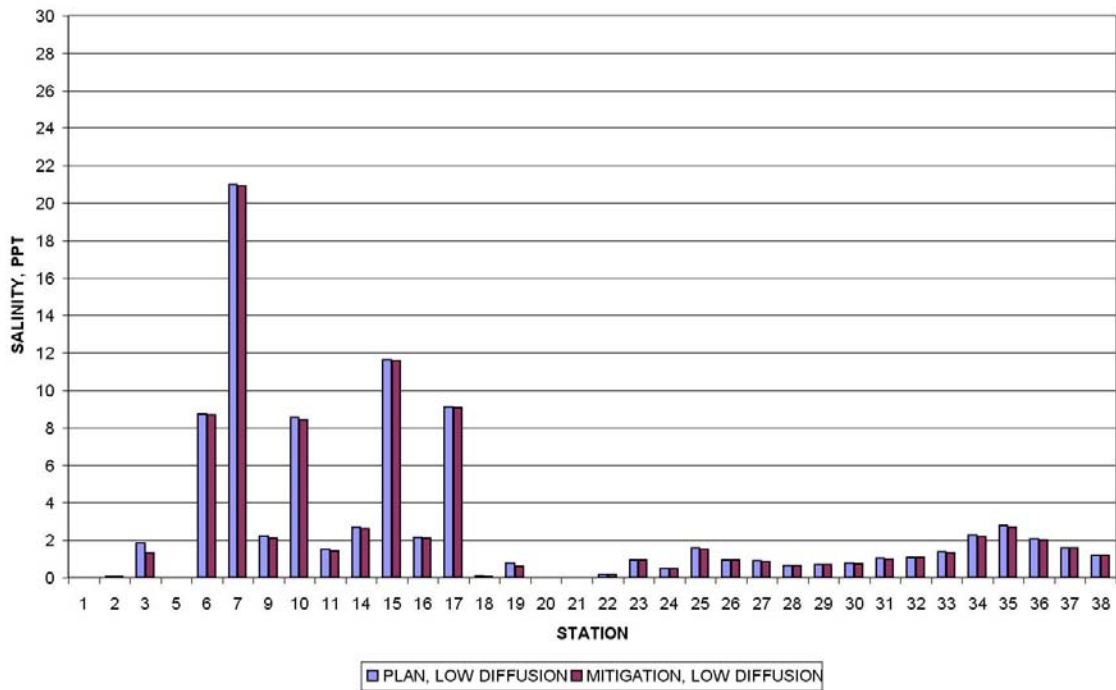


# Mitigation Scenario 2

HIGHEST 33% CONTINUOUS SALINITY, MEDIAN FLOW, LOW DIFFUSION

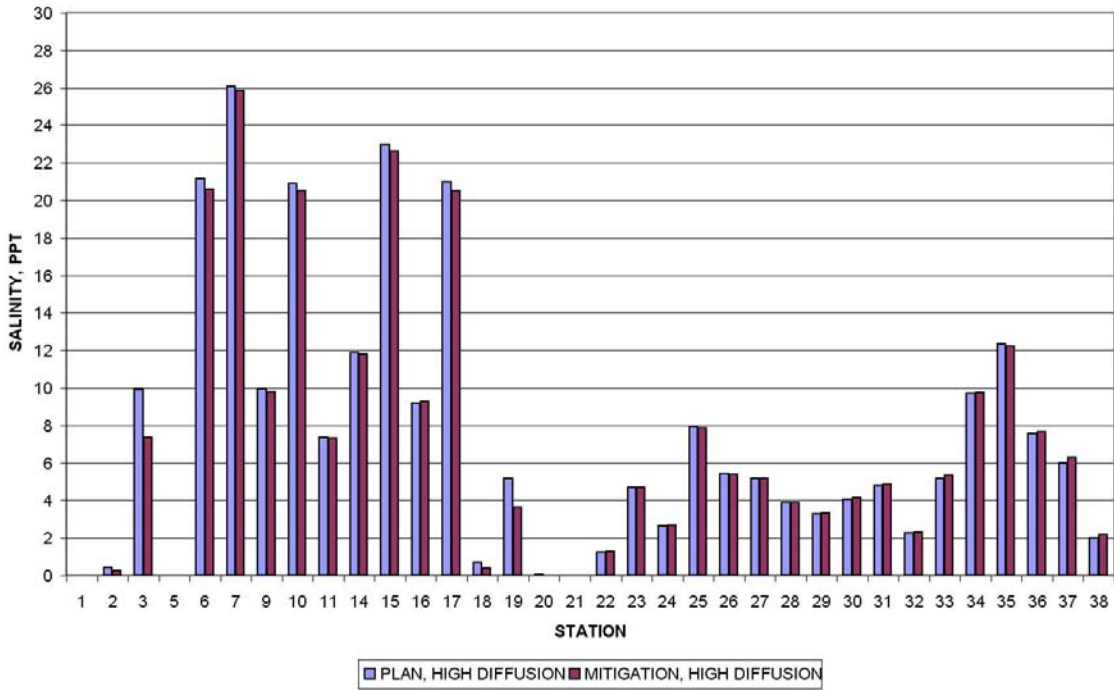


MEAN SALINITY VALUES, MEDIAN FLOW, LOW DIFFUSION

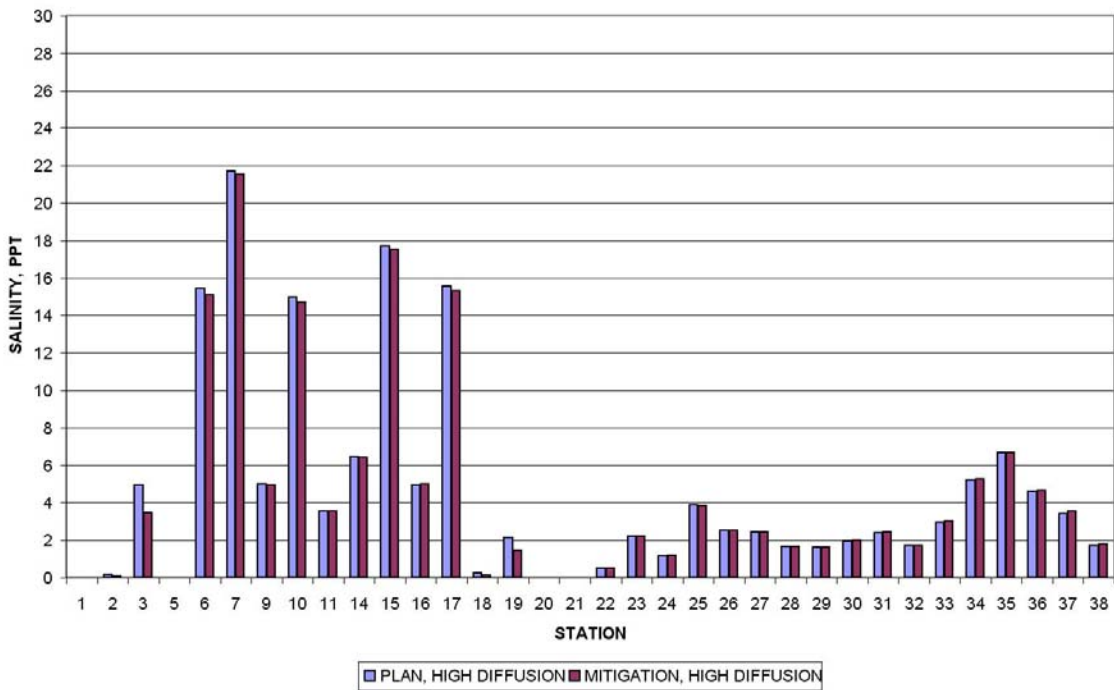


# Mitigation Scenario 2

HIGHEST 33% CONTINUOUS SALINITY, MEDIAN FLOW, HIGH DIFFUSION

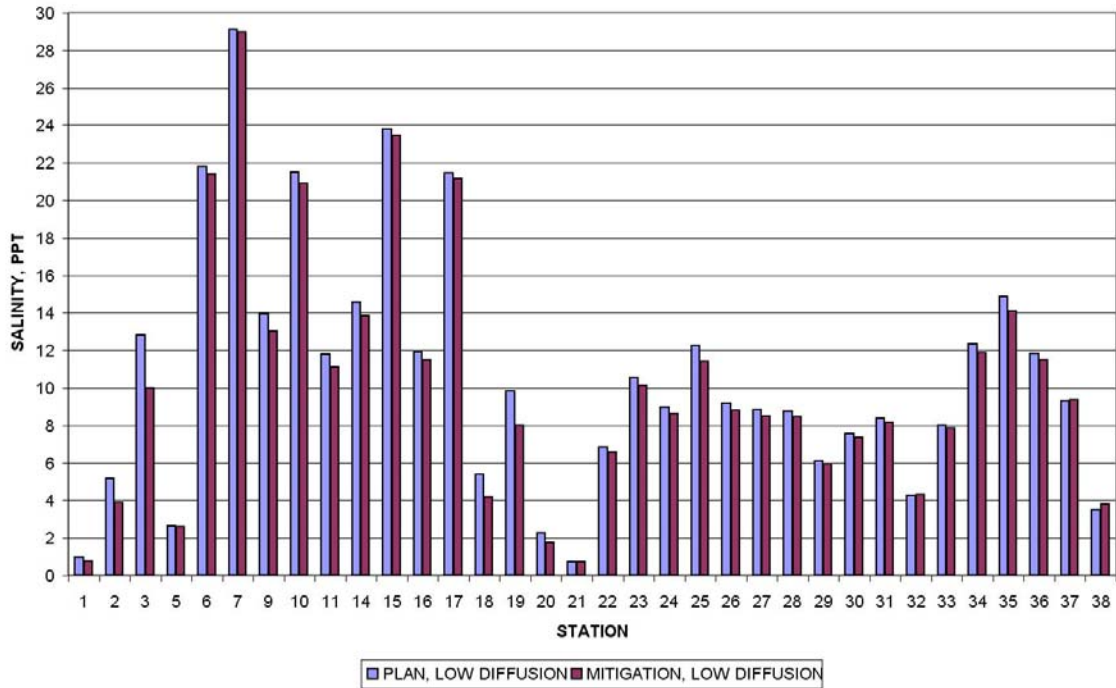


MEAN SALINITY VALUES, MEDIAN FLOW, HIGH DIFFUSION

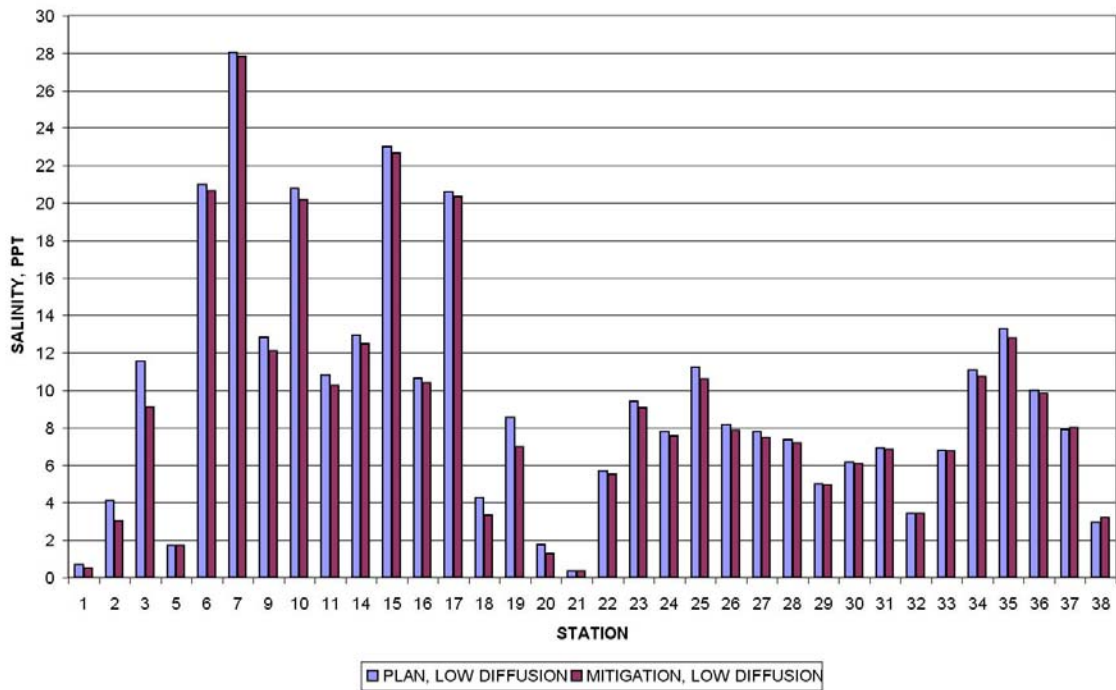


# Mitigation Scenario 3

HIGHEST 33% CONTINUOUS SALINITY, LOW FLOW, LOW DIFFUSION

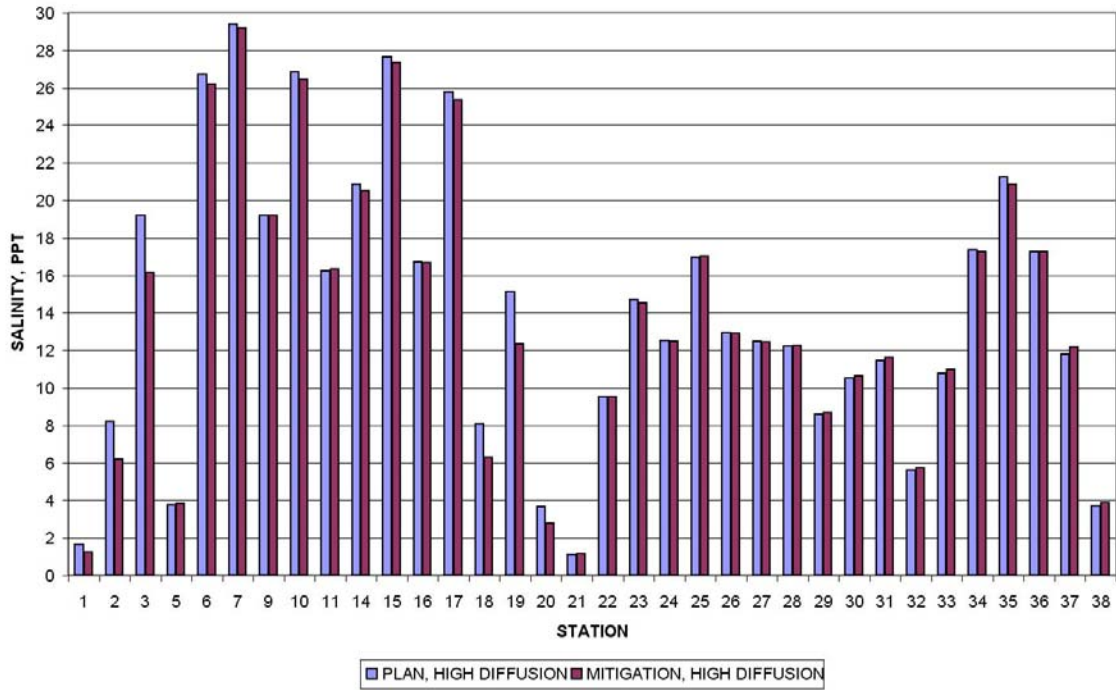


MEAN SALINITY VALUES, LOW FLOW, LOW DIFFUSION

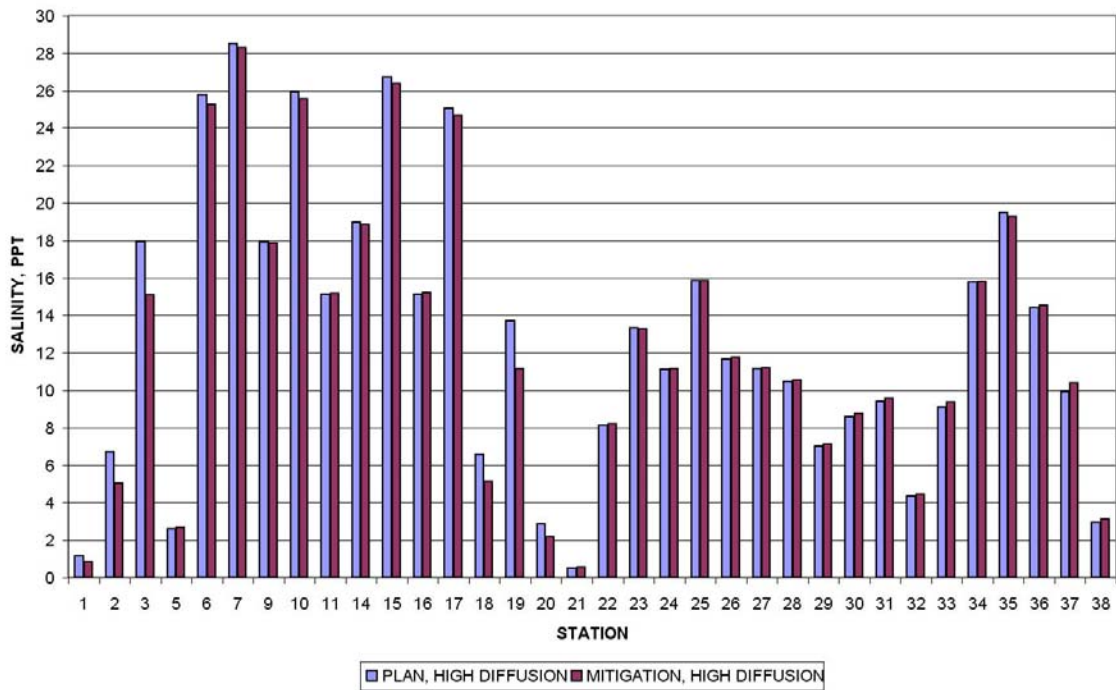


# Mitigation Scenario 3

HIGHEST 33% CONTINUOUS SALINITY, LOW FLOW, HIGH DIFFUSION

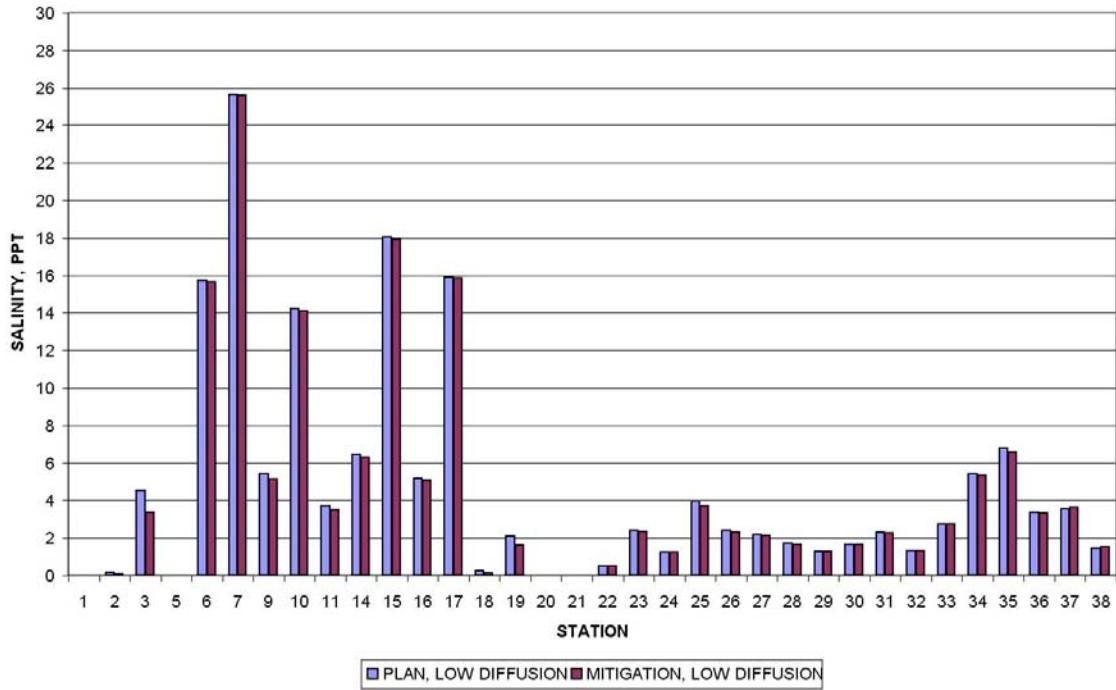


MEAN SALINITY VALUES, LOW FLOW, HIGH DIFFUSION

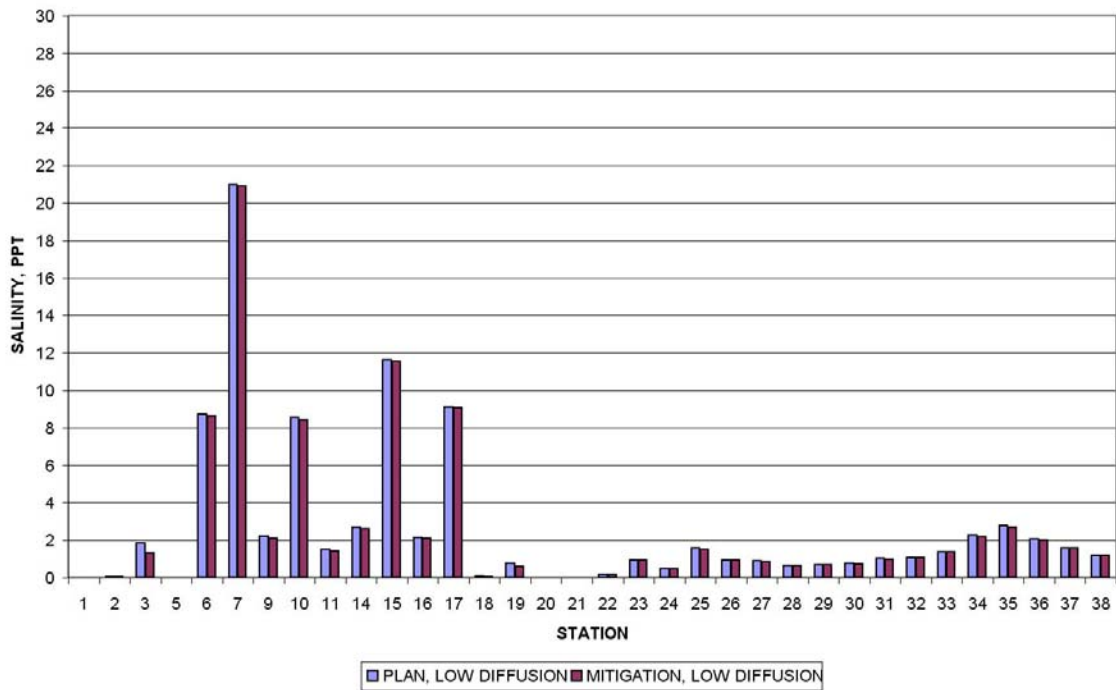


# Mitigation Scenario 3

HIGHEST 33% CONTINUOUS SALINITY, MEDIAN FLOW, LOW DIFFUSION

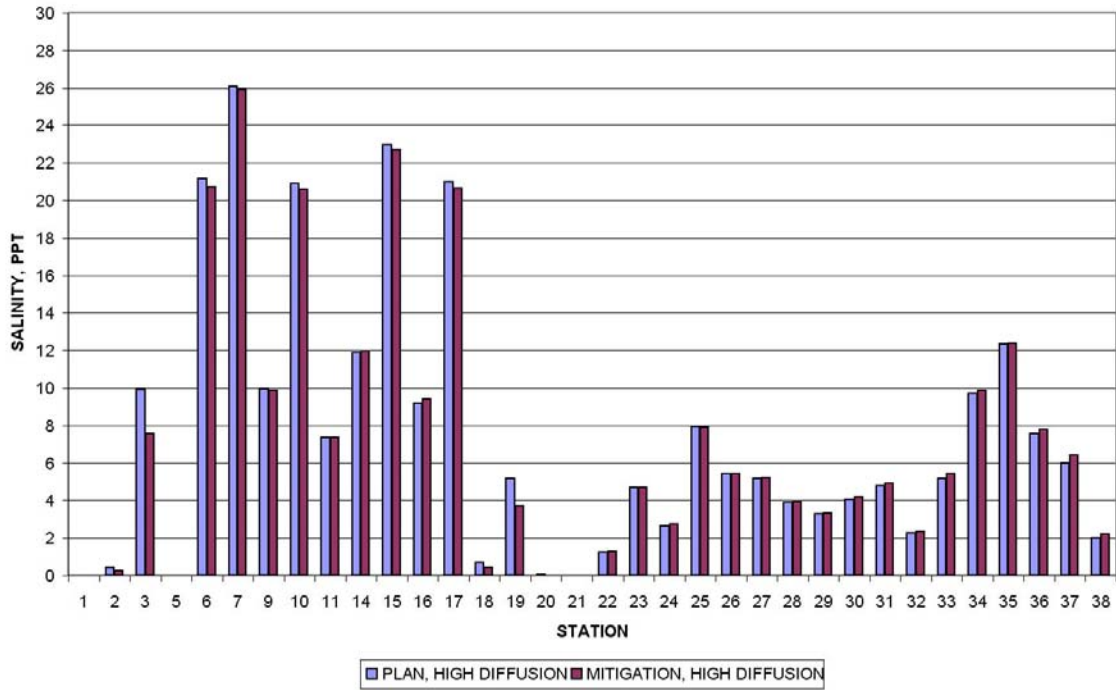


MEAN SALINITY VALUES, MEDIAN FLOW, LOW DIFFUSION

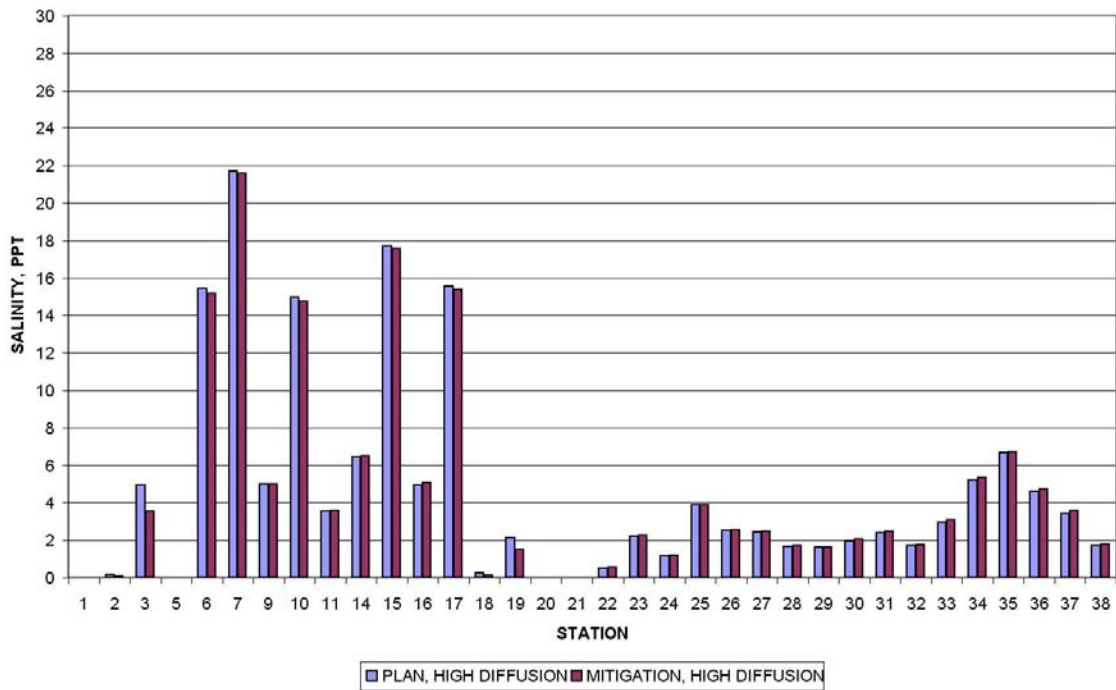


# Mitigation Scenario 3

HIGHEST 33% CONTINUOUS SALINITY, MEDIAN FLOW, HIGH DIFFUSION

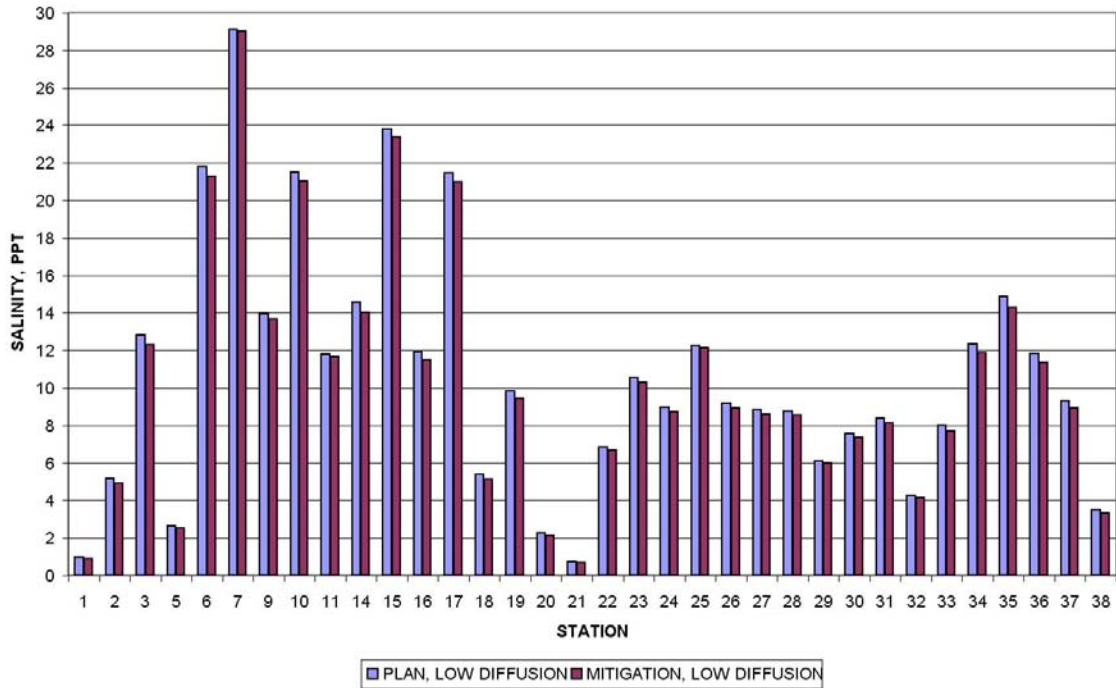


MEAN SALINITY VALUES, MEDIAN FLOW, HIGH DIFFUSION

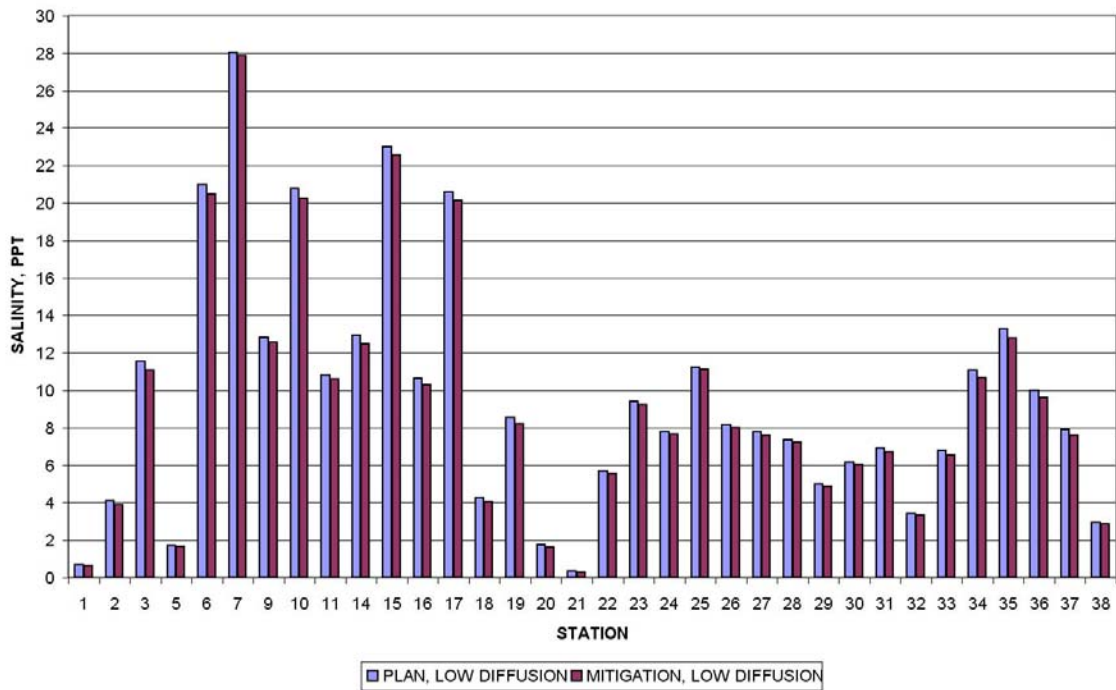


# Mitigation Scenario 5

HIGHEST 33% CONTINUOUS SALINITY, LOW FLOW, LOW DIFFUSION

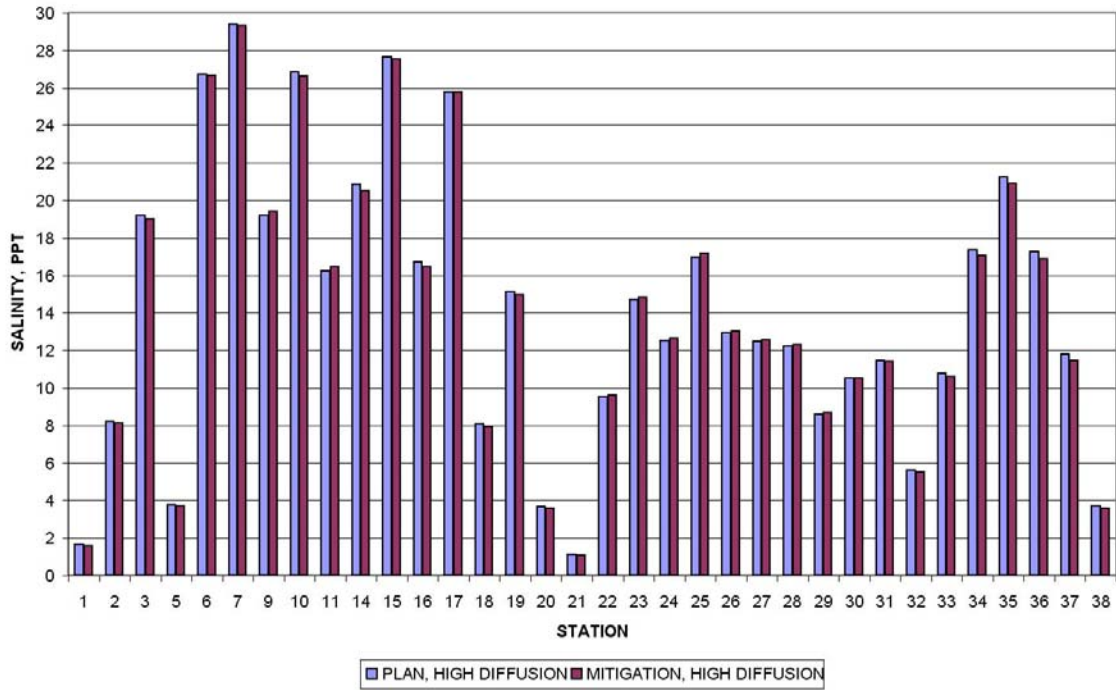


MEAN SALINITY VALUES, LOW FLOW, LOW DIFFUSION

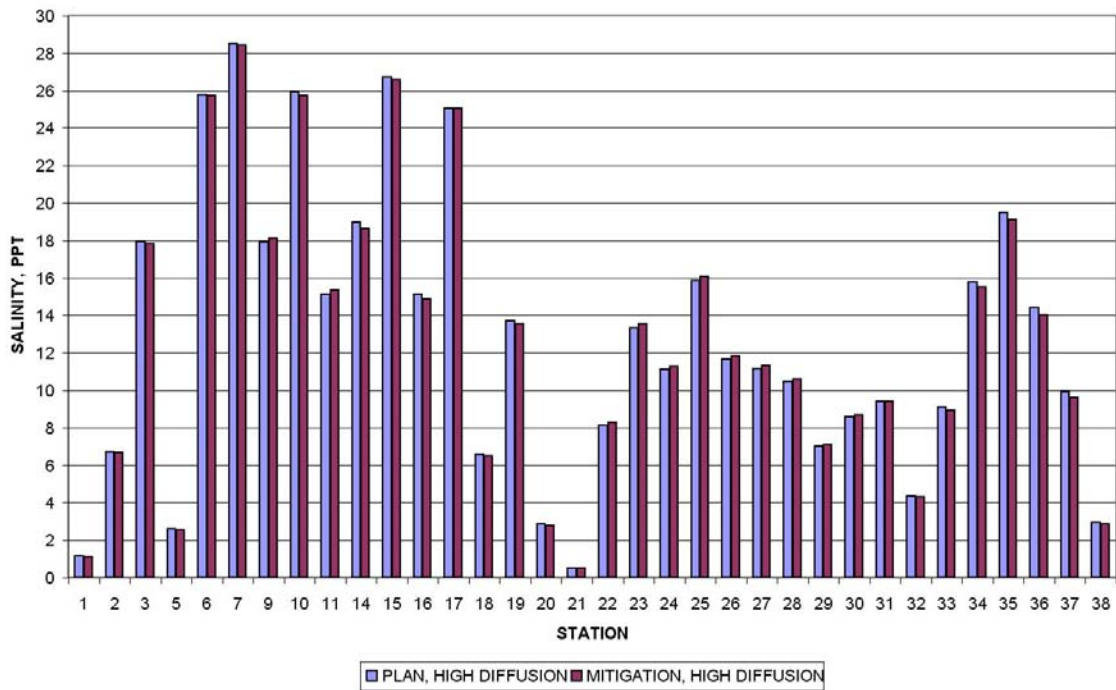


# Mitigation Scenario 5

HIGHEST 33% CONTINUOUS SALINITY, LOW FLOW, HIGH DIFFUSION

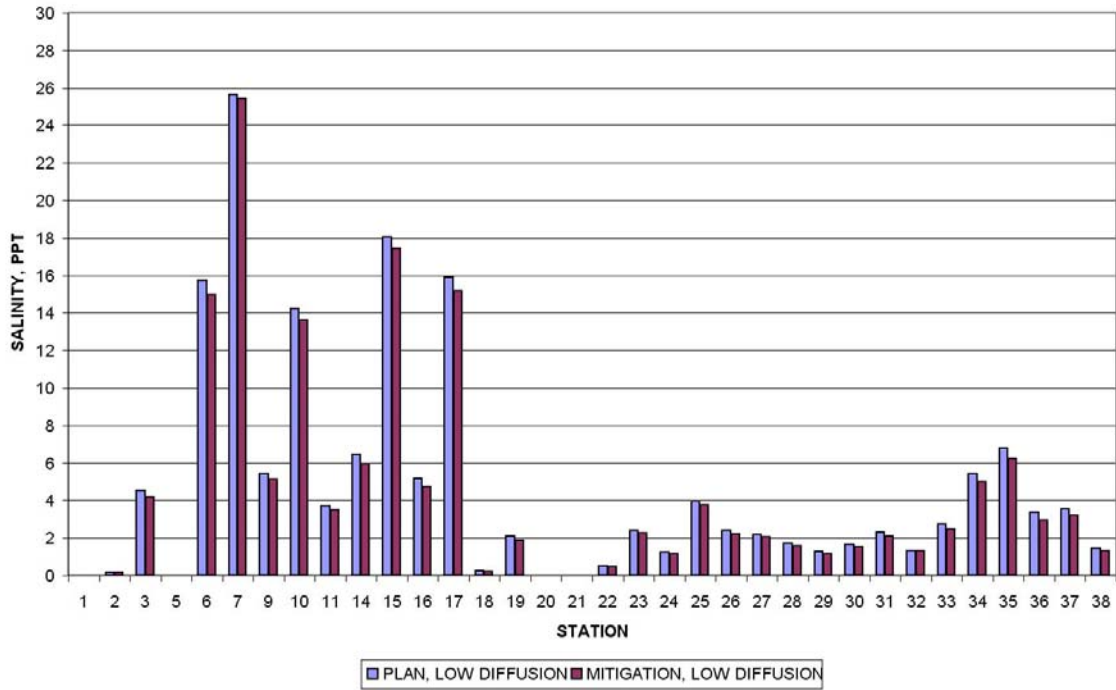


MEAN SALINITY VALUES, LOW FLOW, HIGH DIFFUSION

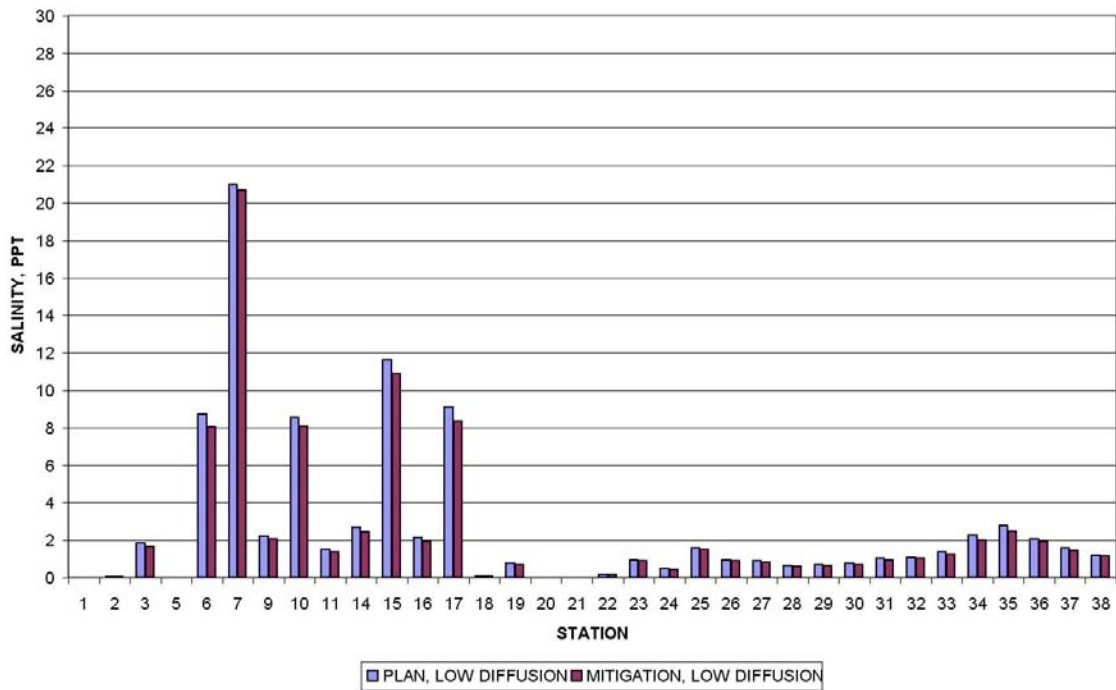


# Mitigation Scenario 5

HIGHEST 33% CONTINUOUS SALINITY, MEDIAN FLOW, LOW DIFFUSION

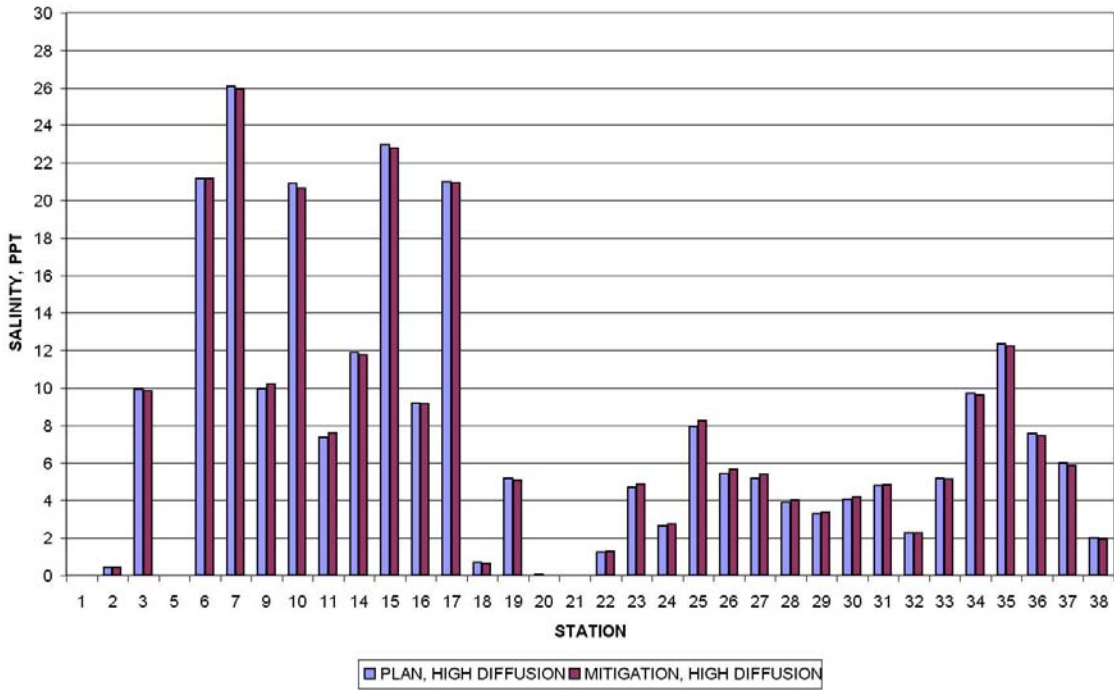


MEAN SALINITY VALUES, MEDIAN FLOW, LOW DIFFUSION

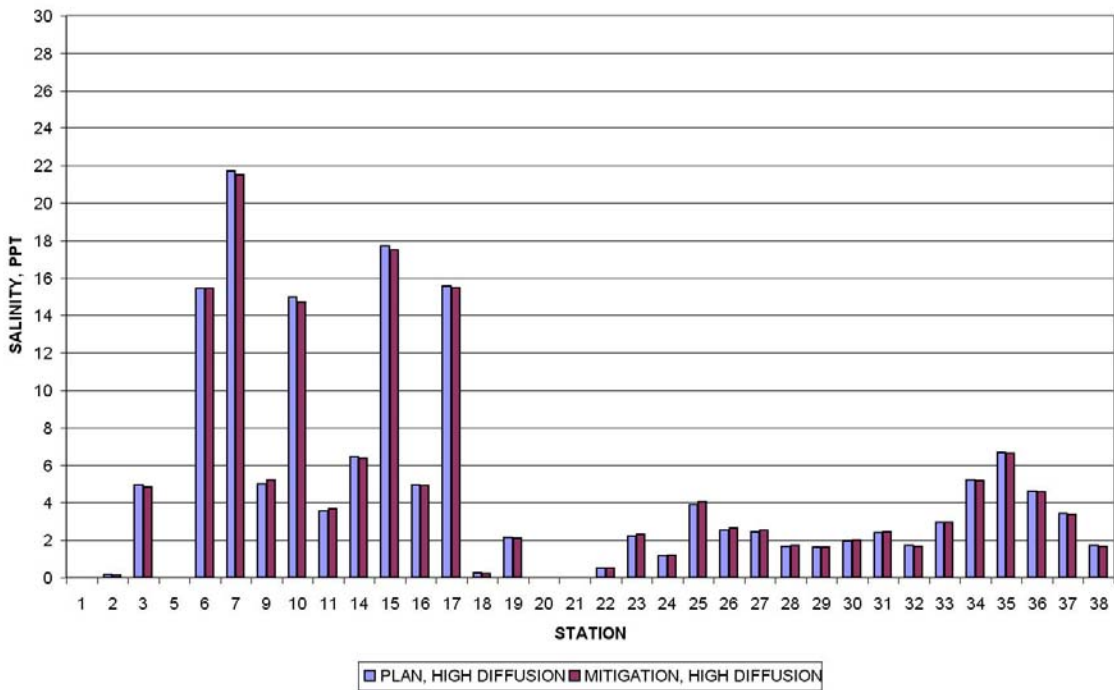


# Mitigation Scenario 5

HIGHEST 33% CONTINUOUS SALINITY, MEDIAN FLOW, HIGH DIFFUSION

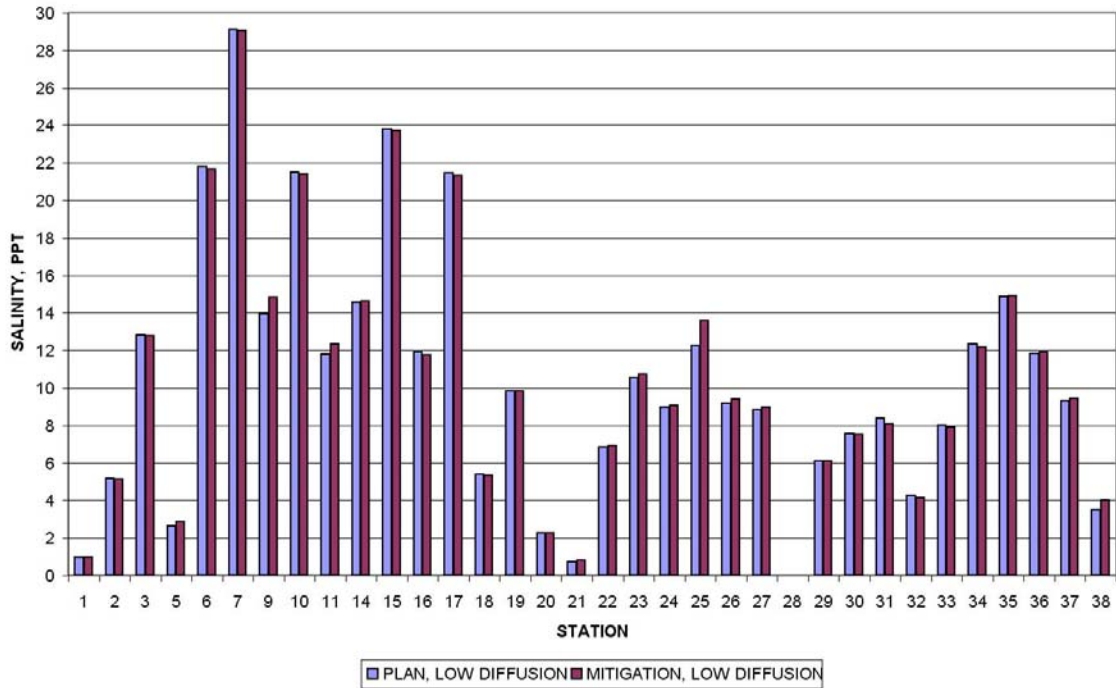


MEAN SALINITY VALUES, MEDIAN FLOW, HIGH DIFFUSION

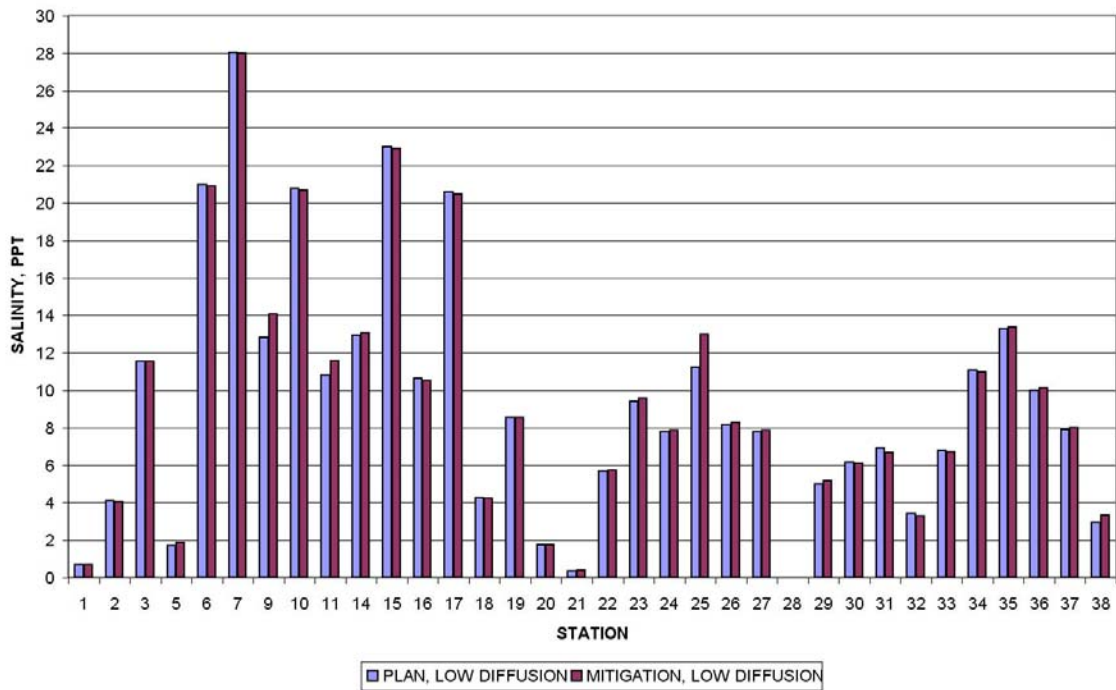


# Mitigation Scenario 6

HIGHEST 33% CONTINUOUS SALINITY, LOW FLOW, LOW DIFFUSION

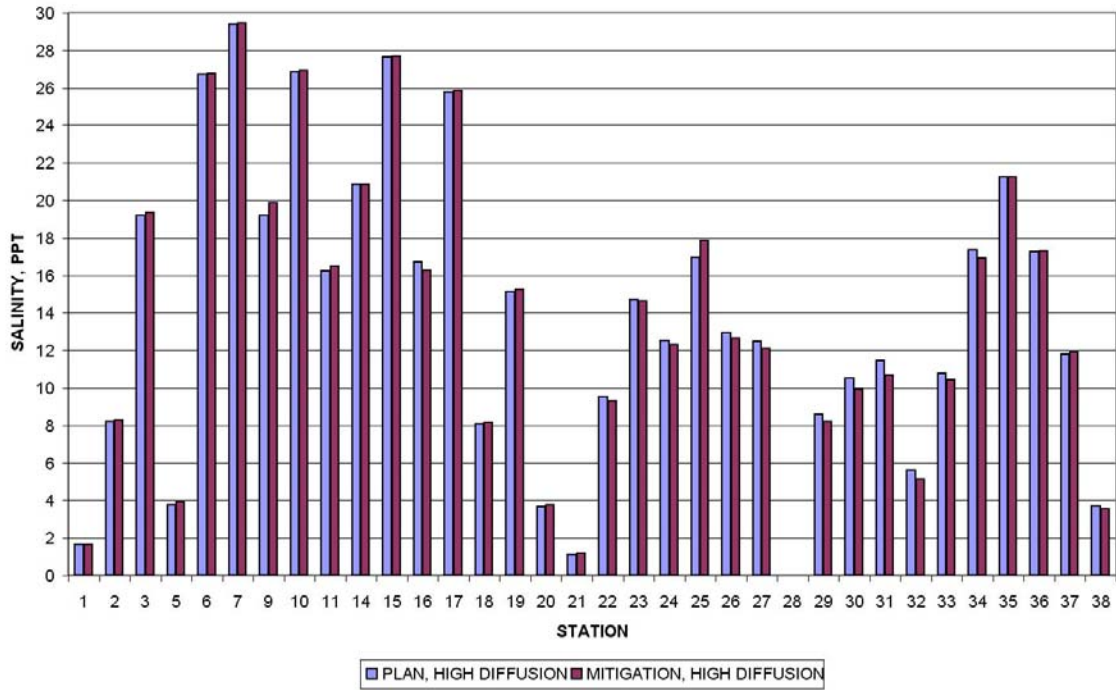


MEAN SALINITY VALUES, LOW FLOW, LOW DIFFUSION

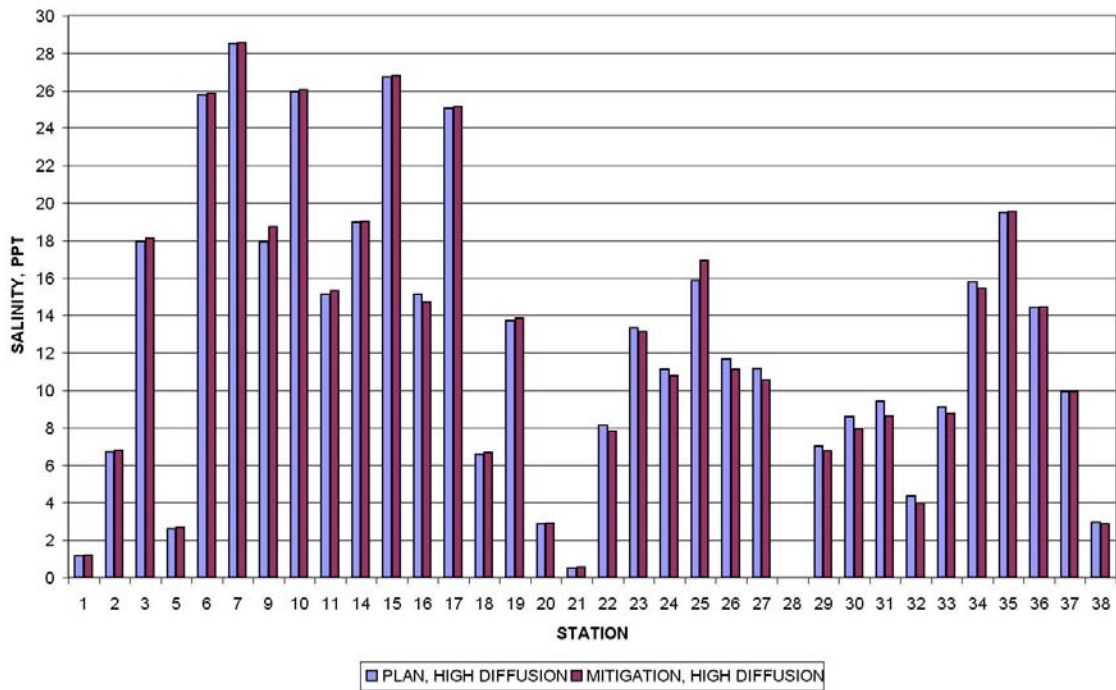


# Mitigation Scenario 6

HIGHEST 33% CONTINUOUS SALINITY, LOW FLOW, HIGH DIFFUSION

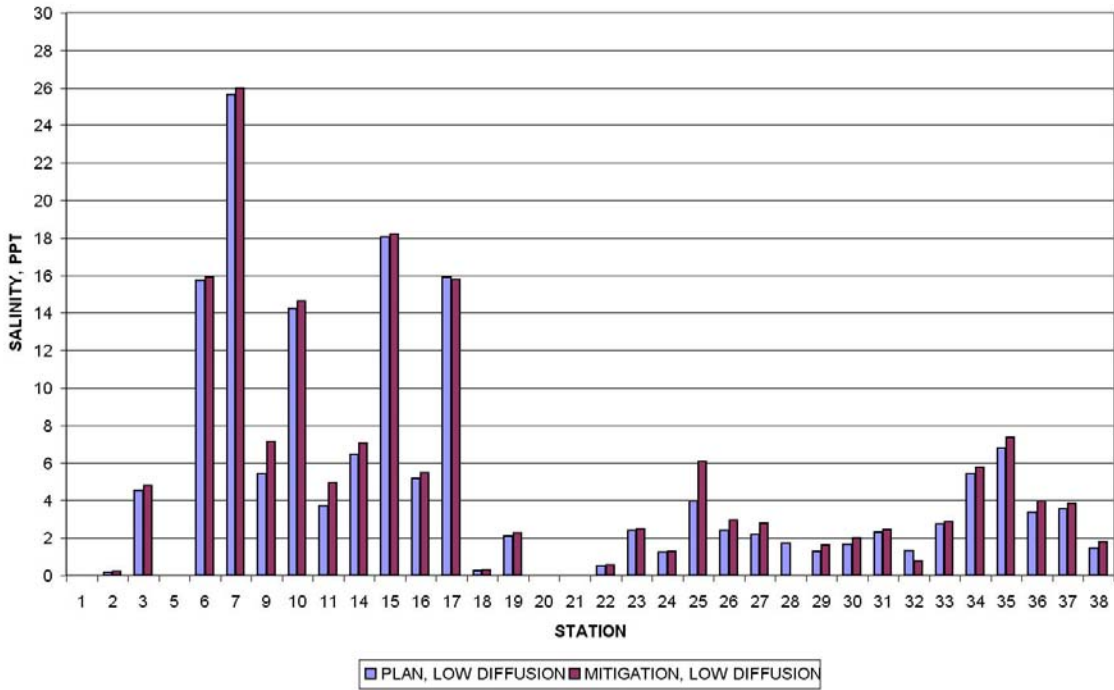


MEAN SALINITY VALUES, LOW FLOW, HIGH DIFFUSION

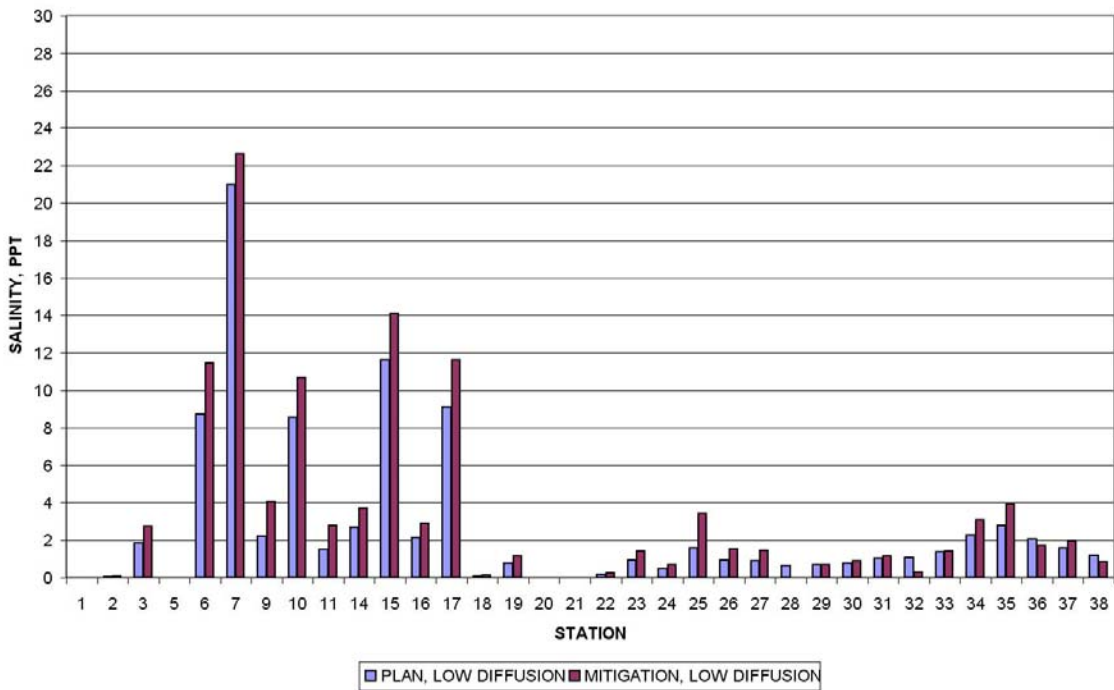


# Mitigation Scenario 6

HIGHEST 33% CONTINUOUS SALINITY, MEDIAN FLOW, LOW DIFFUSION

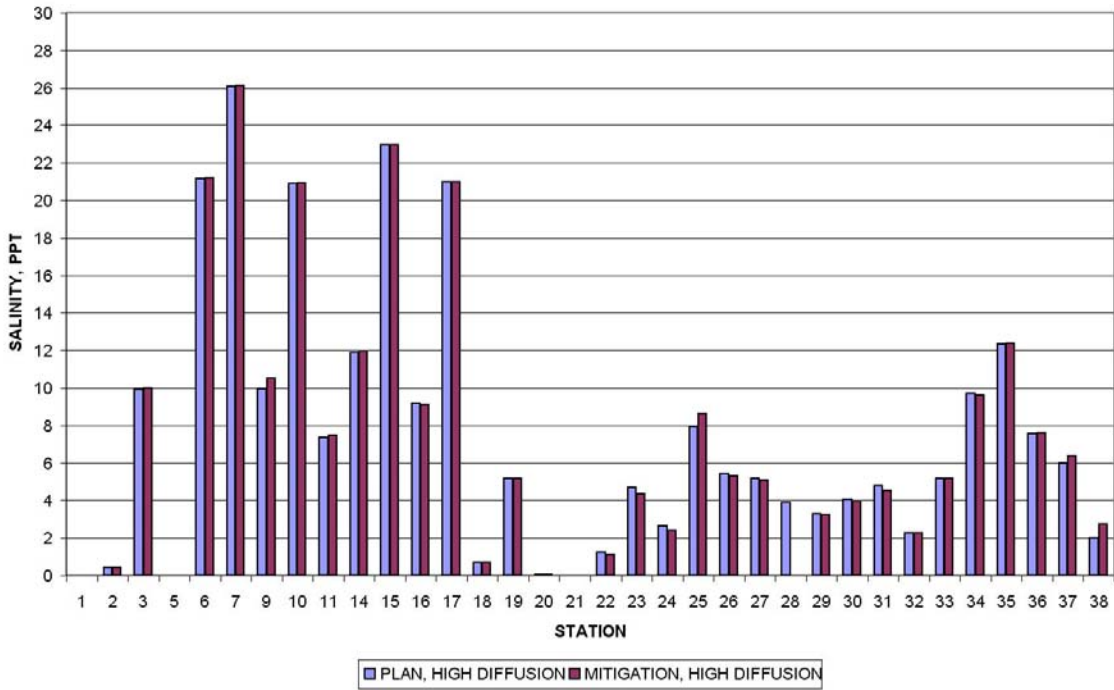


MEAN SALINITY VALUES, MEDIAN FLOW, LOW DIFFUSION



# Mitigation Scenario 6

HIGHEST 33% CONTINUOUS SALINITY, MEDIAN FLOW, HIGH DIFFUSION



MEAN SALINITY VALUES, MEDIAN FLOW, HIGH DIFFUSION

